# NACA

# RESEARCH MEMORANDUM

INVESTIGATION OF THE EFFECTS OF

WING AND TAIL MODIFICATIONS ON THE LOW-SPEED STABILITY

CHARACTERISTICS OF A MODEL HAVING A THIN 40° SWEPT WING

OF ASPECT RATIO 3.5

By Joseph Weil, William C. Sleeman, Jr.,
and Andrew L. Byrnes, Jr.

Langley Aeronautical Laboratory
Langley Field, Va.

# NATIONAL ADVISORY COMMITTEE
# FOR AERONAUTICS
## WASHINGTON
April 28, 1953

NACA RM L53C09

NATIONAL ADVISORY COMMITTEE FOR AERONAUTICS

RESEARCH MEMORANDUM

INVESTIGATION OF THE EFFECTS OF

WING AND TAIL MODIFICATIONS ON THE LOW-SPEED STABILITY

CHARACTERISTICS OF A MODEL HAVING A THIN 40° SWEPT WING

OF ASPECT RATIO 3.5

By Joseph Weil, William C. Sleeman, Jr.,
and Andrew L. Byrnes, Jr.

SUMMARY

An investigation has been made of the effects of wing and tail modifications on the low-speed stability characteristics of a model having a thin 40° swept wing of aspect ratio 3.5. The scope of this investigation was influenced to a large degree by the problem of obtaining a remedy for undesirable longitudinal stability characteristics observed in flight on several airplanes with similar wing geometry. Although some lateral stability and control data were obtained, this paper deals primarily with longitudinal characteristics of the model.

Longitudinal stability characteristics of the original configuration were considered good with the flaps down and slats extended; however with flaps and slats retracted, longitudinal instability was present in the angle-of-attack range between 11° and 16°. The use of either a horizontal-tail location below the fuselage center line or an optimum wing leading-edge chord-extension essentially eliminated the longitudinal instability. Neither the optimum fence configuration developed nor the highest tail position studied (0.65 semispan above the fuselage center line) were quite as effective in improving the longitudinal stability characteristics as the aforementioned modifications. By drooping the portion of the leading edge occupied by the retracted slat and chord-extension, it was possible to obtain almost the same usable lift coefficient with flaps down that was available without chord extension but with slats extended.

Enlarging the wing root inlet accentuated the undesirable longitudinal characteristics encountered with the original configuration and rendered it less responsive to modifications found beneficial with the smaller inlet. A tail location below the fuselage center line appeared to offer the most effective means of providing satisfactory longitudinal stability with the larger root inlet.

## INTRODUCTION

An investigation of the effects of wing and tail modifications on the low-speed stability characteristics of a model having a thin 40° swept wing of aspect ratio 3.5 has been made in an attempt to find means of improving the longitudinal stability characteristics observed in flight on several airplanes with similar wing geometry.

Information is also presented to show effects of wing modifications (such as fences and leading-edge chord-extensions) and changes in horizontal-tail location on the stability characteristics of the model. Longitudinal-stability data were also obtained with an enlarged root inlet with several wing and tail modifications.

## SYMBOLS

The system of stability axes employed, together with an indication of the positive forces, moments, and angles is presented in figure 1. The symbols used in this paper are defined as follows:

$C_L$        lift coefficient,  Lift/qS

$C_X$        longitudinal-force coefficient,  X/qS

$C_Y$        lateral-force coefficient,  Y/qS

$C_l$        rolling-moment coefficient,  L/qSb

$C_m$        pitching-moment coefficient,  M/qSc̄

$C_n$        yawing-moment coefficient,  N/qSb

X         longitudinal force along X-axis (Drag = -X), lb

Y         lateral force along Y-axis, lb

Z         force along Z-axis (Lift = -Z), lb

L         rolling moment about X-axis, ft-lb

M         pitching moment about Y-axis, ft-lb

N         yawing moment about Z-axis, ft-lb

| q | free-stream dynamic pressure, $\frac{\rho V^2}{2}$, lb/sq ft |
|---|---|

$\sigma$ tail effectiveness parameter, $\dfrac{\left(\partial c_m / \partial i_t\right)_{\text{wing on}}}{\left(\partial c_m / \partial i_t\right)_{\text{max}_{\text{wing off}}}}$

S      wing area, sq ft (excluding area of inlet ducts)

$\bar{c}$      wing mean aerodynamic chord, ft

c      local streamwise chord, ft

b      wing span, ft

V      free-stream velocity, ft/sec

A      aspect ratio, $b^2/S$

$\rho$      mass density of air, slugs/cu ft

$\alpha$      angle of attack of fuselage center line, deg

$\beta$      angle of sideslip, deg

$\epsilon$      effective downwash angle at tail, deg

$\Lambda$      angle of sweep of quarter-chord line, deg

$i_t$      angle of incidence of stabilizer with respect to fuselage center line (positive when trailing edge down), deg

$\delta_{a_L}$      left-aileron deflection (positive with trailing edge down), deg

$\delta_f$      flap deflection, deg

$\delta_s$      slat deflection, deg

$\delta_1$      deflection of leading edge between 48 and 65 percent semispan, deg

$\delta_2$      deflection of leading edge between 65 and 94 percent semispan, deg

Subscripts:

$\beta$        denotes partial derivative of a coefficient with respect to

sideslip; for example, $C_{l_\beta} = \dfrac{\partial C_l}{\partial \beta}$

max        maximum

## MODEL AND APPARATUS

### Description of Model and Airplane

Details of the physical characteristics of the model are presented
in figures 2 and 3 and table I.

Inasmuch as no provision was made to allow air flow through the
model inlet, the forward portion of the inlet was faired to afford
a good aerodynamic shape. (See fig. 2.)

Various modifications to the wing and tail geometry were made to
study their effects on the longitudinal stability characteristics of
the proposed configuration.

Tail modifications.- Six alternate tail locations were investigated
in addition to the original position. (See fig. 4.) The primary vari-
able in this study was tail height; however, some increase in tail
length occurred when the horizontal tail was raised on the swept vertical
tail.

Wing modifications.- A fairly systematic series of fence and leading-
edge chord-extension configurations was investigated. The scope of this
study is indicated in figures 5 and 6. Two segments of the portion of
wing originally occupied by the retracted slat (including the chord-
extensions) were drooped various amounts, pivoting about the lower wing
surface at the 15-percent-chord station. (See fig. 7.)

In order to determine the effect of inlet size on the various aero-
dynamic characteristics, a glove conforming to a large inlet was fash-
ioned out of soft wood and placed over the original inlet. The differ-
ences between the two inlet configurations are shown in figure 8. Some
of the most beneficial fence and chord-extension configurations investi-
gated with the smaller inlet were also studied with the wing having the
larger inlet. Additional modifications attempted with the larger inlet
alone consisted of a large fence at the outboard edge of the inlet and a
spoiler on the inlet nose (fig. 8).

## Flow Studies

The effects of wing modifications on the flow over the upper wing surface were obtained from photographs of wool tufts placed on the wing surface.

The effects of wing modifications on the flow field at the tail plane were determined by use of the tuft grid described in reference 1. For these studies, the tail surfaces were replaced by unswept $\frac{1}{8}$ - inch rods to indicate the position occupied by the vertical tail and also the proposed and extreme horizontal-tail positions investigated. The tuft grid was placed approximately 1.5 wing semispans behind the wing quarter-chord line and extended over the tunnel cross section except for the supporting frame. Photographs of the tuft grid were obtained with a camera mounted 75 feet downstream of the grid and approximately on the tunnel center line. Further details of the tuft-grid technique can be found in reference 2.

## TESTS AND CORRECTIONS

### Tests

The tests were conducted in the Langley 300 MPH 7- by 10-foot tunnel at a dynamic pressure of 40 pounds per square foot which, for average test conditions, corresponds to a Mach number of about 0.17 and a Reynolds number of approximately $2.0 \times 10^6$, based on the wing mean aerodynamic chord of 1.67 feet.

The lateral-stability derivatives of the model were determined from tests through the angle-of-attack range at sideslip angles of $\pm 5^\circ$.

In all instances the tricycle landing gear was in the extended position when the trailing-edge flaps were deflected. Unless otherwise noted, a tail height of 25 percent wing semispan above the fuselage center line was used.

### Corrections

The angle-of-attack, drag, and pitching-moment results have been corrected for jet-boundary effects, computed on the basis of unswept-wing theory by the method of reference 3. Independent calculations have shown that the effects of sweep on these corrections are negligible.

No systematic tare evaluation has been made. It is felt, however, on the basis of limited data and past experience that appreciable tare effects were present only in minimum drag and longitudinal trim. It was estimated from reference 4 that the blockage correction to the measured dynamic pressure was of the order of 1 percent. This correction has not been applied to the data.

## PRESENTATION OF RESULTS

The figures presenting the results are grouped as follows:

### Longitudinal Characteristics

### Lateral Characteristics

## DISCUSSION

### Basic Longitudinal Characteristics

The data of figure 10 with $\delta_f = 0°$ indicate longitudinal stability characteristics at about $\alpha = 10°$ which might cause the airplane

to be uncontrollable and to pitch up to undesirably high angles of attack in certain flight conditions. For this configuration, the cause of the higher-lift instability is clearly traceable to the extremely large increase in $\partial\epsilon/\partial\alpha$ (fig. 12) arising from the inward and upward displacement of the center of wing vorticity. (See tuft-grid photographs, fig. 37.) The untapered horizontal-tail plan form also places a large portion of the tail outboard in a region of higher downwash slope. It is perhaps of some interest that the fuselage alone contributes only about 0.14 to $\partial\epsilon/\partial\alpha$ in the range of greatest instability.

At the highest angles of attack the stabilizer effectiveness, as indicated by the parameter $\sigma$, is reduced to about 50 to 75 percent of the maximum wing-off value (fig. 12). This adverse stability effect, however, is more than counteracted by the large stabilizing decrease in downwash slope.

With the flaps deflected $40^\circ$ and slats extended, acceptable stability characteristics are indicated. (See fig. 11.) The desirable flow characteristics obtained over the tip wing sections in this configuration are shown in figure 38.

A short study was made to determine the effect of the slat and slat modifications on the lift coefficient attainable at moderately high angles of attack with the flaps deflected $40^\circ$. It is seen (fig. 13) that the slat was very effective in delaying the wing stall and contributed as much as 0.3 to the available lift coefficient at moderately high angles of attack. The data of figure 13 indicate, furthermore, that the lift characteristics are essentially unaffected by slat gap. Reducing the slat deflection from $21.7^\circ$ to $14.5^\circ$ effected only a slight reduction in maximum lift but produced less desirable longitudinal stability characteristics above $\alpha = 14^\circ$.

Modifications Designed to Improve

Longitudinal Characteristics

The longitudinal-stability difficulties encountered with the basic configuration, $\delta_f = 0^\circ$, were considered serious enough to warrant the study of various means for alleviating the pitch-up tendency. In the interpretation of the effects of the modifications it was felt that, although the variation of $C_m$ with $C_L$ provides a direct indication of the stability characteristics below stall, it usually does not produce data in a convenient form for a quantitative evaluation of the pitch-up that occurs at or near the stall. The motion associated with this type of instability can produce high angular acceleration of the airplane without necessarily causing excessive load factors and is

considered very undesirable by pilots.  It appeared that a linear variation of  $C_m$  with  $\alpha$  on the other hand would result in close to optimum stability characteristics with little overshoot or pitch-up apt to occur in either maneuvers or 1 g flight near stall and this attainment is the goal of the various modifications.

Although the data are presented about the rather far forward center-of-gravity location ($0.15\bar{c}$), every attempt will be made to discuss the results in a fairly general manner.

Effect of tail height.- The effect of relocating the horizontal tail is shown in figures 14 to 16.  Raising the tail to 36 percent  $b/2$  above the fuselage center line actually resulted in increased severity of the break although the instability was delayed to a slightly higher lift coefficient.  With the tail located on top of the vertical tail (65 percent  $b/2$  above the fuselage center line) the lift coefficient at which pitch-up might be expected is delayed to  $C_{L_{max}}$, but this configuration might still produce undesirable overshoot at the stall.  The instability above  $\alpha = 17^\circ$  for the highest tail location (fig. 14) results from the unfavorable downwash variation encountered as the tail approaches the plane of the rolled-up wing vortices.  (See tuft-grid photographs, fig. 37.)

Lowering the tail to 19 percent  $b/2$  above the fuselage center line or use of an inverted vee tail (root and tip chords 19 and 2 percent semispan above fuselage center line, respectively, fig. 4) produced little beneficial effect on the pitch-up tendency (see fig. 15). When the tail was lowered to 7 percent semispan below the fuselage center line, however, the longitudinal stability seems acceptable throughout the angle-of-attack range probably because the tail is emerging from the wake in this condition.

With flaps deflected 40° and slats extended, no serious longitudinal-stability problems would appear to exist for any of the raised tail locations although some pitch-up tendency is indicated for the highest tail location at angles of attack greater than 20°.  (See fig. 16.)  No force data were obtained for the lowest tail investigated with flaps deflected. The tuft-grid photographs (fig. 38), however, show very unsteady flow in the region of the lowest tail which might indicate a buffet problem.

Use of fences.- Fences have frequently been used in the past to improve the longitudinal stability characteristics of swept wings.  A number of fence configurations were studied on the subject model (fig. 5) and the results are shown in figures 17 to 20.  With the flaps undeflected, fence 2 was located at various spanwise stations from 65 to 80 percent  $b/2$.  The data (fig. 17) indicate that the high-lift longitudinal stability was considerably improved by the fence at all

locations.  None of the fence installations was successful in pro-
ducing a configuration free from pitch-up in the angle-of-attack range
below 20°; however, a fence location at 75 percent  b/2  appeared
slightly superior to some of the other locations.

The sensitivity of the pitching-moment characteristics to fence
size was determined for the 75-percent-$\frac{b}{2}$ location.   (See fig. 18.)
It is seen that there are relatively minor changes in stability brought
about by using a fence larger than fence 4.  This result appears to be
reasonable in view of the leading-edge separation encountered on thin
swept wings.  A small inboard leading-edge spoiler added as a means of
providing a sharp leading edge (fig. 5) and used in conjunction with
fence 2 improved the over-all stability somewhat (fig. 18).  Several
multiple-fence installations were investigated in the flap-retracted
condition (fig. 19).  The results showed that in neither instance did
the use of two fences add to the gains obtained through use of a single
well-placed fence.  (See figs. 17 and 19.)

With flaps and slats extended it is seen (fig. 20) that the lift
coefficient in the angle-of-attack range between 12° and 16° is reduced
by from 0.04 to 0.08 when fences 1 and 2 are used; moreover, the gains
in  $\Delta C_L$  attributable to slat deflection in the same angle-of-attack
range are about halved.  The multiple fences did not change the already
satisfactory pitching-moment variations obtained with slats extended.
In the high angle-of-attack range with slats retracted, however, the
use of fences 1 and 2 did improve the longitudinal stability.

<u>Undrooped chord-extensions.</u>- Another means of securing improved
high-lift longitudinal stability on thin-, swept-wing airplanes is
afforded by the use of leading-edge chord-extensions.  A systematic
investigation of various chord-extension configurations (see fig. 6)
was undertaken and the results are presented in figures 21 to 26.  The
effects of varying the inboard end of a 0.10c extension with  $\delta_f = 0°$
are shown in figure 21.  The improvement in the pitching-moment char-
acteristics is similar to, but somewhat greater than, that obtained with
fences at a given spanwise location (cf. figs. 21 and 17).  This is
particularly true of the 65- and 70-percent-$\frac{b}{2}$  inboard-end locations
where the variations of  $C_m$  with both  $\alpha$  and  $C_L$  indicate essentially
no pitch-up tendency in the practical angle-of-attack range ($\alpha < 20°$).

It is generally conceded that the gains derived from use of chord-
extensions are dependent to a large extent on the action of the vortex
shed from the inboard edge, which is of such direction as to retard the
spread of low-energy air over the outboard wing sections and, conse-
quently, maintain a greater proportion of the total lift over the tip.

Thus, the effects of the chord-extension in some respects are the aerodynamic counterpart of the physical barrier created by the use of a fence. This line of reasoning is illustrated by a comparison of photographs made of surface tufts with and without a chord-extension (cf. figs. 37 and 39).

From figure 21 it was evident that 65 to 70 percent $b/2$ represented the optimum inboard extension location for the configuration under study. A further investigation was made to determine the effect of spanwise extent of the chord-extension with the inboard end fixed at 65 percent $b/2$. The results (fig. 22) show that an outboard location of 80 percent $b/2$ did not produce the abrupt instability at $\alpha = 24^\circ$ that existed when the extension was carried to 94 percent $b/2$. In the practical angle-of-attack range, however, there would appear to be very little difference between the two installations, particularly with a large initial static margin present. Moving the outboard end of the extension in to the 75-percent-$\frac{b}{2}$ location resulted in longitudinal stability characteristics that were definitely inferior (above $\alpha = 10^\circ$) to those for the larger span extensions previously discussed. A similar comparison for an inboard location of 70 percent $b/2$ showed that a span of 0.24 $b/2$ (70 to 94 percent $b/2$) produced somewhat more desirable results than a span of 0.10 $b/2$ (cf. figs. 21 and 22).

Increasing the overhang of the leading-edge chord-extension from 0.10c to 0.15c produced very little effect up to $\alpha = 20^\circ$ but delayed and reduced the magnitude of the abrupt pitch-up tendency at very high angles of attack. (See fig. 23.)

A fairly complete set of data was obtained for one of the more promising chord-extension configurations evolved (extension of 0.10c from 70 to 94 percent $b/2$) and the results are presented in figures 24 and 25. A comparison of these results with those obtained for the original configurations (figs. 10 and 11) are presented in figure 26. It is evident that for $\delta_f = 0^\circ$ the gains in stability in the angle-of-attack range from $12^\circ$ to $16^\circ$ are less attributable to a more rearward wing-fuselage aerodynamic center than to the reduction in $\partial\epsilon/\partial\alpha$. The stability characteristics with flaps deflected $40^\circ$ are about equally satisfactory with either the original extended slats or chord-extensions.

Drooped chord-extensions.- In order to realize maximum landing performance, it is desirable to obtain the highest possible lift at reasonable angles of attack ($12^\circ$ to $16^\circ$). The lift characteristics pertinent to the landing problem have been summarized in figure 31; the values are for trimmed flight about the 0.15$\bar{c}$ center-of-gravity location. When a chord-extension was used in combination with $\delta_f = 40^\circ$, the usable

$C_{L_{max}}$ was about 0.15 less than that obtained for the original configu-
ration with slats extended. In order to increase the usable $C_{L_{max}}$, it
was decided to droop the area forward of 0.15c and outboard of the
48-percent-$\frac{b}{2}$ station (including the chord-extension) by various amounts
(see fig. 7). Note that the region of the wing drooped corresponded to
the portion of the wing occupied by the retracted slat. It is apparent
from figure 31 that a leading-edge droop of 10° provided substantially
the same $C_{L_{max}}$ as with slats extended but at the expense of somewhat
deteriorated higher-lift stability characteristics (fig. 27). Drooping
the chord-extension alone weakened the stability and produced essen-
tially no gain in $C_{L_{max}}$. (See fig. 28.)

The effect of leading-edge droop was obtained with flaps neutral
(fig. 30) on the assumption that a small amount of permanent droop could
be tolerated in the high-speed condition. It is evident that even 5° of
leading-edge droop seriously reduced the effect of the chord-extension
on the stability in the angle-of-attack range between 10° and 12°.

### Longitudinal Stability Characteristics With Enlarged Inlet

Basic configuration.- It is seen from figure 32 that increasing the
size of the root inlet does not alter the angle of attack for instability.
However, the model with the original inlet was unstable in the angle-of-
attack range from 11° to 16°, primarily because of the extremely high
values of downwash slope encountered. The instability of the model with
the larger inlet persisted to $\alpha = 19°$ because of the pronounced
unstable tendency of the wing-fuselage combination in conjunction with
the later occurrence of peak $\partial\epsilon/\partial\alpha$. (See figs. 32 and 33.)

The more unfavorable wing-fuselage pitching-moment characteristics
obtained with the larger inlet probably stem from two sources. It would
appear from a comparison of the tuft photographs in figures 37 and 41
that the vortices shed from the outboard edge of the large inlet might
be responsible for an accentuation of spanwise boundary-layer flow which
promotes earlier tip separation. At $\alpha = 13°$ and 17°, although the flow
over the most of the outboard wing sections is almost completely stalled
with either inlet, the flow near the leading edge appears to be somewhat
better for the smaller inlet. In addition to this indirect effect of
the larger inlet, a further inspection of the tuft photographs shows that
the larger inlet, acting much like a low-aspect-ratio wing, remained
unstalled even at very high angles of attack and this effect is probably
responsible for a direct destabilizing increment in lift of perhaps 0.1
to 0.2 $C_L$.

Modifications to model.- The results of some attempts to improve
the pitching-moment characteristics of the model with the larger inlet
are presented in figures 34 to 36.  A chord-extension from 0.65b/2 to
0.94b/2 (which was so effective when used with the smaller inlet)
reduced the severity of the pitch-up tendency in the angle-of-attack
range from 11° to 18° (fig. 34), but the characteristics indicated are
far from desirable.  Lowering the tail to 19 percent  b/2  above the
fuselage reference line with chord-extensions (fig. 35) caused no addi-
tional improvement in the stability characteristics.  The addition of
either a large fence at the outboard edge of the inlet or a spoiler
located 2 inches behind the inlet leading edge for the model equipped
with chord-extensions actually produced less desirable pitching-moment
characteristics than were obtained with chord extensions alone.  (See
fig. 34.)  The use of fences 1 and 2 at 75 and 40 percent  b/2, respec-
tively, had little effect on the characteristics of the basic model with
the larger inlet.

Placing the horizontal tail 7 percent  b/2  below the fuselage
center line resulted in pitching-moment characteristics that probably
would be acceptable (fig. 36).

Aileron Characteristics

The results of aileron-effectiveness tests are presented in fig-
ures 42 and 43 for the original configurations and for the wing with
chord-extensions from 70 to 94 percent  b/2.  The lateral-control data
for the basic configuration indicate that about two-thirds of the low-
lift effectiveness is maintained in the high angle-of-attack range.  The
data of figure 42(b) also show an abrupt roll-off tendency on the left
wing at the initiation of stall with flaps deflected, which might indi-
cate extreme sensitivity to small model asymmetry in this attitude.
This same sensitivity is also shown with flaps up (fig. 42(a)) by the
presence of double-value points at  $\alpha = 13°$  for the up-aileron settings.

When the wing was modified with chord-extensions from 70 to 94 per-
cent  b/2  the abruptness of roll-off at stall was considerably reduced
for the flaps-deflected condition (without slats), and no unstable flow
conditions, as indicated by double-value points, were observed in the
flaps-retracted condition.  (See fig. 43.)  The effects of chord-
extensions on the aileron control effectiveness at several angles of
attack are shown in figure 44.  The use of chord-extensions did not
alter the aileron effectiveness much with flaps deflected or at low
angles of attack with flaps neutral, but the effectiveness of the down-
going aileron is improved with flaps neutral at very high angles of
attack.

## Lateral-Stability Derivatives

$C_{n_\beta}$.- For all complete-model configurations investigated the directional stability is high (generally greater than 0.004) below the stall. (See figs. 45 and 46.) The tail contribution to $C_{n_\beta}$ was estimated to be 0.0062 by the method of reference 5 and lift-effectiveness charts of reference 6. This compares with 0.0052 from wing-off tests at zero lift and an average value of 0.0065 with flaps down and drooped chord-extensions. The greater effectiveness with the wing on is probably attributable to stabilizing sidewash effects. There was not much effect of either chord-extension configuration on $C_{n_\beta}$ below the stall. At the stall a large decrease in weathercock stability was always present; however, a small degree of positive stability was retained at the highest test angle of attack. The loss in effectiveness at high angles of attack is probably traceable to the blanketing of the vertical tail by fuselage separation inasmuch as the wing-off configuration showed a similar, although more gradual, decrease in $C_{n_\beta}$ with $\alpha$. (See fig. 45.)

$C_{l_\beta}$.- In the high angle-of-attack range and with flaps down, the drooped chord-extensions (fig. 46) would appear to prevent the occurrence of neutral or slightly negative dihedral effect which was present for the original slats-out condition and with the undrooped chord-extension (fig. 45(b)). In the flaps-neutral condition the use of the chord-extension increased $C_{l_\beta}$ in the higher angle-of-attack range. (See fig. 45(a).)

## CONCLUSIONS

An investigation of the effects of wing and tail modifications on the low-speed stability characteristics of an airplane configuration having a thin 40° swept wing of aspect ratio 3.5 indicated the following conclusions:

1. Longitudinal instability was present for the basic model configuration with flaps neutral at angles of attack between 11° and 16°. With flaps down and slats extended the longitudinal stability was considered good.

2. The use of slats with flaps down contributed as much as 0.3 to the lift coefficient at moderately high angles of attack and was to a large extent responsible for the desirable longitudinal stability characteristics. Slat gap was found to be unimportant for this configuration.

3. Raising the horizontal tail to 65 percent semispan above the fuselage center line (highest tail position investigated) delayed the onset of instability from an angle of attack of 11° to 17°. A tail location of 7 percent semispan below the fuselage center line resulted in acceptable pitching-moment characteristics with flaps neutral throughout the test angle-of-attack range.

4. Although the longitudinal stability characteristics at higher angles of attack were considerably improved by the use of outboard wing fences, none of the fence installations were successful in producing a configuration free from flat spots or instability below an angle of attack of 20°. In no instance did the gains obtained with two fences add to the improvement obtainable through use of a single well-placed fence.

5. Leading-edge chord-extensions were more effective in improving the pitching-moment characteristics than fences. An extension of 0.10 local chord extending from 0.70 to 0.94 semispan, for example, essentially eliminated the pitch-up tendency.

6. Replacing the wing slats with leading-edge chord-extensions in the landing condition resulted in a loss of 0.15 lift coefficient in the usable range of landing attitudes. Drooping that portion of the leading edge occupied by the retracted slat and the chord-extension 10° provided substantially the same lift characteristics as with slats extended and deflected 21.7°, at the expense, however, of somewhat deteriorated higher-lift stability characteristics.

7. With an enlarged wing root inlet and flaps neutral, the attitude at which longitudinal instability occurred was not altered, but the instability was extended over a considerably greater angle-of-attack range than with the smaller inlet. The use of a leading-edge chord-extension reduced the severity of pitch-up tendency in the angle-of-attack range from 11° to 18° but the resultant characteristics would still appear unacceptable. The addition of various wing fences or spoilers located near the inlet leading edge had no beneficial effect. Lowering the horizontal tail to a position 7 percent semispan below the fuselage center line produced what would appear to be acceptable pitching-moment characteristics throughout the lift range with flaps neutral.

8. About two-thirds of the low-lift aileron effectiveness is maintained at the highest angles of attack for the basic configuration. The use of chord-extensions did not materially alter the aileron effectiveness but improved the flow stability near the stall (flaps neutral) and reduced the abruptness of roll-off with flaps deflected.

9. In the higher angle-of-attack range and with flaps down, the drooped chord-extensions prevented the occurrence of neutral or slightly

negative dihedral effect which was present for the original slats-out condition and with undrooped chord-extensions.

Langley Aeronautical Laboratory,
     National Advisory Committee for Aeronautics,
          Langley Field, Va.

## REFERENCES

1. Sleeman, William C., Jr., and Linsley, Edward L.:  Low-Speed Wind-Tunnel Investigation of the Effects of Propeller Operation at High Thrust on the Longitudinal Stability and Trim of a Twin-Engine Airplane Configuration.  NACA RM L52D04, 1952.

2. Bird, John D., and Riley, Donald R.:  Some Experiments on the Visualization of Flow Fields Behind Low-Aspect-Ratio Wings by Means of a Tuft Grid.  NACA TN 2674, 1952.

3. Gillis, Clarence L., Polhamus, Edward C., and Gray, Joseph L., Jr.: Charts for Determining Jet-Boundary Corrections for Complete Models in 7- by 10-Foot Closed Rectangular Wind Tunnels.  NACA WR L-123, 1945.  (Formerly NACA ARR L5G31.)

4. Herriot, John G.:  Blockage Corrections for Three-Dimensional-Flow Closed-Throat Wind Tunnels, With Consideration of the Effect of Compressibility.  NACA Rep. 995, 1950.  (Supersedes NACA RM A7B28.)

5. Queijo, M. J., and Wolhart, Walter D.:  Experimental Investigation of the Effect of Vertical-Tail Size and Length and of Fuselage Shape and Length on the Static Lateral Stability Characteristics of a Model With 45° Sweptback Wing and Tail Surfaces.  NACA Rep. 1049, 1951.  (Supersedes NACA TN 2168.)

6. DeYoung, John, and Harper, Charles W.:  Theoretical Symmetric Span Loading at Subsonic Speeds for Wings Having Arbitrary Plan Form. NACA Rep. 921, 1948.

TABLE I

SUMMARY OF BASIC MODEL GEOMETRY

Wing:
 Area (not including inlet area), sq ft . . . . . . . . . . . . . 9.03
 Span, ft . . . . . . . . . . . . . . . . . . . . . . . . . . . 5.59
 Sweepback of quarter-chord line, deg . . . . . . . . . . . . . 40
 Aspect ratio . . . . . . . . . . . . . . . . . . . . . . . . . 3.45
 Taper ratio . . . . . . . . . . . . . . . . . . . . . . . . . 0.578
 Dihedral . . . . . . . . . . . . . . . . . . . . . . . . . . . $-3^\circ\ 30'$
 Incidence . . . . . . . . . . . . . . . . . . . . . . . . . . $2^\circ\ 30'$
 Geometric twist, deg . . . . . . . . . . . . . . . . . . . . . 0
 Mean aerodynamic chord, ft . . . . . . . . . . . . . . . . . . 1.67
 Airfoil section (normal to quarter-chord line) . . . . . . NACA 64A010
 Root chord, ft . . . . . . . . . . . . . . . . . . . . . . . . 2.063
 Tip chord, ft . . . . . . . . . . . . . . . . . . . . . . . . 1.195

Flap:
 Type . . . . . . . . . . . . . . . . . . . . . . . . Plain trailing edge
 Area (one flap), sq ft . . . . . . . . . . . . . . . . . . . . 0.420
 Span, ft . . . . . . . . . . . . . . . . . . . . . . . . . . . 1.009
 Hinge line, percent  c . . . . . . . . . . . . . . . . . . . . 75
 Maximum deflection, deg . . . . . . . . . . . . . . . . . . . 40

Aileron:
 Area (one aileron), sq ft . . . . . . . . . . . . . . . . . . 0.38
 Span, ft . . . . . . . . . . . . . . . . . . . . . . . . . . . 1.24
 Hinge line, percent  c . . . . . . . . . . . . . . . . . . . . 75
 Maximum deflection (normal to hinge line), deg . . . . . . . . $\pm 18$

Leading-edge slat:
 Span of one slat (normal to model center line), ft . . . . . . 1.33
 Ratio of slat chord to wing chord (normal to c/4) . . . . . . 0.140
 Inboard edge (from model center line), ft . . . . . . . . . . 1.347
 Forward extension of slat, percent  c . . . . . . . . . . . . 8.4
 Downward extension of slat, percent  c . . . . . . . . . . . . 7.24

Horizontal tail:
 Type . . . . . . . . . . . . . . . . . . . . . . . . . . All-movable
 Area, sq ft . . . . . . . . . . . . . . . . . . . . . . . . . 1.55
 Span, ft . . . . . . . . . . . . . . . . . . . . . . . . . . . 2.36
 Sweepback (quarter chord), deg . . . . . . . . . . . . . . . . 40
 Taper ratio . . . . . . . . . . . . . . . . . . . . . . . . . 1.0
 Dihedral, deg . . . . . . . . . . . . . . . . . . . . . . . . 0
 Chord, ft . . . . . . . . . . . . . . . . . . . . . . . . . . 0.67

TABLE I.- Concluded

SUMMARY OF BASIC MODEL GEOMETRY

Maximum deflection, deg . . . . . . . . . . . . . . . . . . -6 to 15
Airfoil section . . . . . . . . . . . . . . . . . . . . . . NACA 64A009

Vertical tail:
  Area, sq ft . . . . . . . . . . . . . . . . . . . . . . . 1.73
  Span, ft . . . . . . . . . . . . . . . . . . . . . . . . . 1.815
  Sweepback of quarter-chord line . . . . . . . . . . . . . 41° 16' 10"
  Aspect ratio . . . . . . . . . . . . . . . . . . . . . . . 1.90
  Taper ratio . . . . . . . . . . . . . . . . . . . . . . . 0.34
  Mean aerodynamic chord, ft . . . . . . . . . . . . . . . . 0.955
  Airfoil section . . . . . . . . . . . . . . . . . . . . . NACA $64_{(10)}A011$
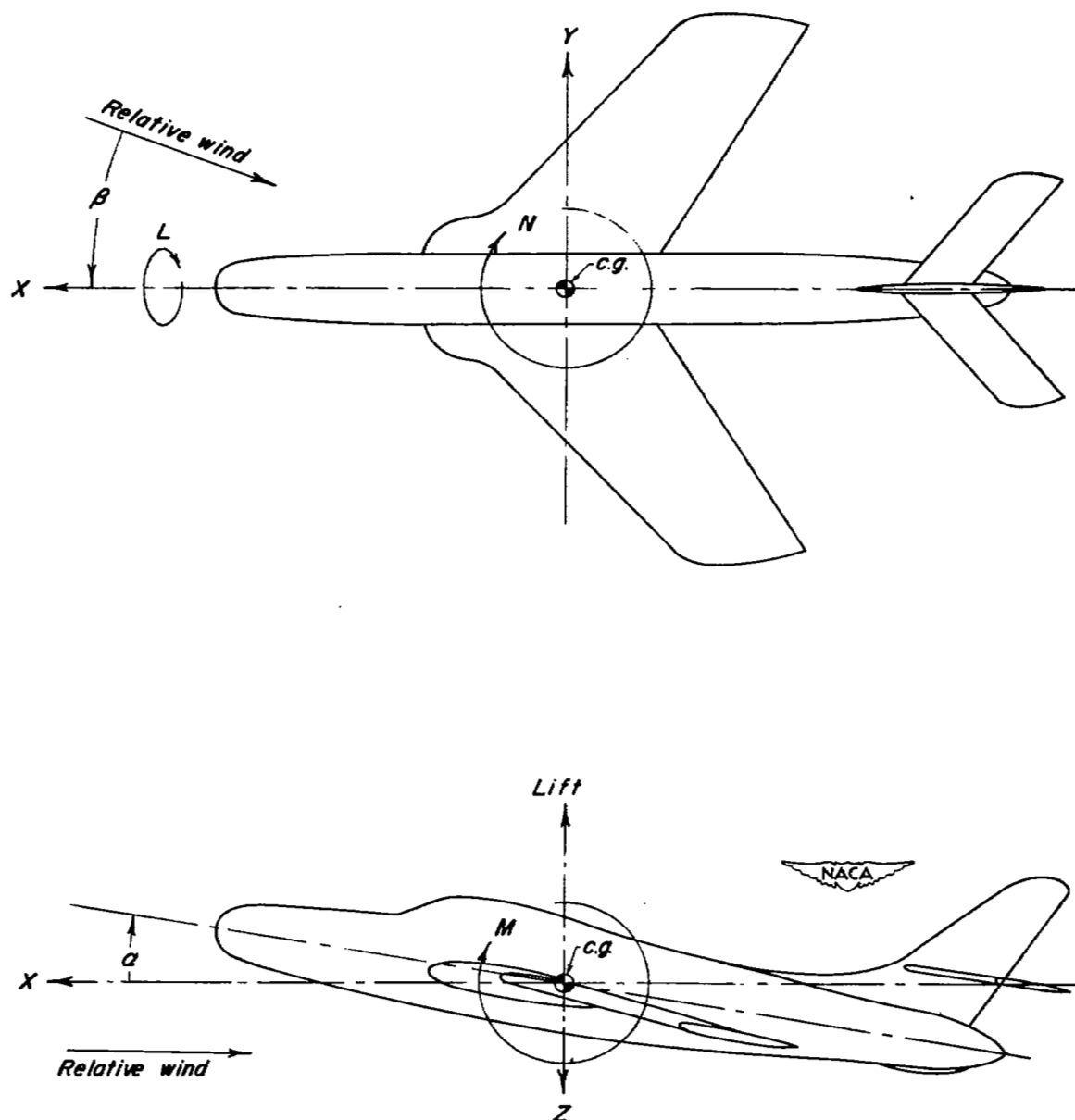
Figure 1.- System of axes and control-surface deflections. Positive
values of forces, moments, and angles are indicated by arrows.

Figure 2.- Two-view drawing showing details of basic model. All dimensions in inches.

.10

Partially extended slat

14.5°

.12

Fully extended slat

21.7°

Typical streamwise sections

outline of fully extended slat

retracted slat position

16.06

16.16

Fuselage ₵

NACA
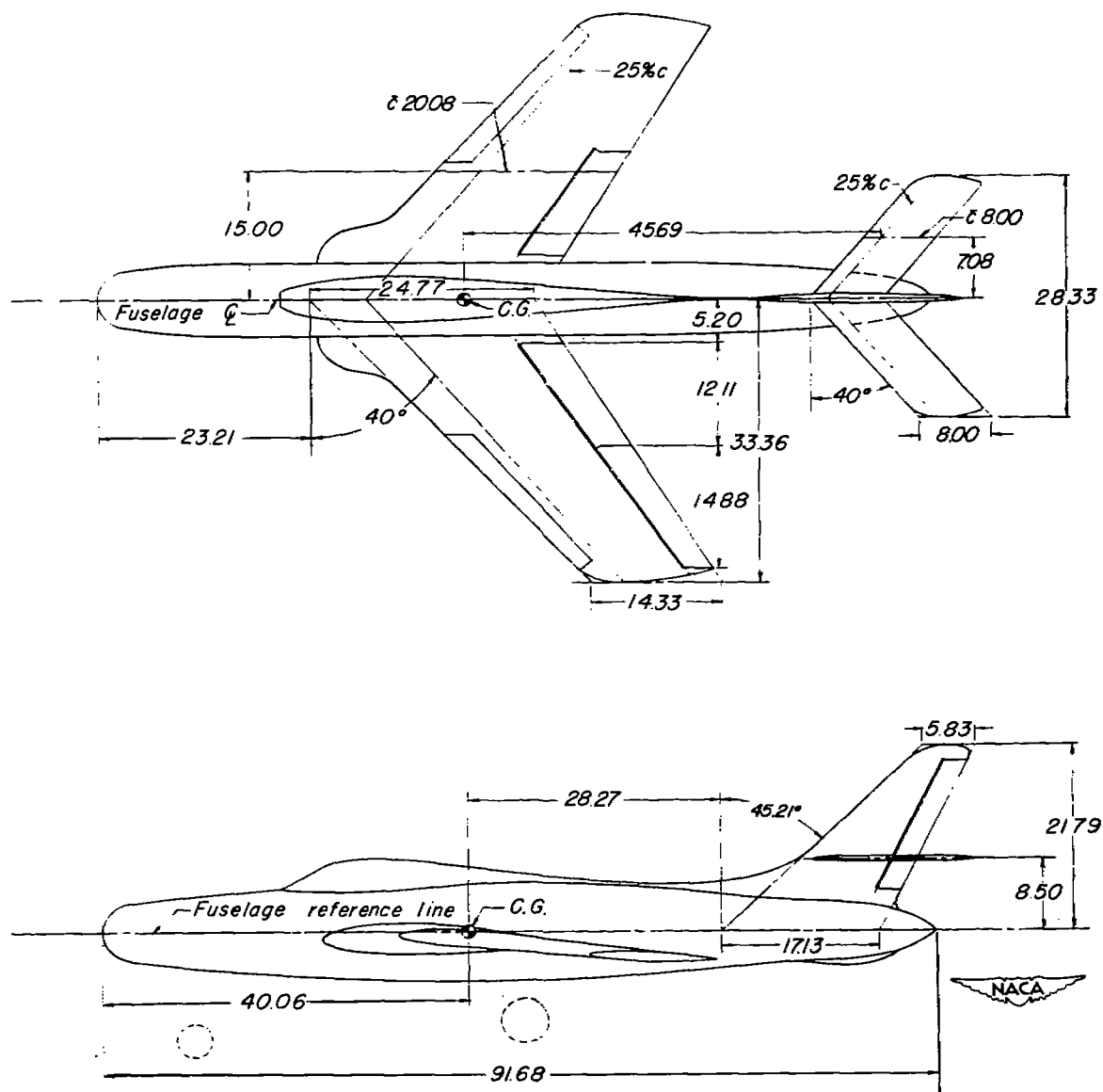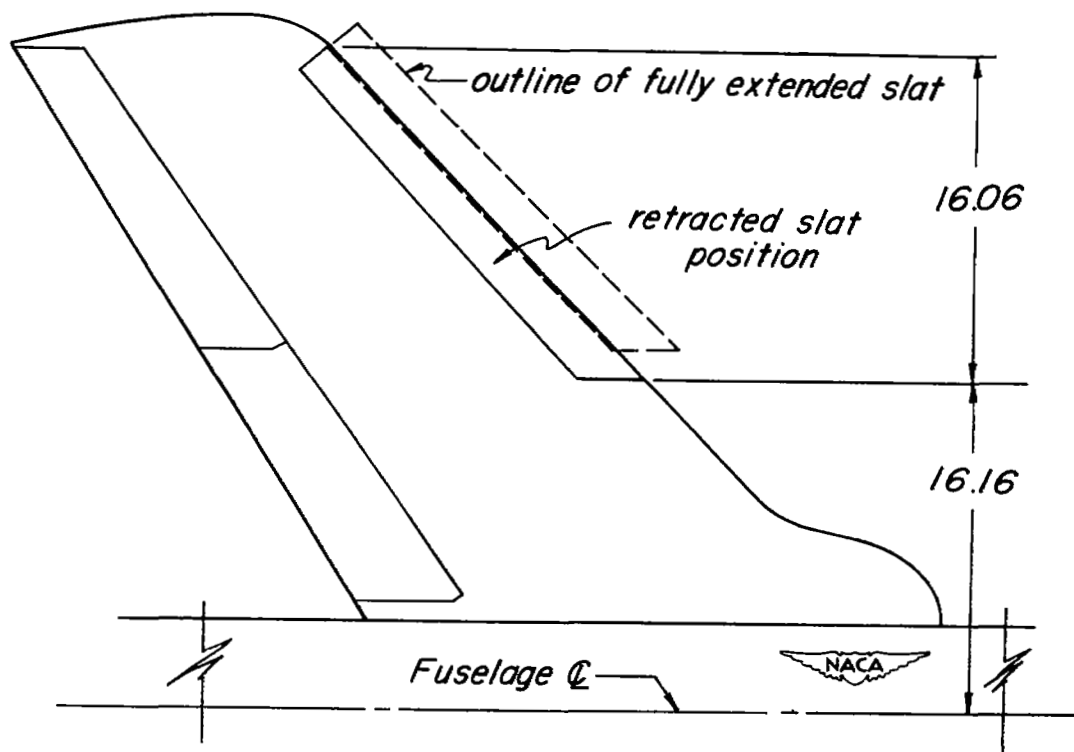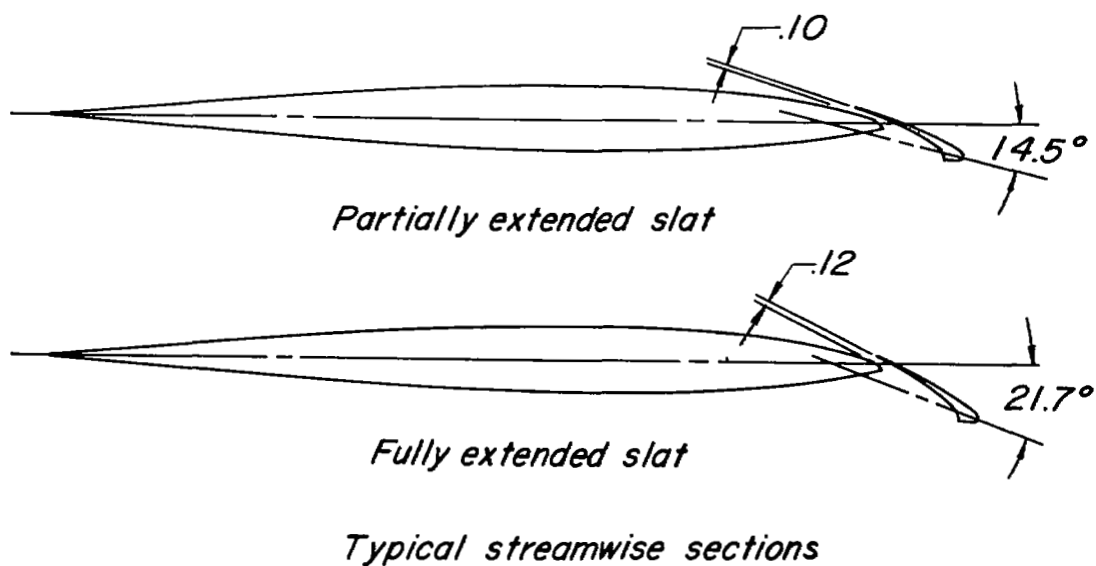
Figure 3.- Details of slat configurations investigated.  All dimensions
in inches.
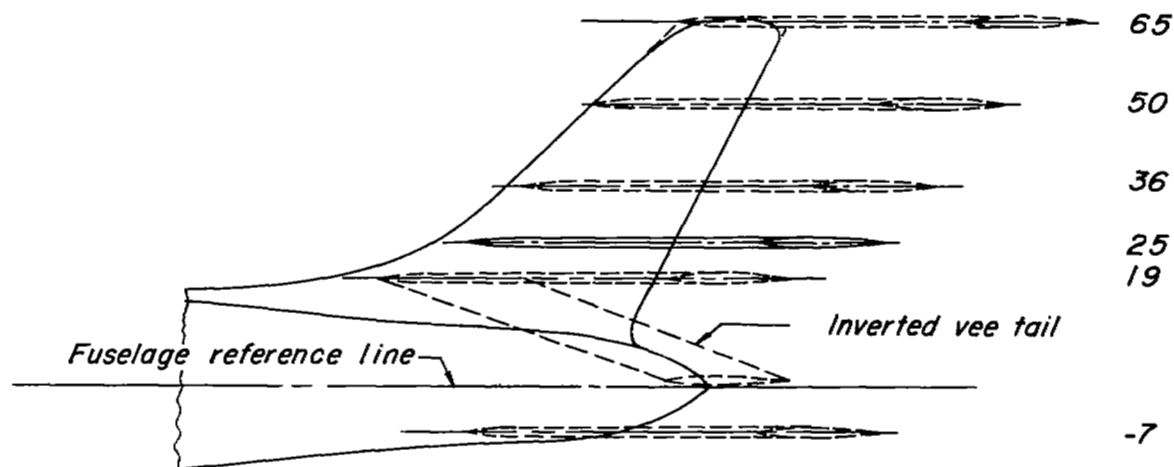
Tail height from fuselage reference line, percent wing semispan  $h_t$

Inverted vee tail

Fuselage reference line

65
50
36
25
19
-7

28.33

5.98

25°

19 $h_t$
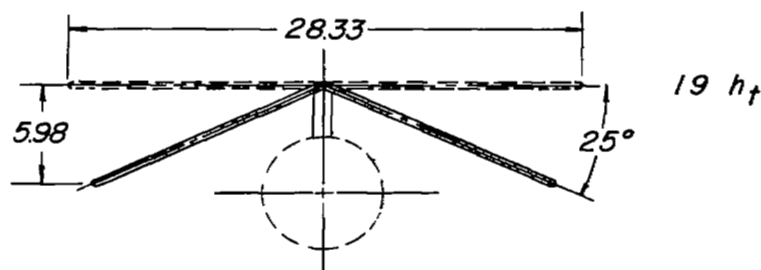
Front view of inverted vee tail

| Tail length, percent $\bar{c}$ | 228 | 202 | 228 | 243 | 262 | 286 |
|---|---|---|---|---|---|---|
| Tail height, percent semispan | -7 | 19 | 25 | 36 | 50 | 65 |

Figure 4.- Summary of horizontal-tail configurations investigated.
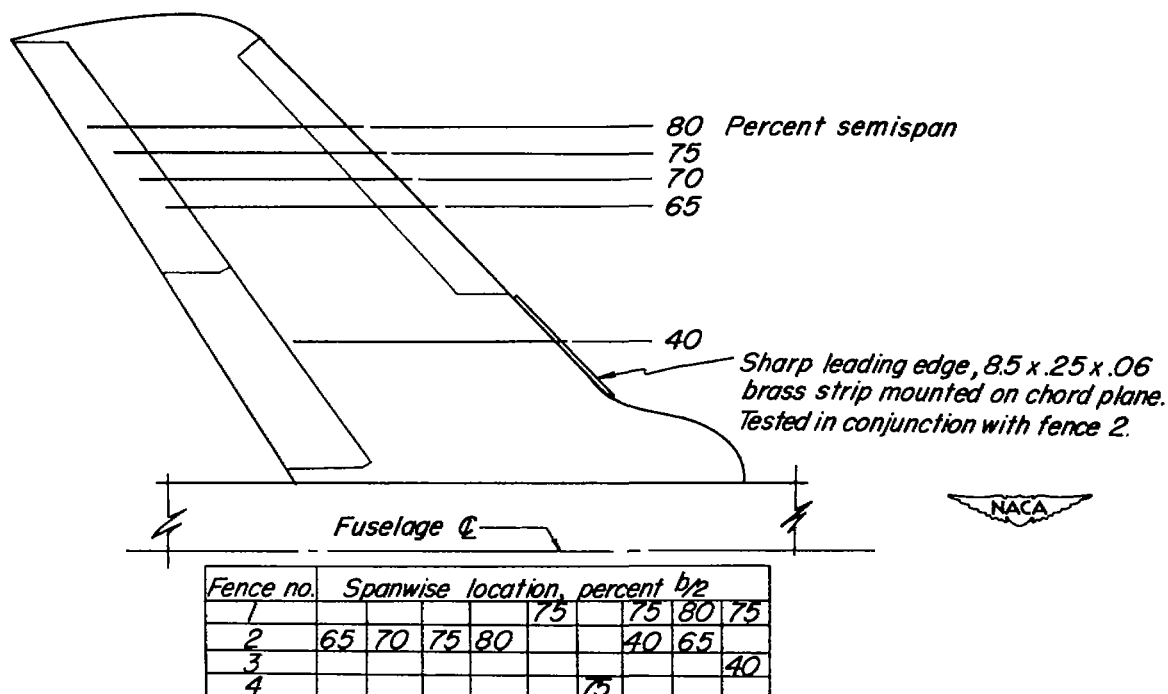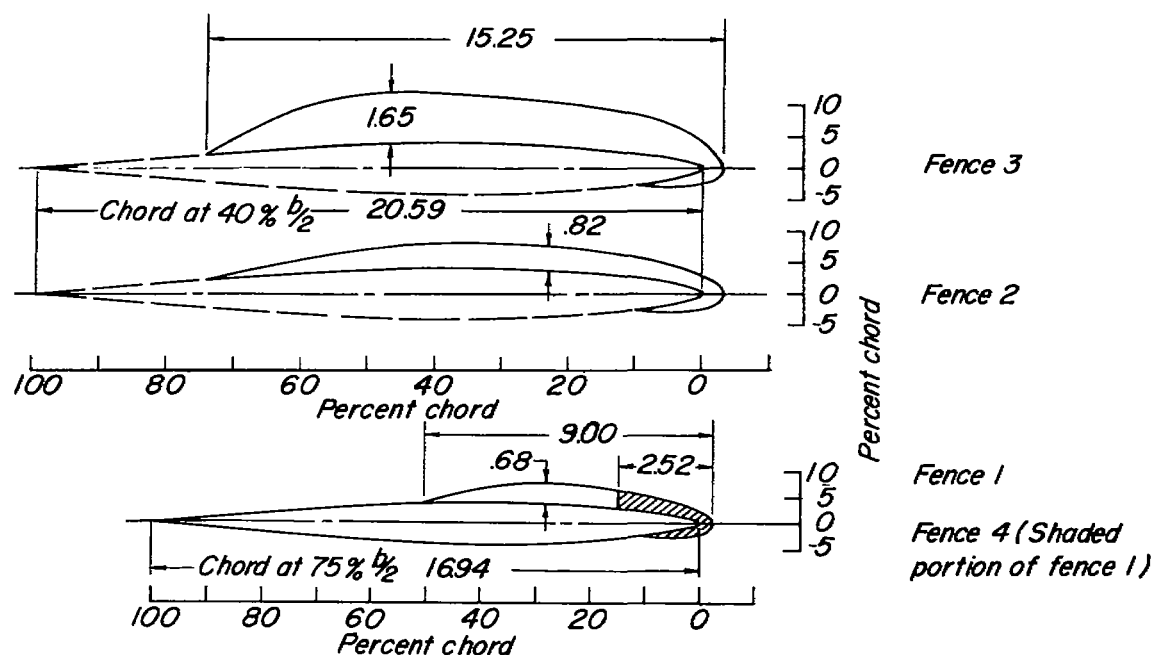
Figure 5.- Details of fence configurations investigated. All dimensions in inches unless otherwise specified. All fences made from 1/8-inch aluminum sheet.
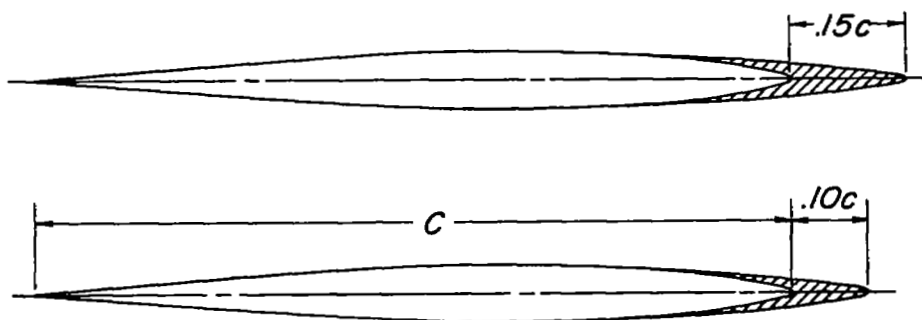
Typical streamwise sections of wing with leading-edge extension

94 Percent semispan

80
75
70
65

50

Fuselage ₵
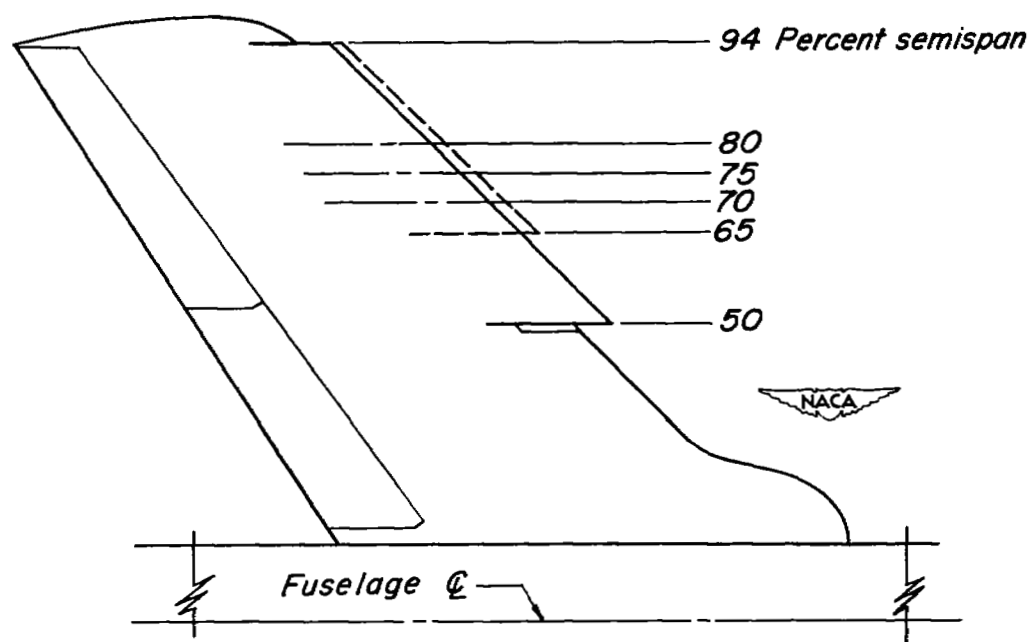
Spanwise extent of chord-extensions tested, Percent semispan

| Chord-extension | 10% c | | | | | | | | 15% c | |
|---|---|---|---|---|---|---|---|---|---|---|
| Inboard edge | 50 | 65 | 70 | 75 | 80 | 65 | 65 | 70 | 65 | 65 |
| Outboard edge | 94 | 94 | 94 | 94 | 94 | 80 | 75 | 80 | 94 | 80 |

Figure 6.- Details of leading-edge chord-extensions investigated.

*Typical streamwise section showing wing with drooped 10% c leading-edge extension*

*A-A*

Hinge

30° Max. $\delta_2$

*Typical streamwise section showing drooped leading edge*

*B-B*

Hinge

30° Max. $\delta_1$

Hinge line, 15 percent chord

94 Percent semispan

A      A

65

B      B

48

NACA

Fuselage $\mathcal{C}$
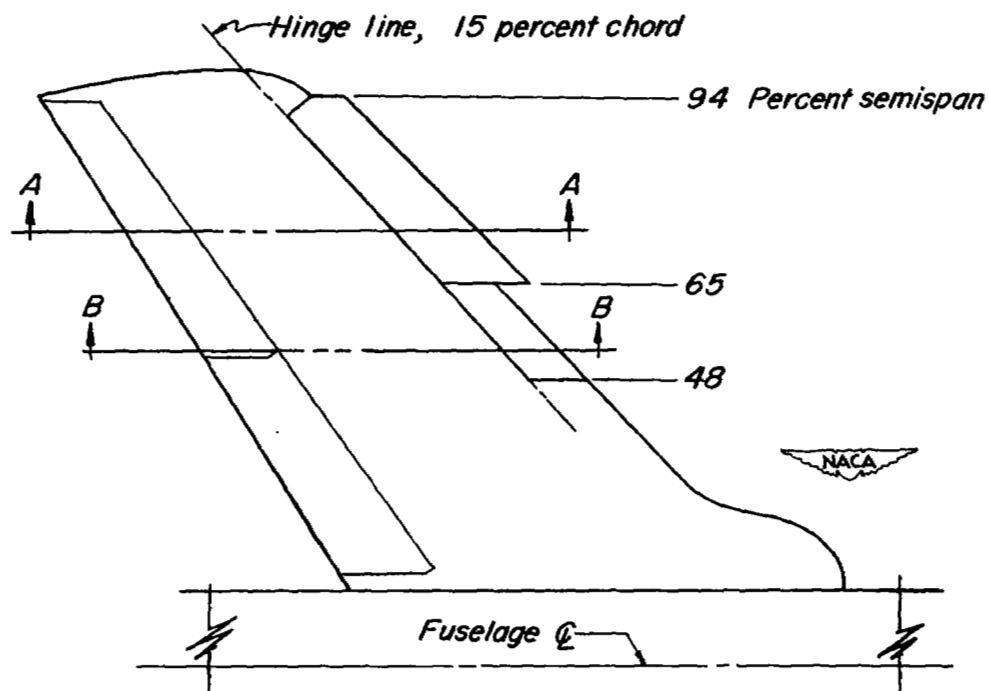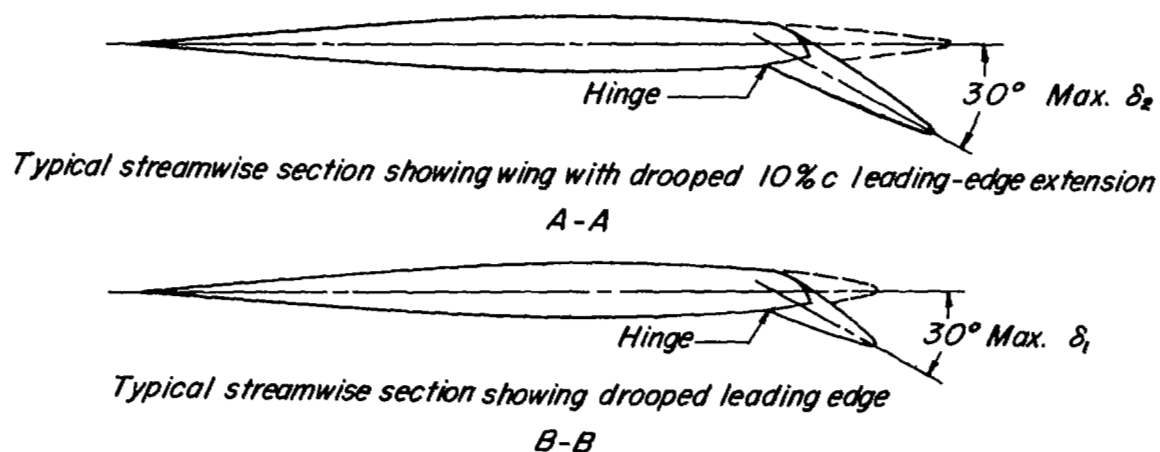
| | Deflection, deg | | | | | |
|---|---|---|---|---|---|---|
| Drooped chord-extension | $\delta_1$ | 0 | 0 | 5 | 10 | 20 | 30 |
| Combinations tested | $\delta_2$ | 0 | 10 | 5 | 10 | 20 | 30 |

Figure 7.- Details of drooped leading-edge chord-extensions investigated.

Streamwise contours

Spanwise contours

Station c    Station b
             Station a

Station 2

Station 1

Station 0   (Fuselage)

Plan view

Detail A - Contours of Large inlet

6      3      0

Scale, inches

2.25                          Fence

23.50

.3  6.75

Spoiler

Large inlet

Outline of small inlet

Fence

See detail A

30% b/2

2

Spoiler

Wing leading edge
extended

Fuselage ₵

6   3   0

Scale, inches
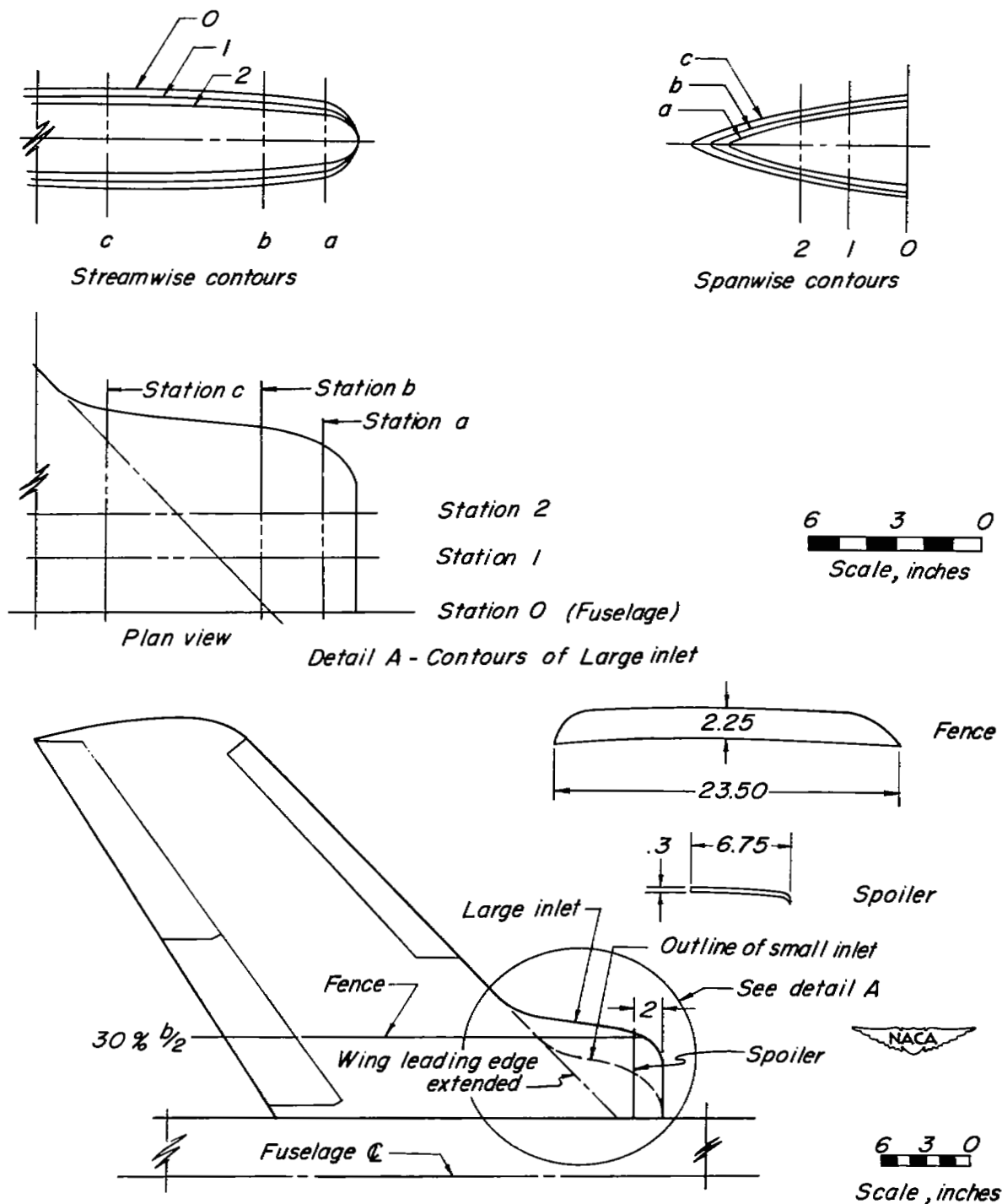
Figure 8.- Details of enlarged inlet and several wing modifications used
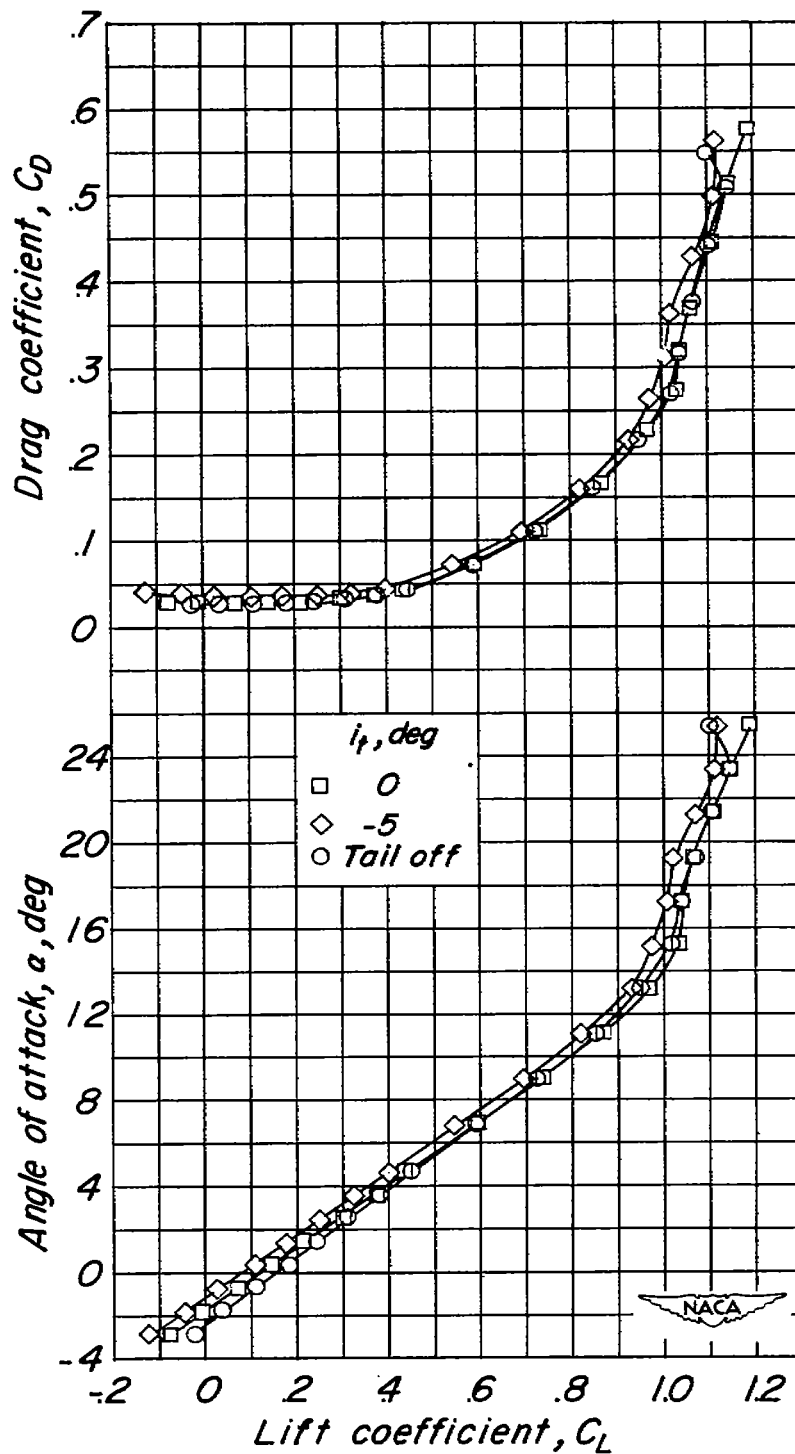in conjunction with enlarged inlet.
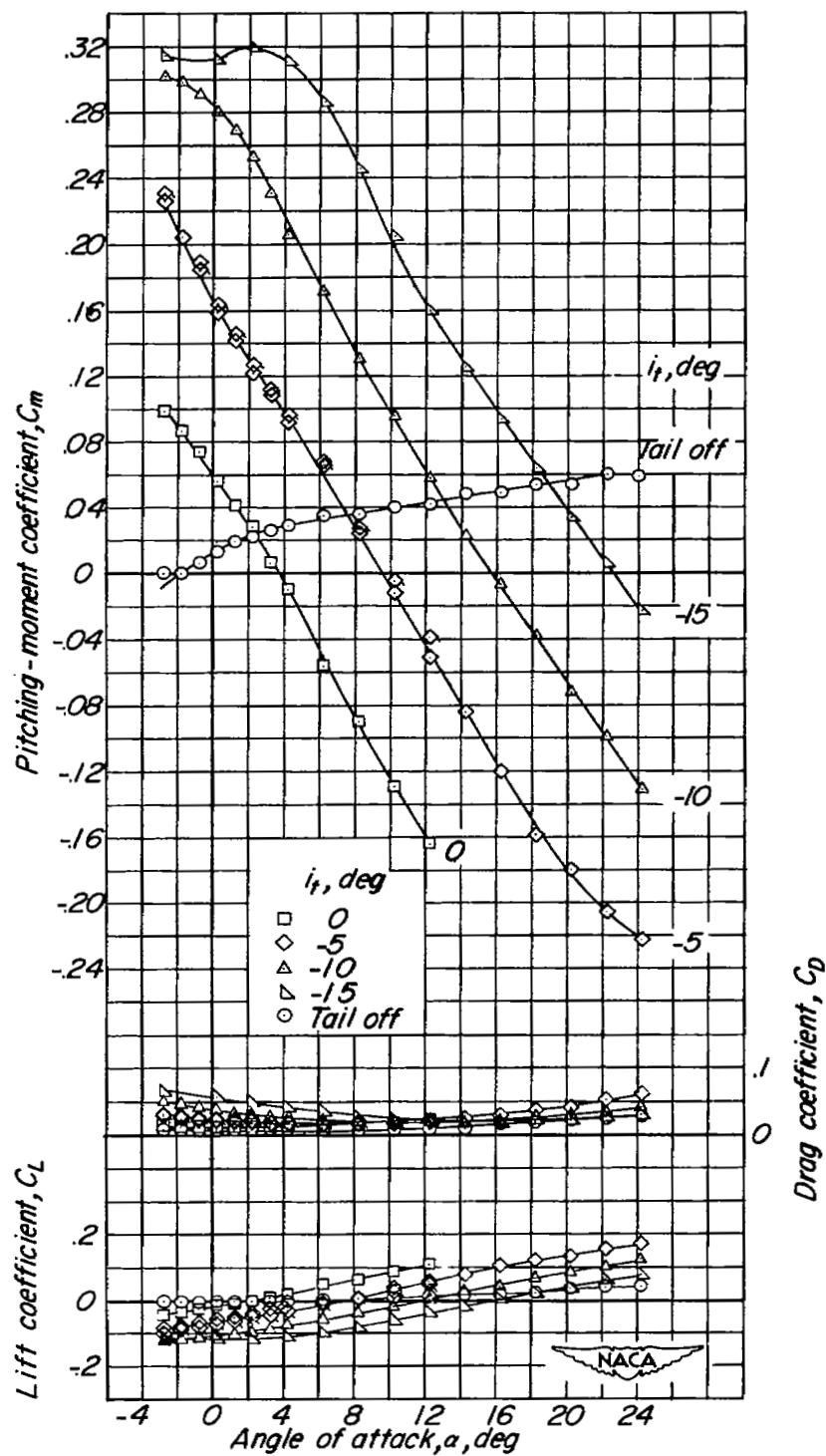
Figure 9.- Wing-off aerodynamic characteristics.
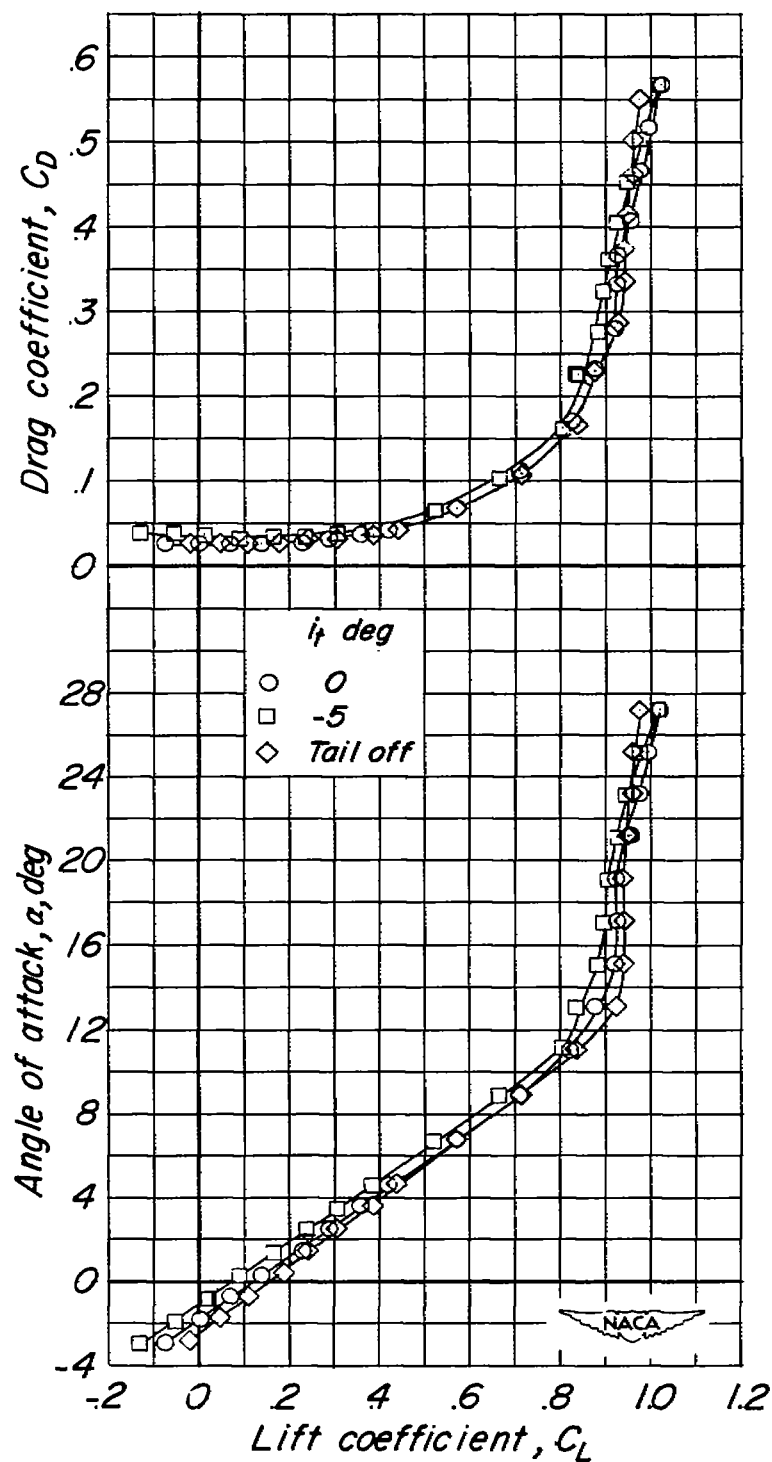
Figure 10.- Effect of stabilizer deflection on the aerodynamic character-
istics of the basic model. $\delta_f = \delta_s = 0^\circ$.
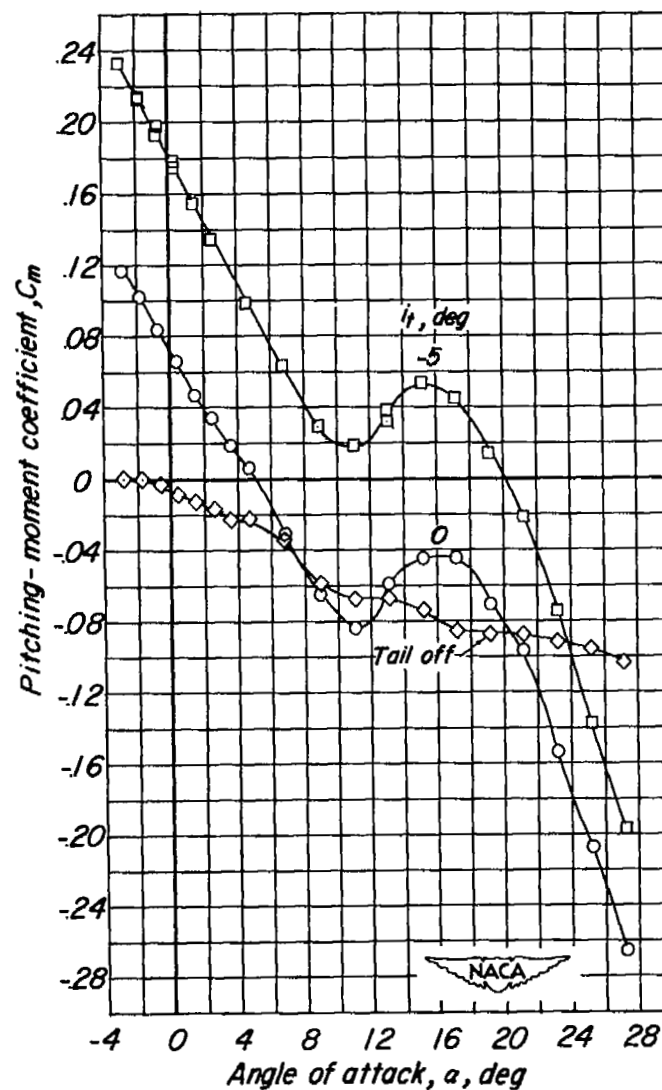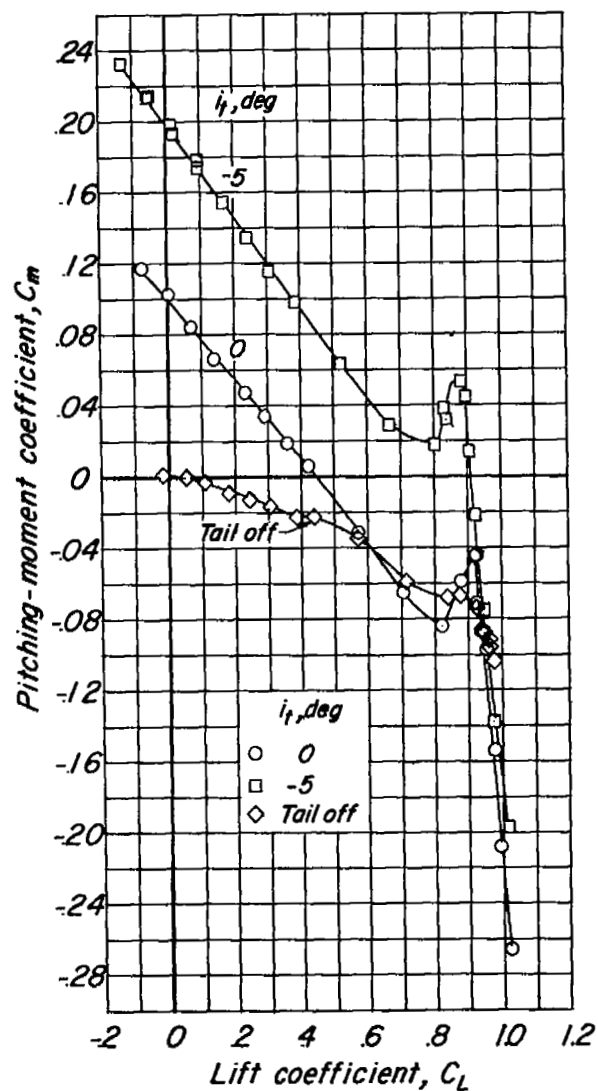
Figure 10.- Concluded.
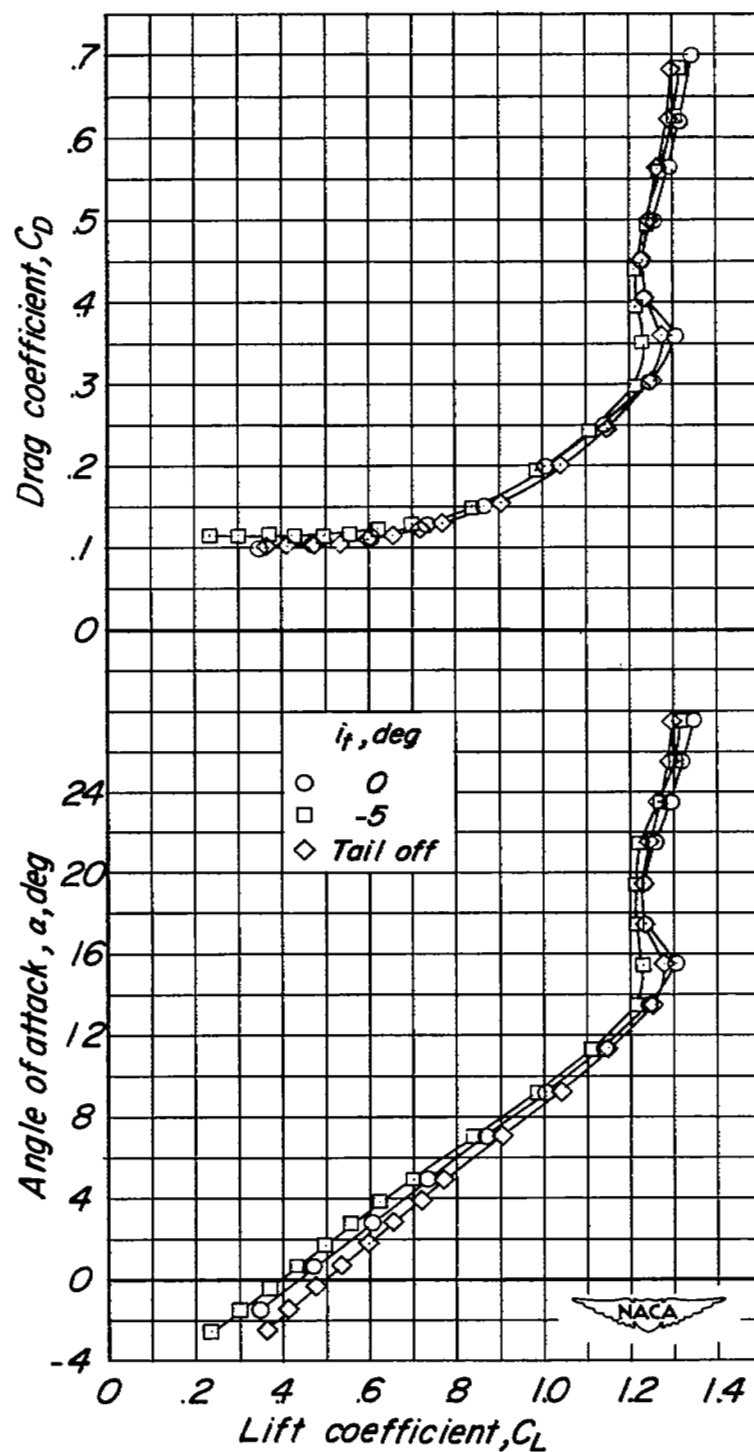
Figure 11.- Effect of stabilizer deflection on the aerodynamic character-istics of the basic model. $\delta_f = 40°$; $\delta_s = 21.7°$.
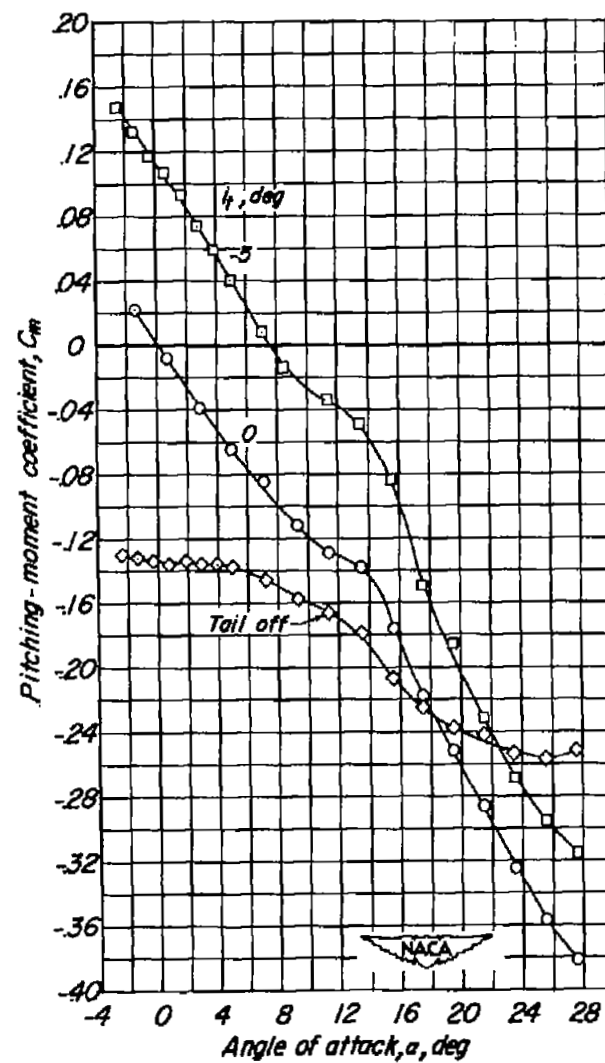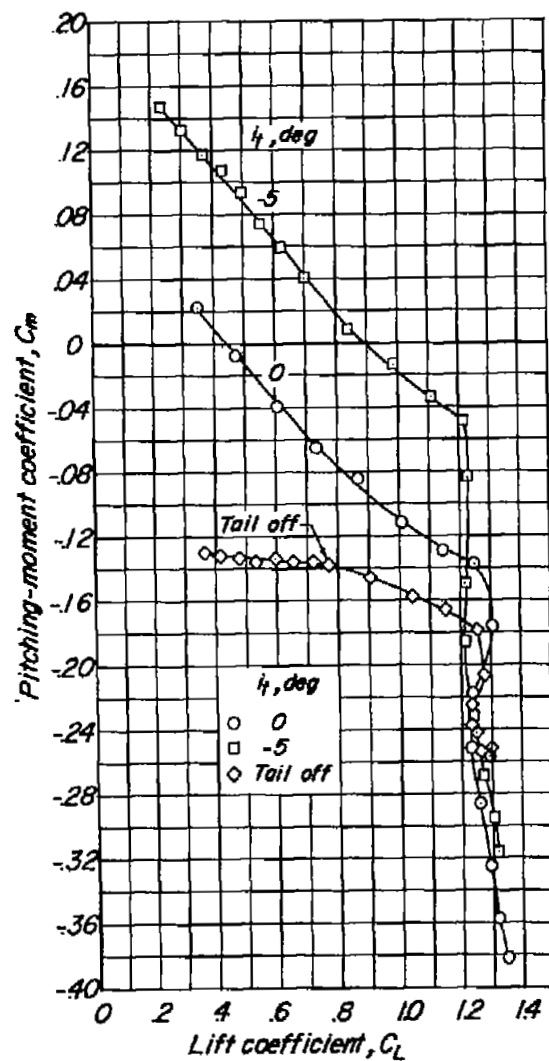
Figure 11.- Concluded.
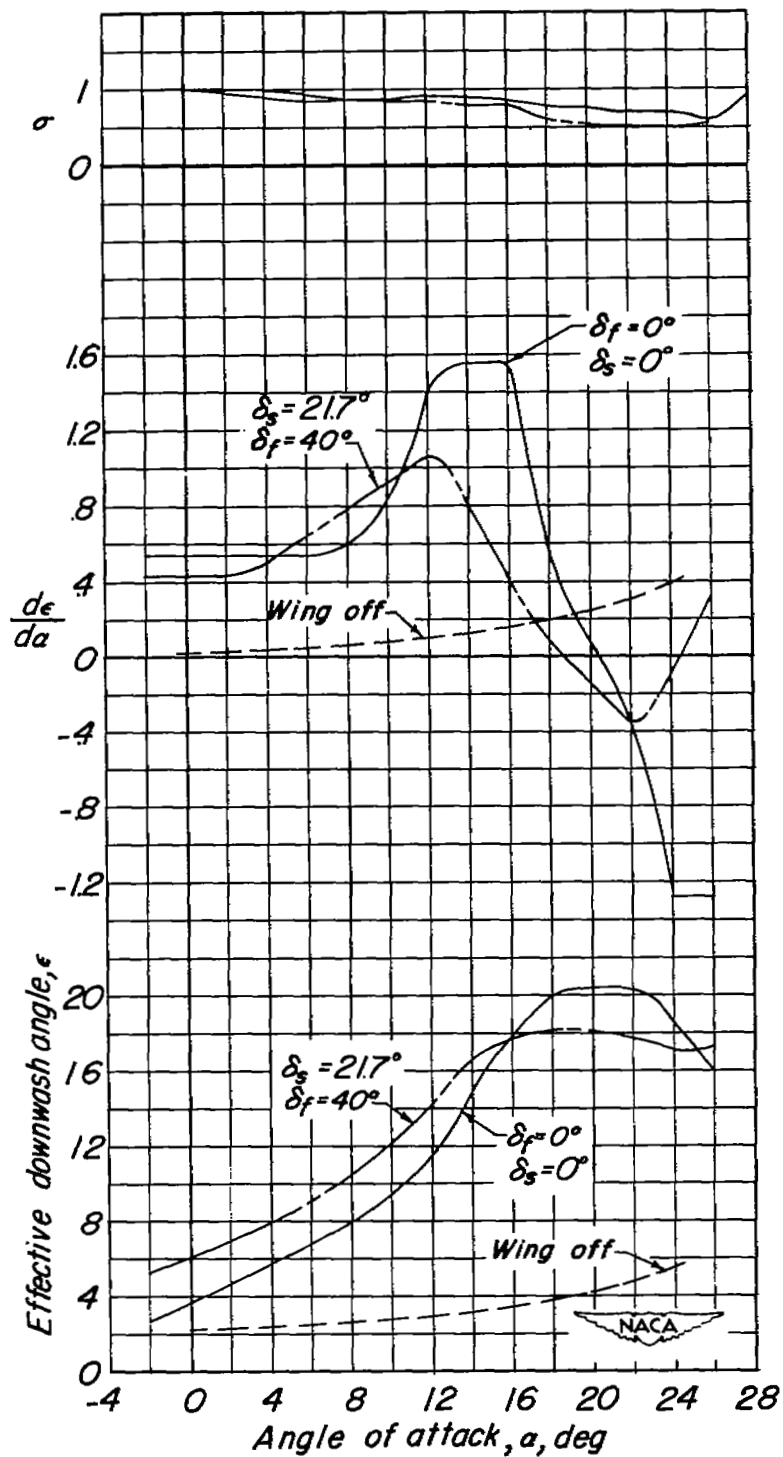
Figure 12.- Summary of effective downwash and tail effectiveness parameter for basic model.
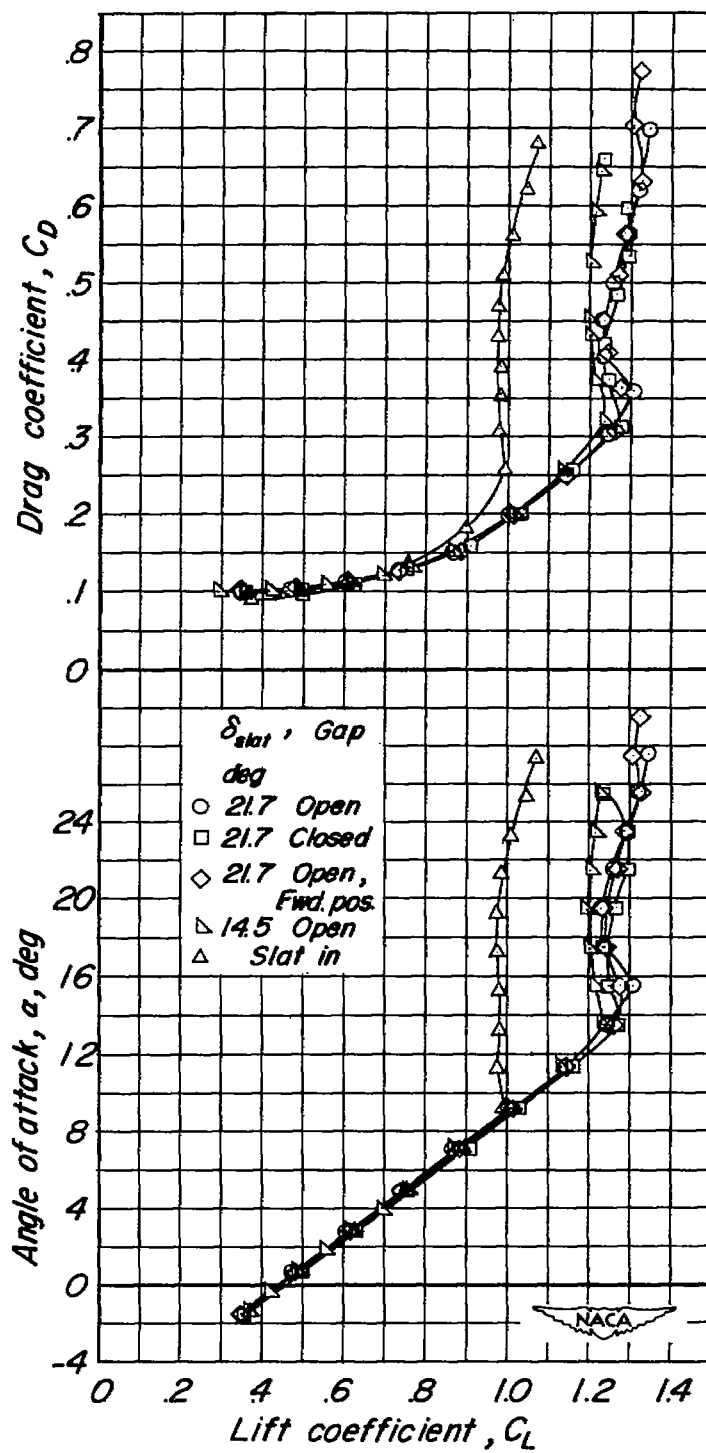
Figure 13.- Effect of slat deflection and modifications. $\delta_f = 40^\circ$; $i_t = 0^\circ$.
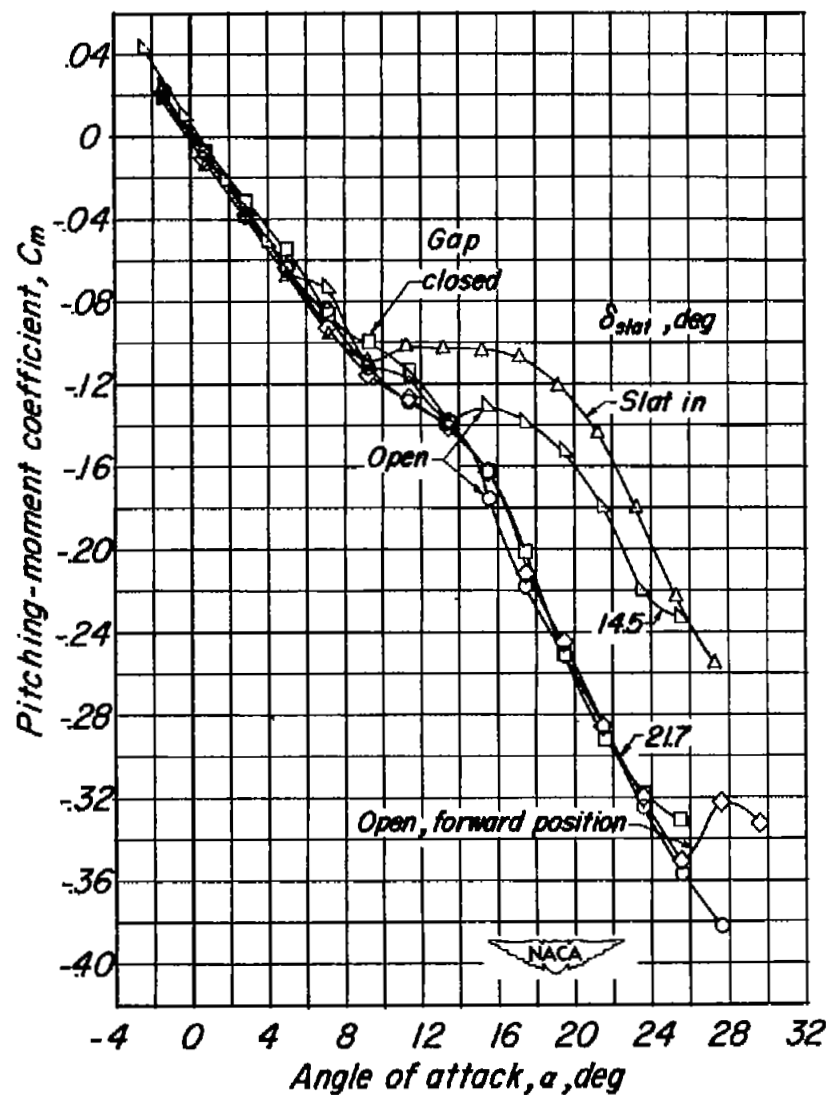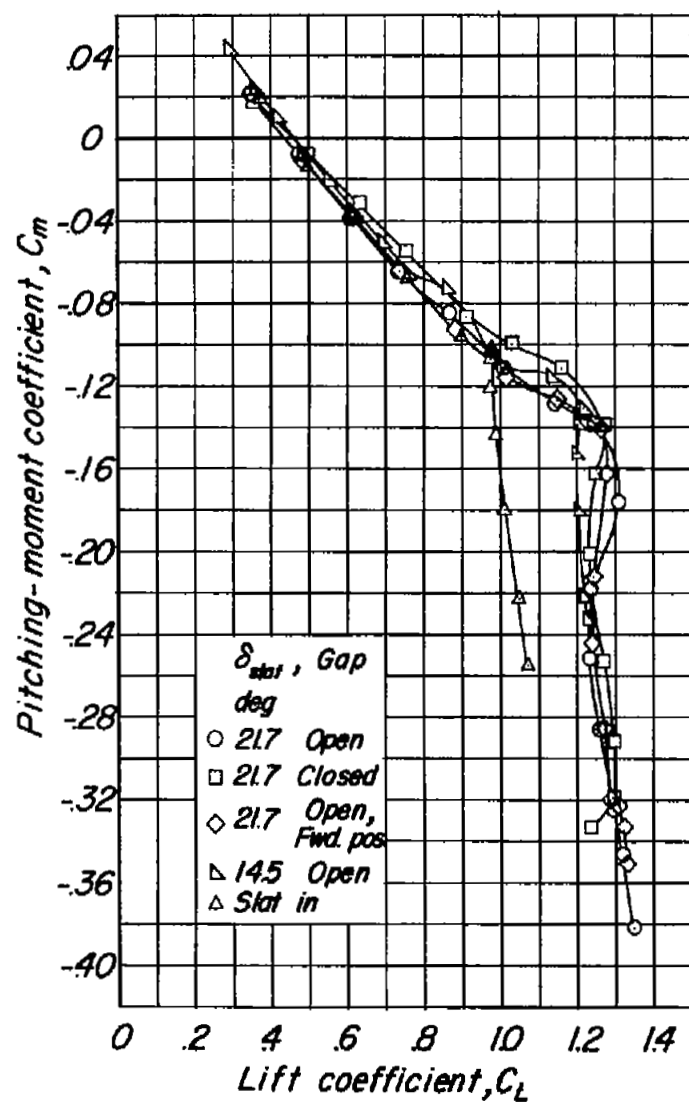
Figure 13.- Concluded.
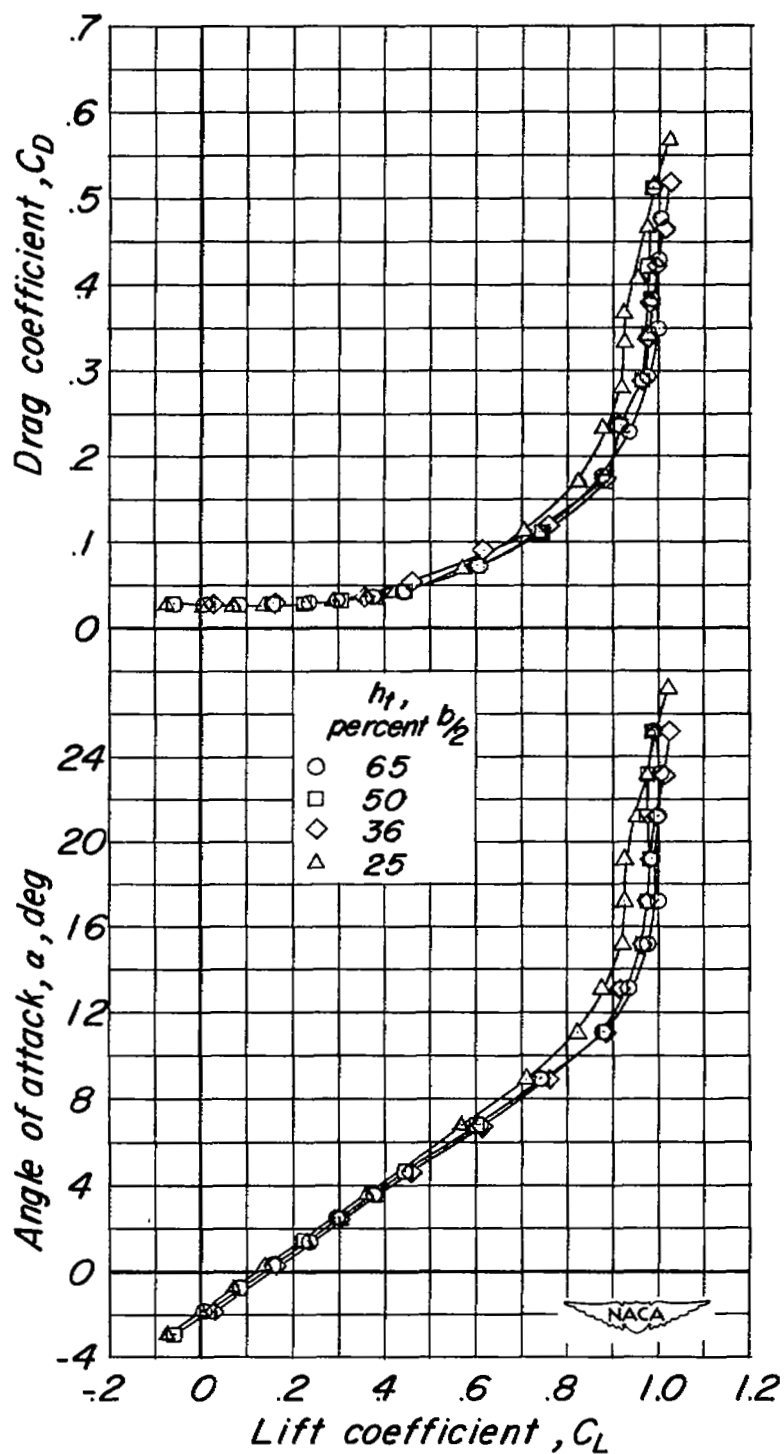
Figure 14.- Effect of raising the horizontal tail on the aerodynamic characteristics of the model. $\delta_f = \delta_s = i_t = 0°$.
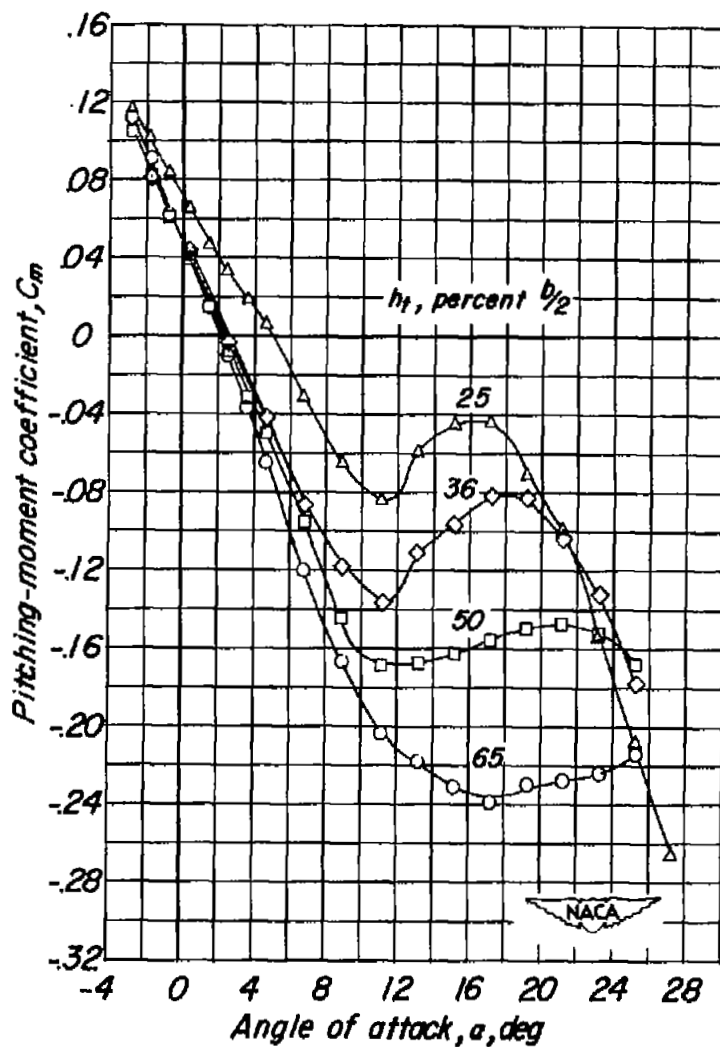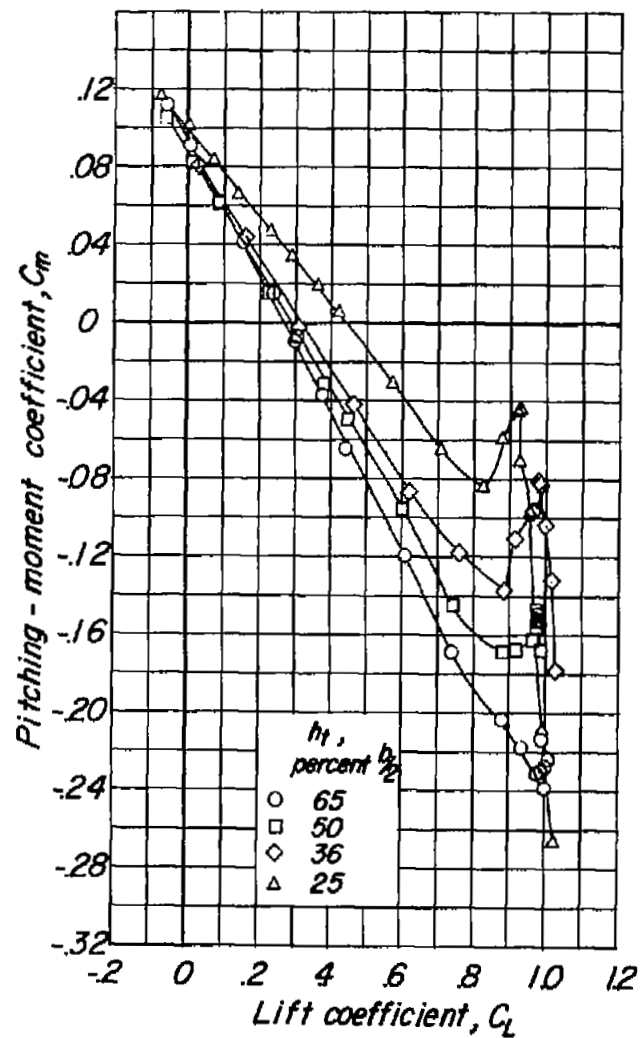
Figure 14.- Concluded.
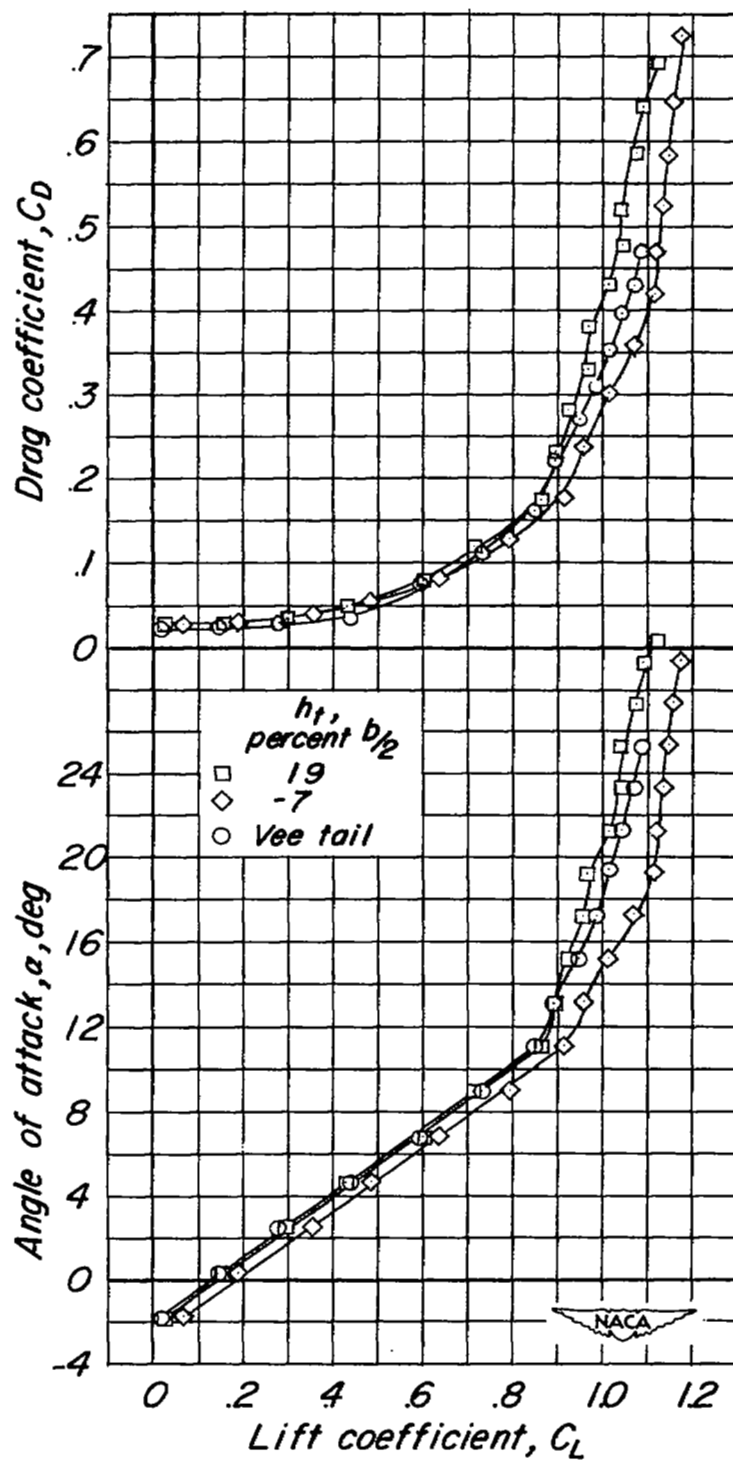
Figure 15.- Effect of lowering the horizontal tail on the aerodynamic characteristics of the model. $\delta_f = \delta_g = i_t = 0^\circ$.
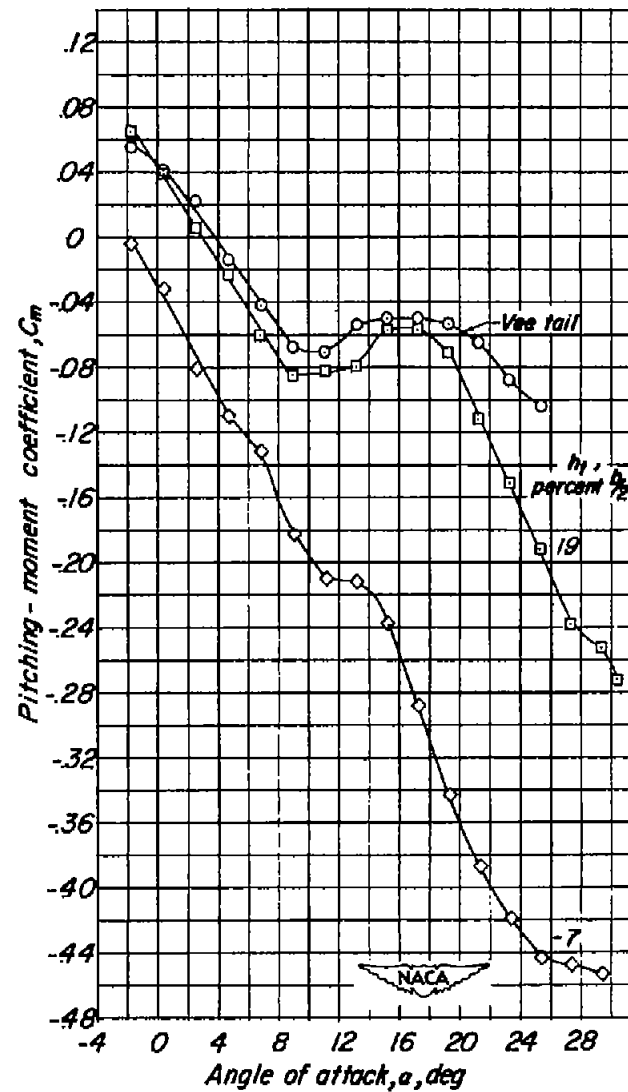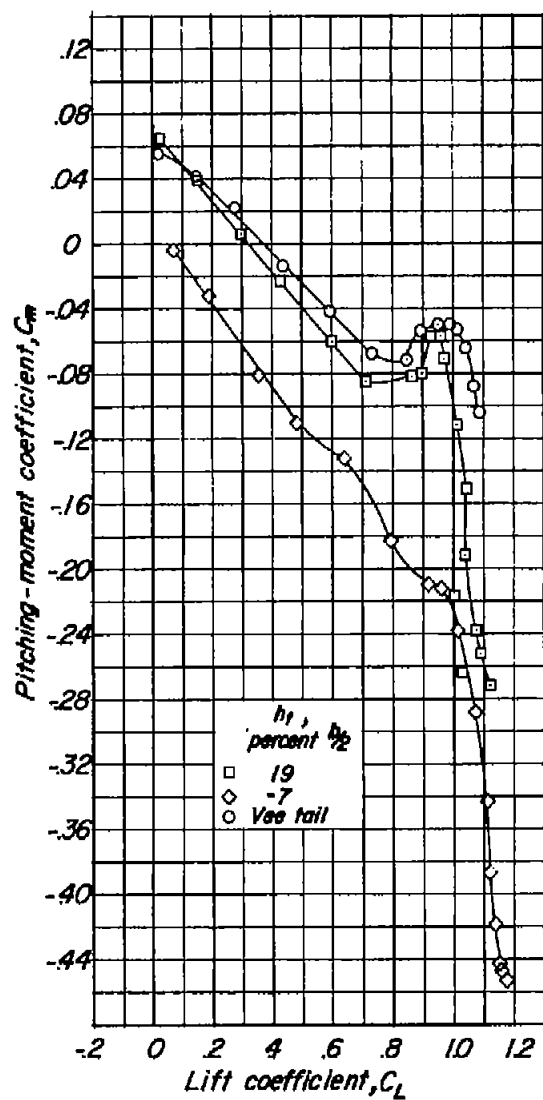
Figure 15.- Concluded.
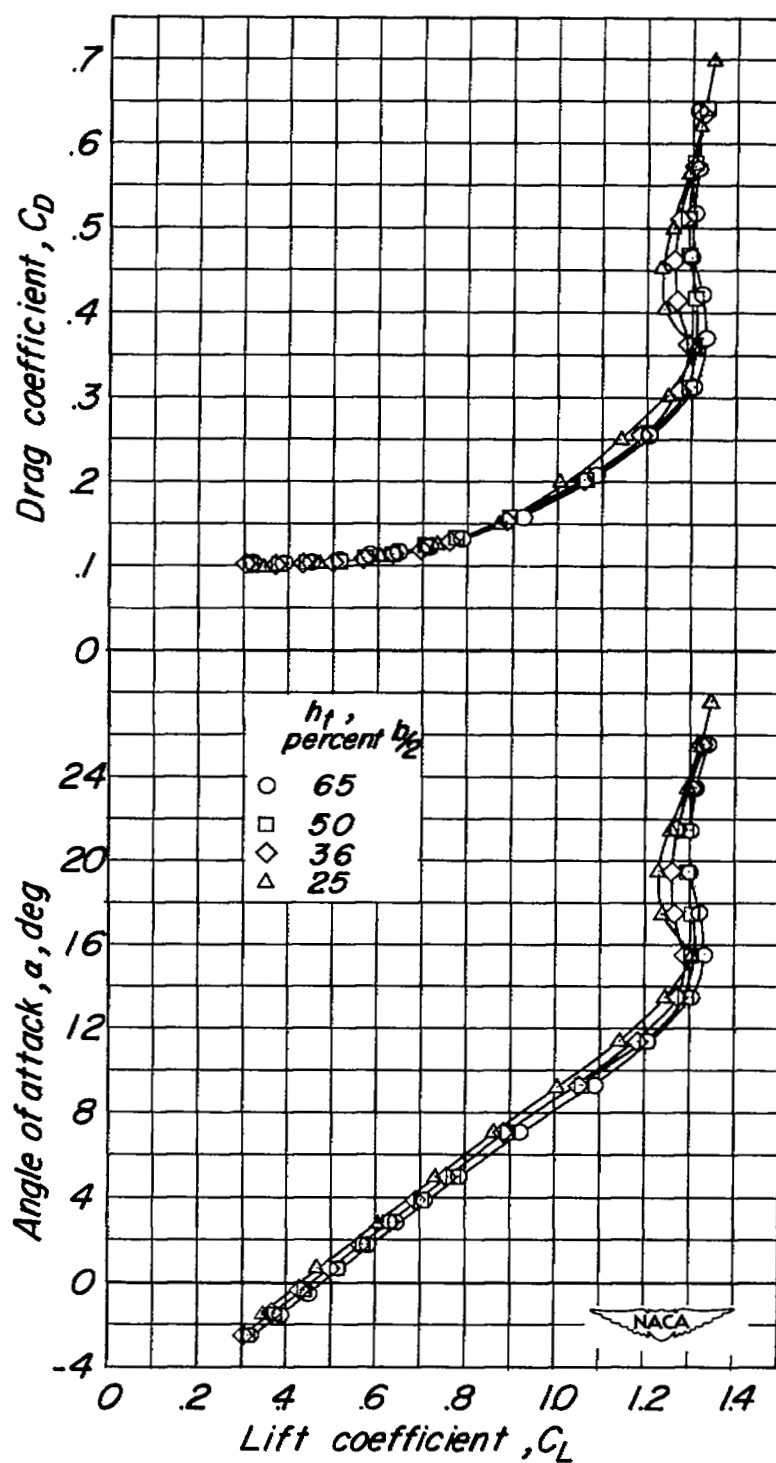
Figure 16.- Effect of raising the horizontal tail on the aerodynamic characteristics of the model. $\delta_f = 40^\circ$; $\delta_s = 21.7^\circ$; $i_t = 0^\circ$.
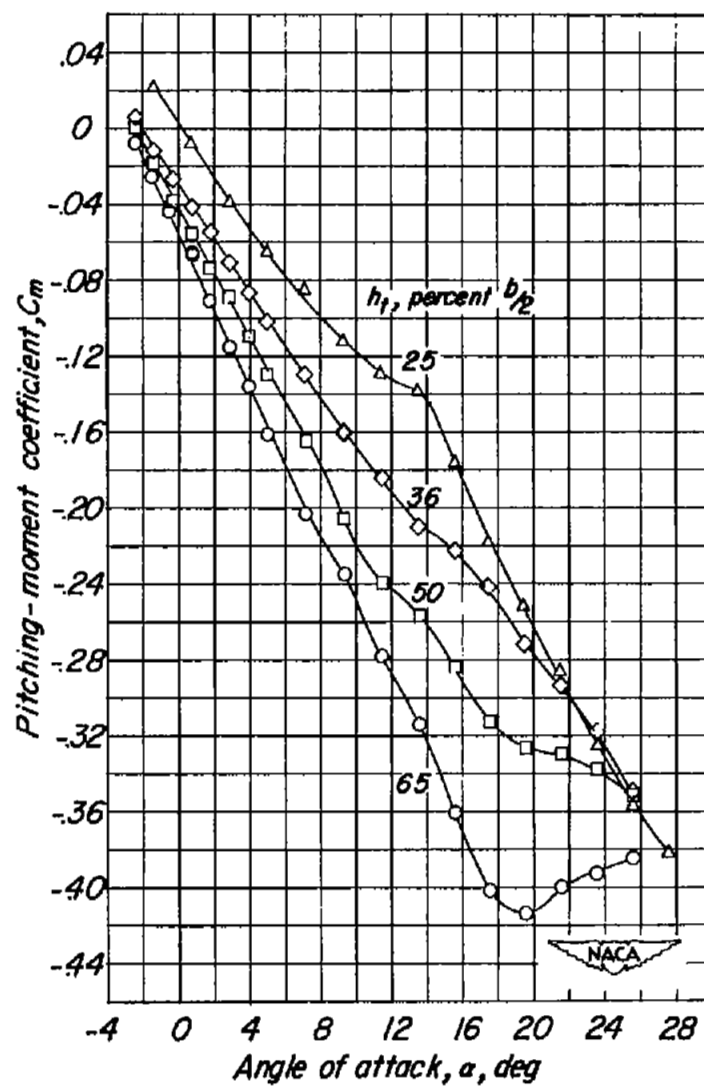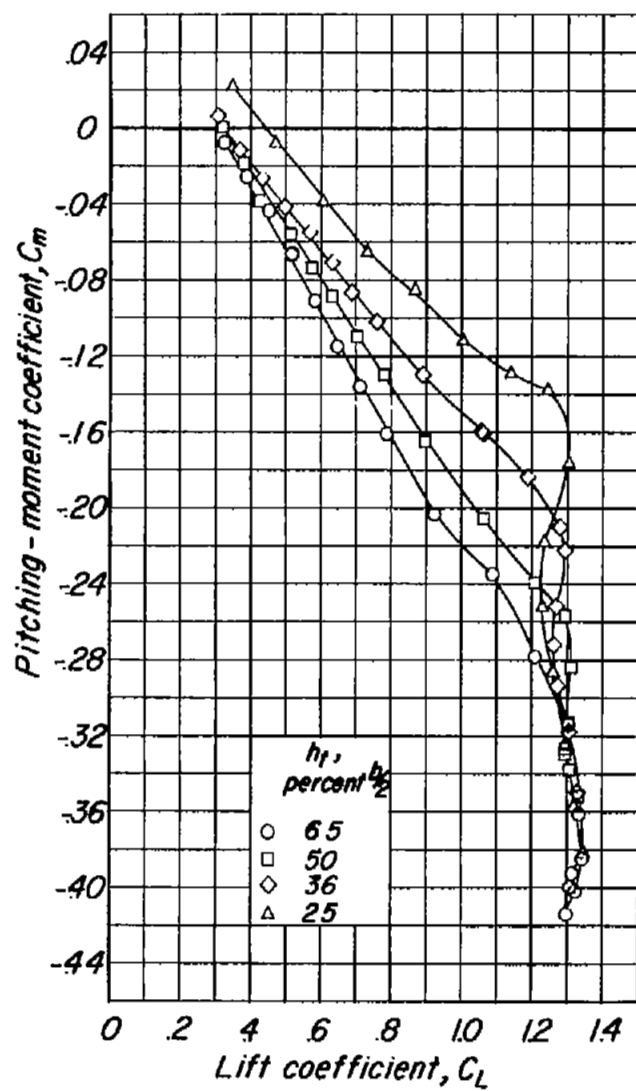
Figure 16.- Concluded.
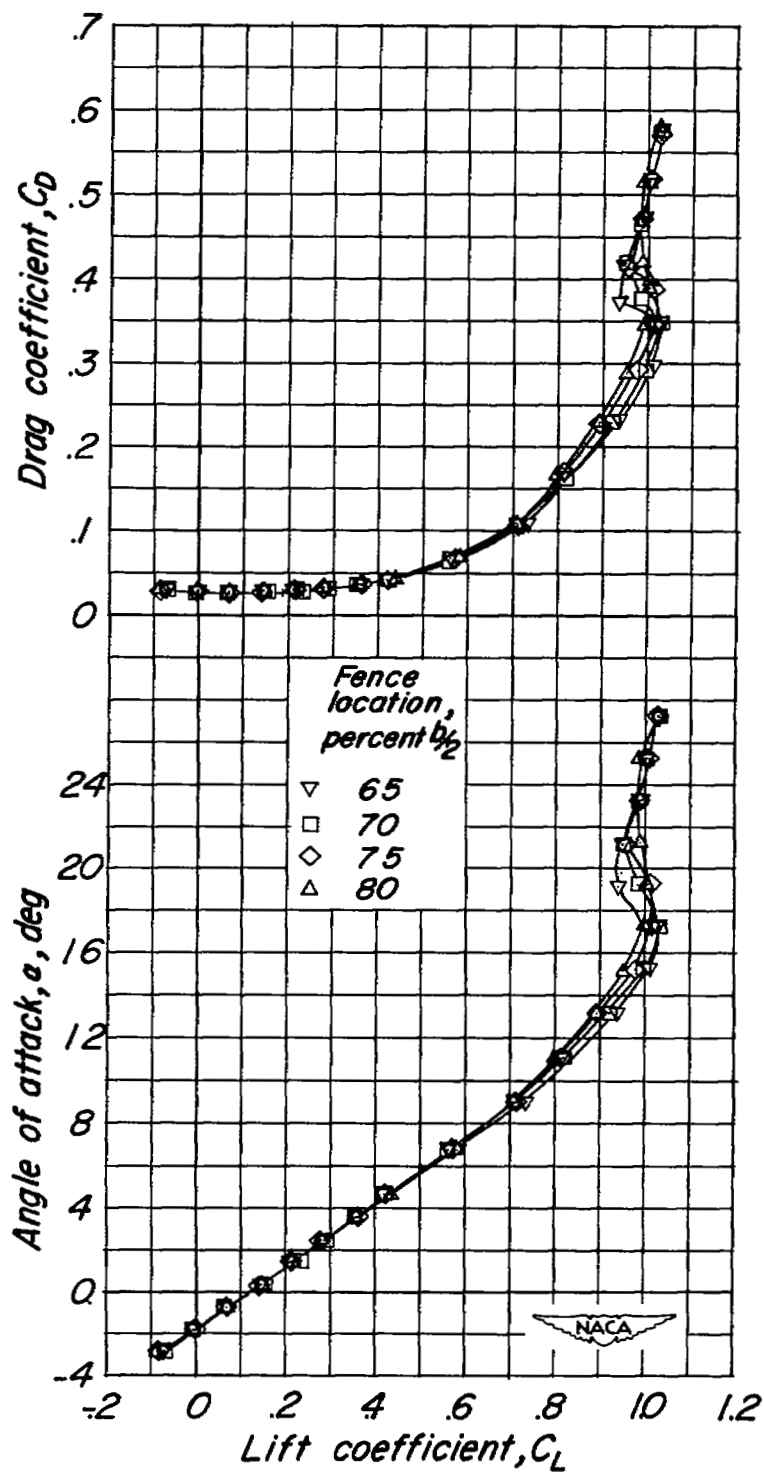
Figure 17.- Effect of spanwise location of wing fence 2. $\delta_f = \delta_s = i_t = 0^\circ$.
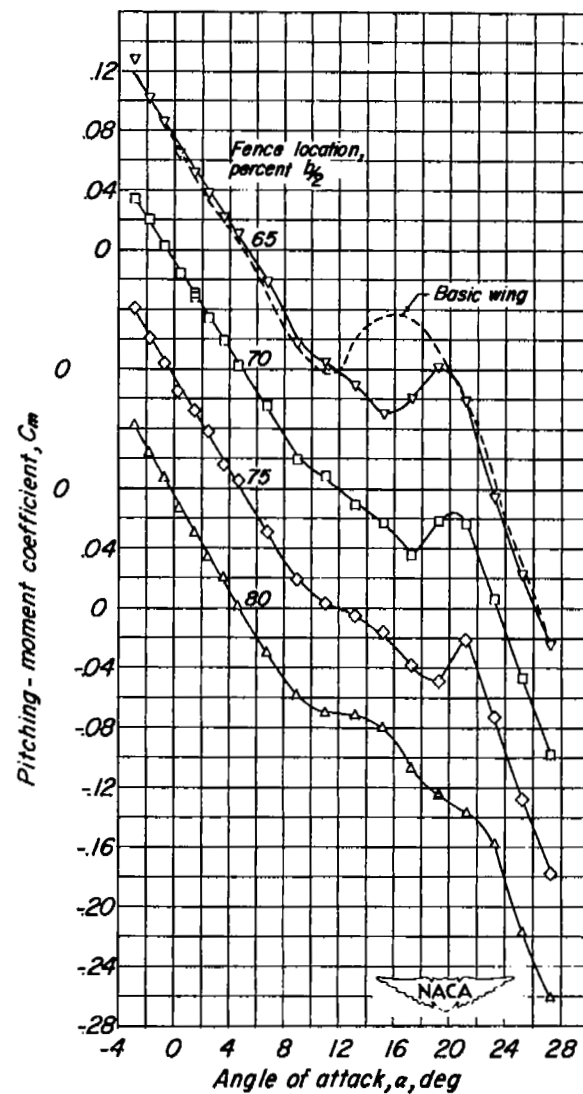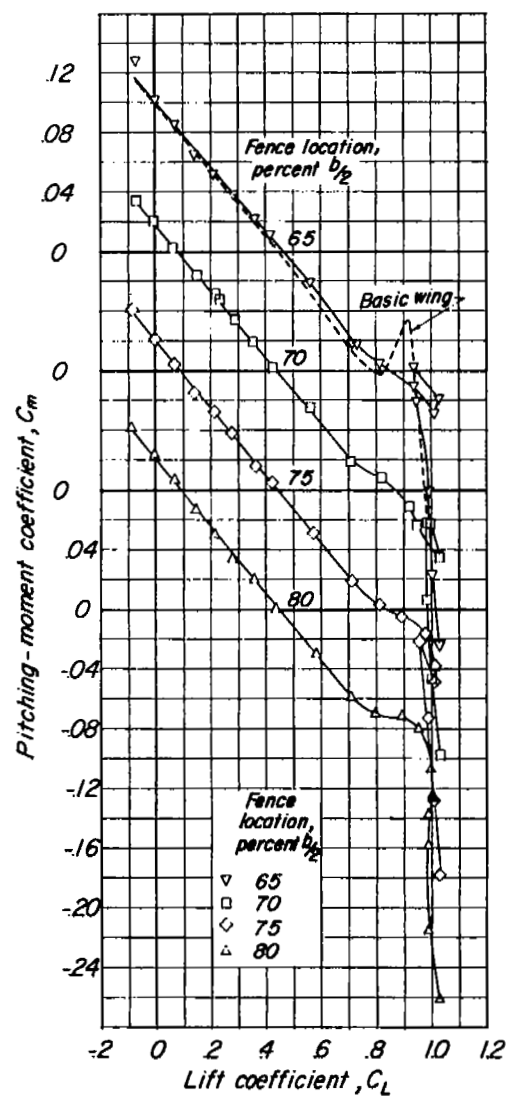
Figure 17.- Concluded.
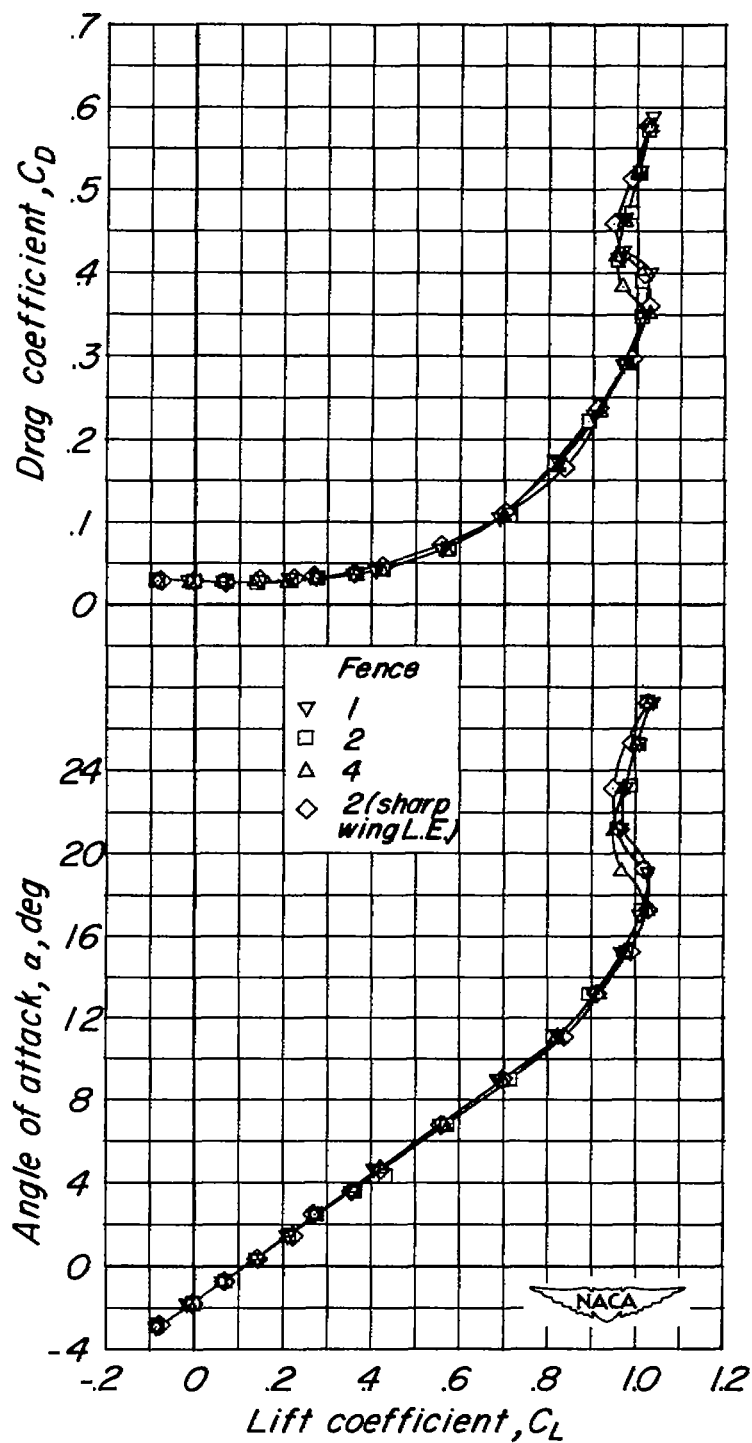
Figure 18.- Effect of fence size with fences located at 75 percent semispan. $\delta_f = \delta_s = i_t = 0°$.
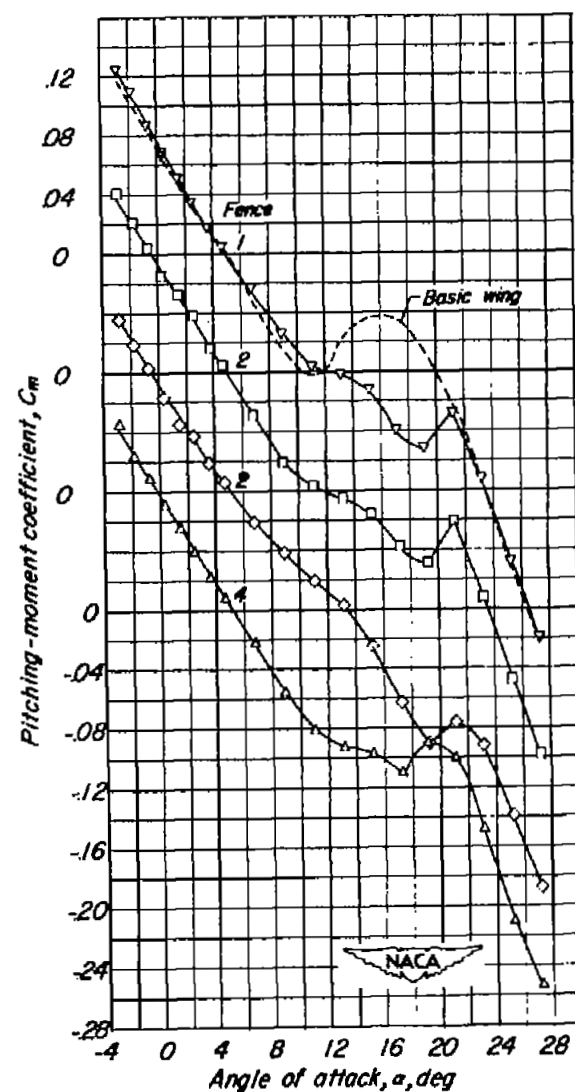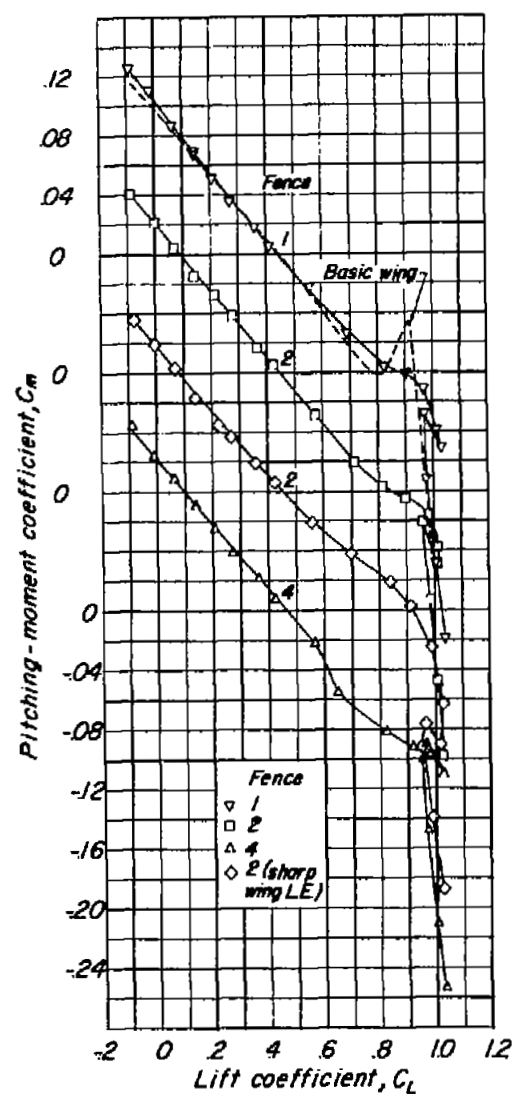
Figure 18.- Concluded.
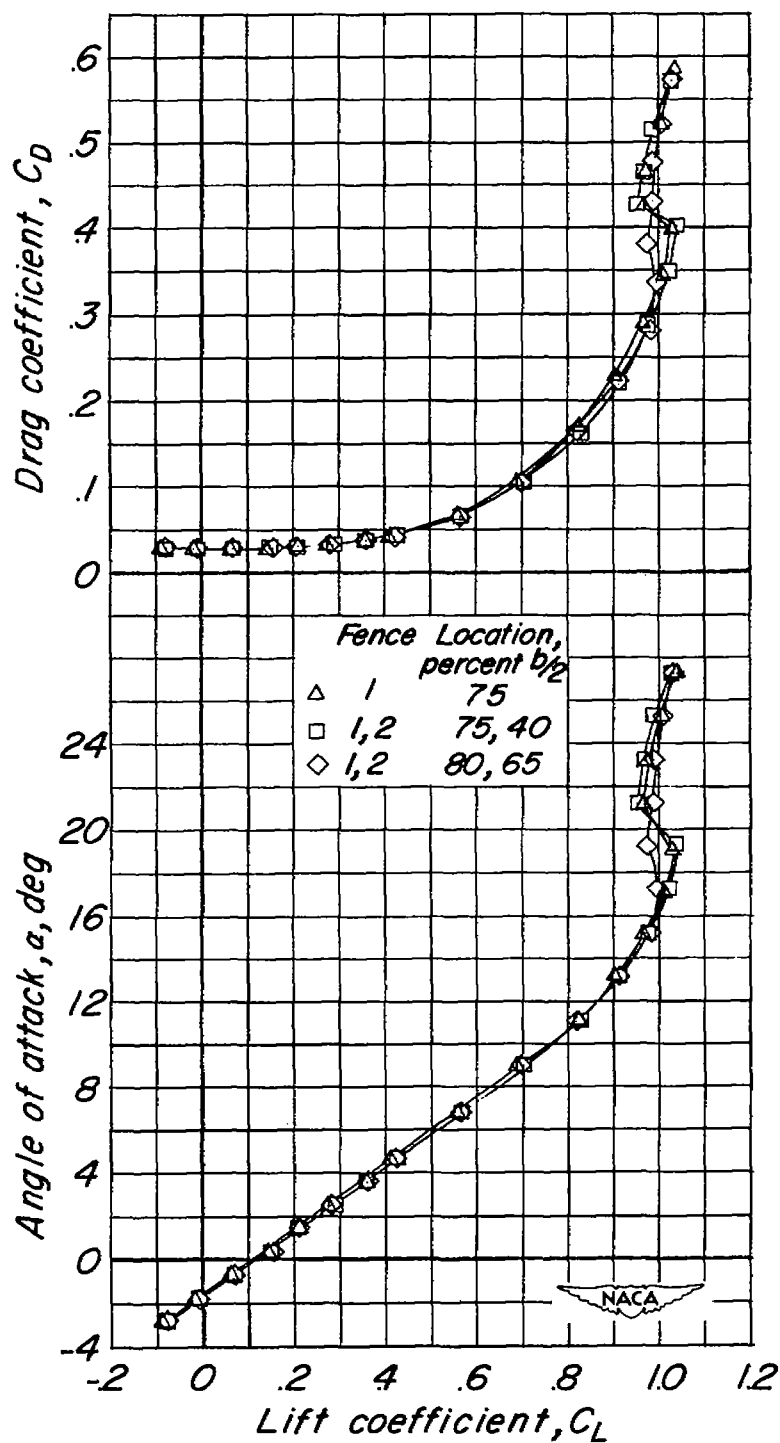
Figure 19.- Effect of multiple fences and spanwise location of fences. $\delta_f = \delta_s = i_t = 0^\circ$.
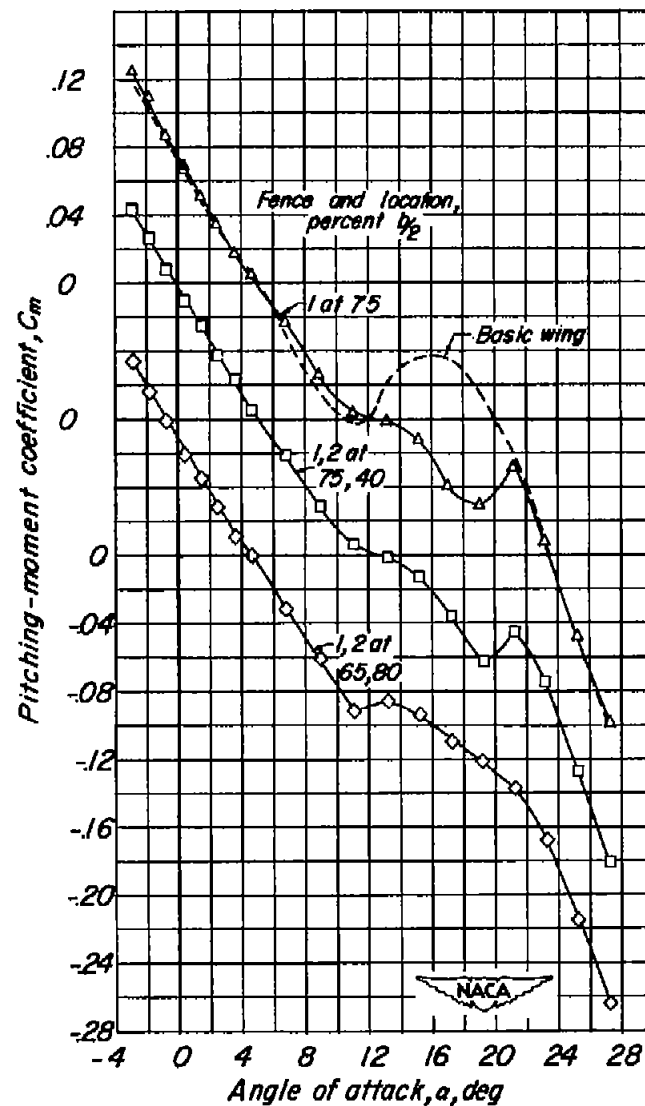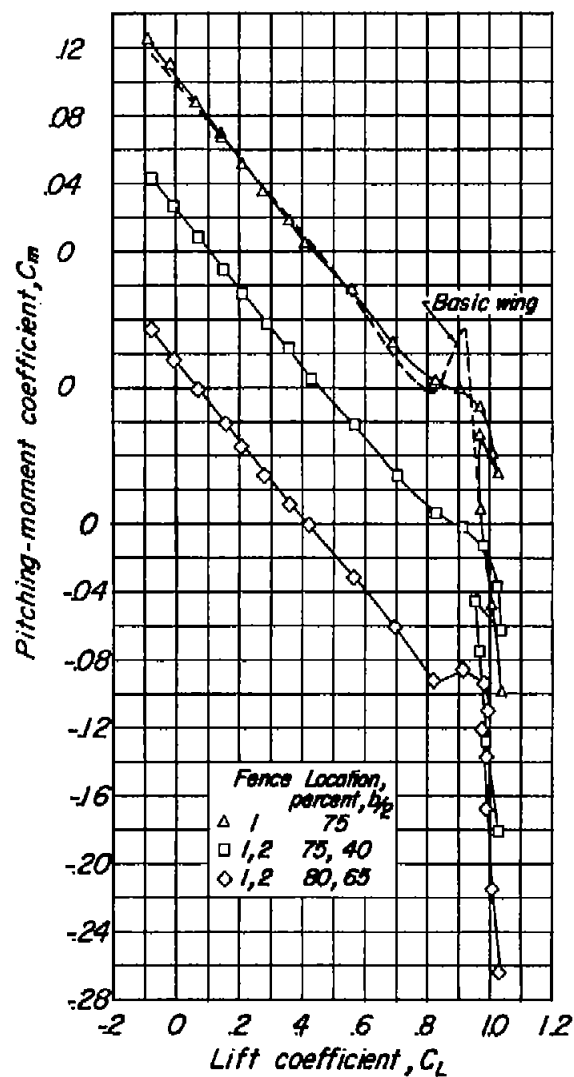
Figure 19.- Concluded.
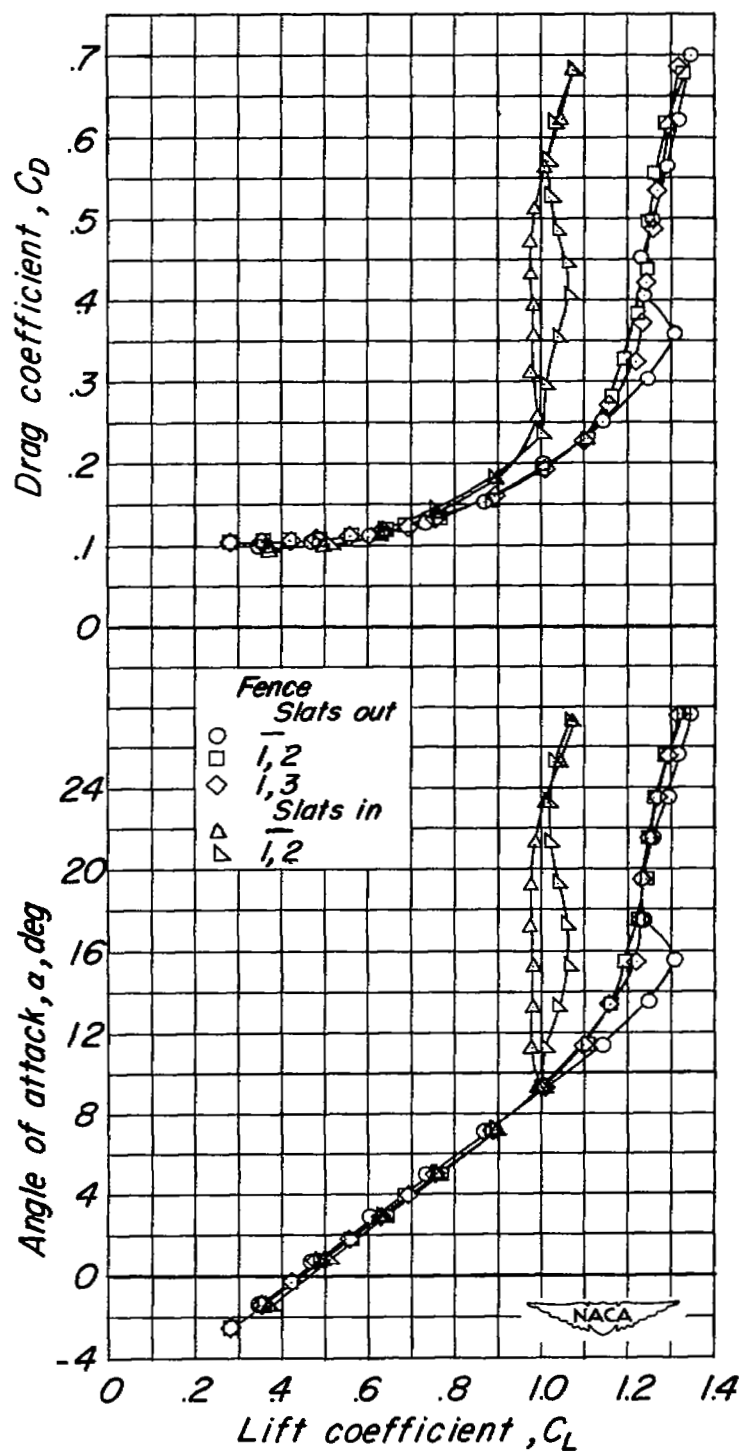
Figure 20.- Effect of multiple fences located at 75 and 40 percent semispan.
$\delta_f = 40°$; $\delta_s = 21.7°$; $i_t = 0°$.
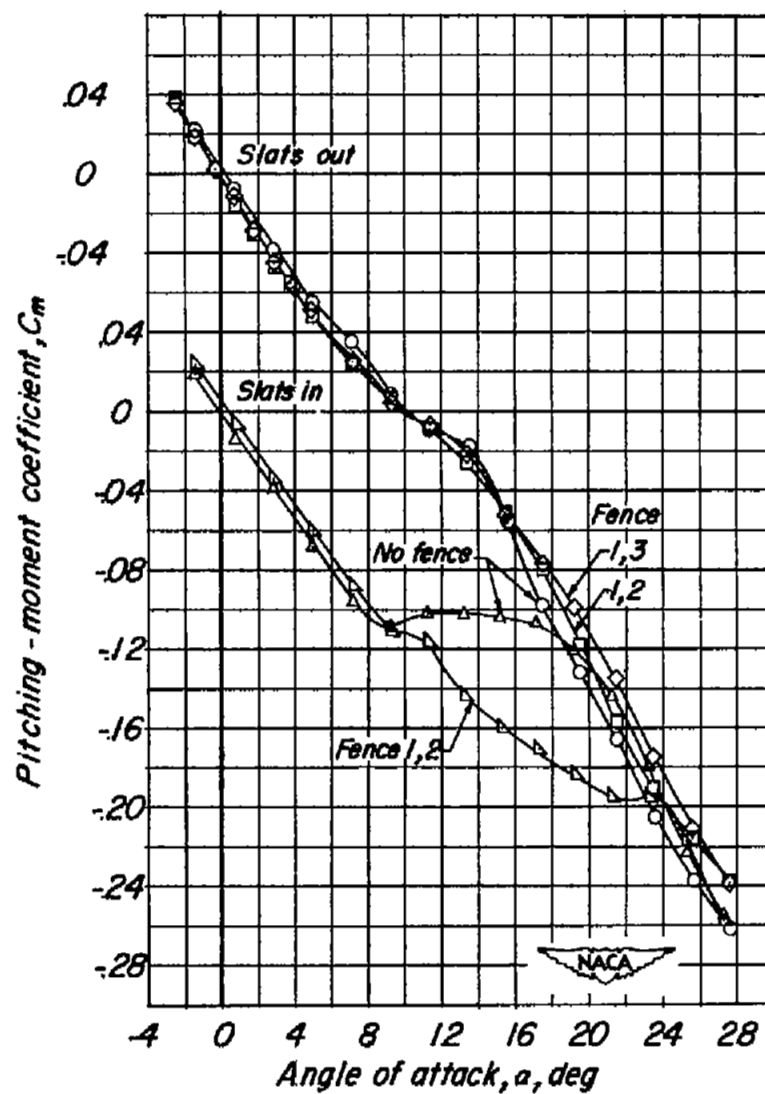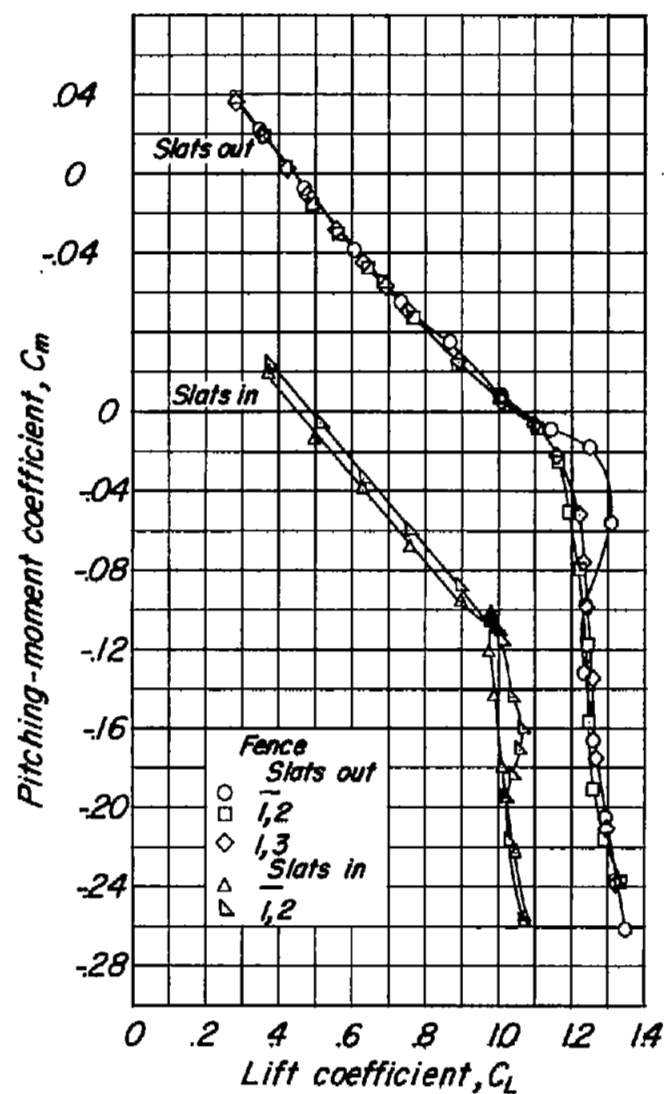
Figure 20.- Concluded.
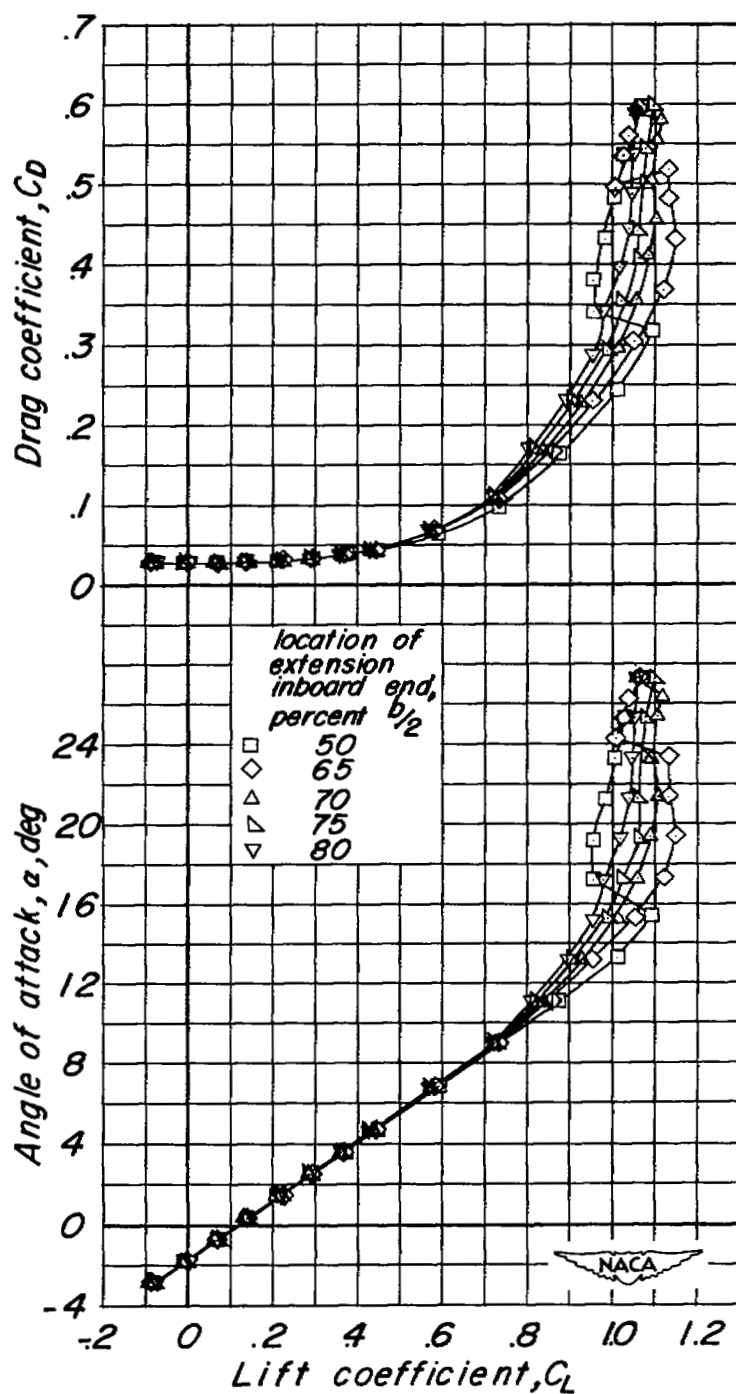
Figure 21.- Effect of inboard-end location of 0.10c leading-edge chord-extensions having the outboard end at 94 percent semispan. $\delta_f = \delta_s = i_t = 0^\circ$.
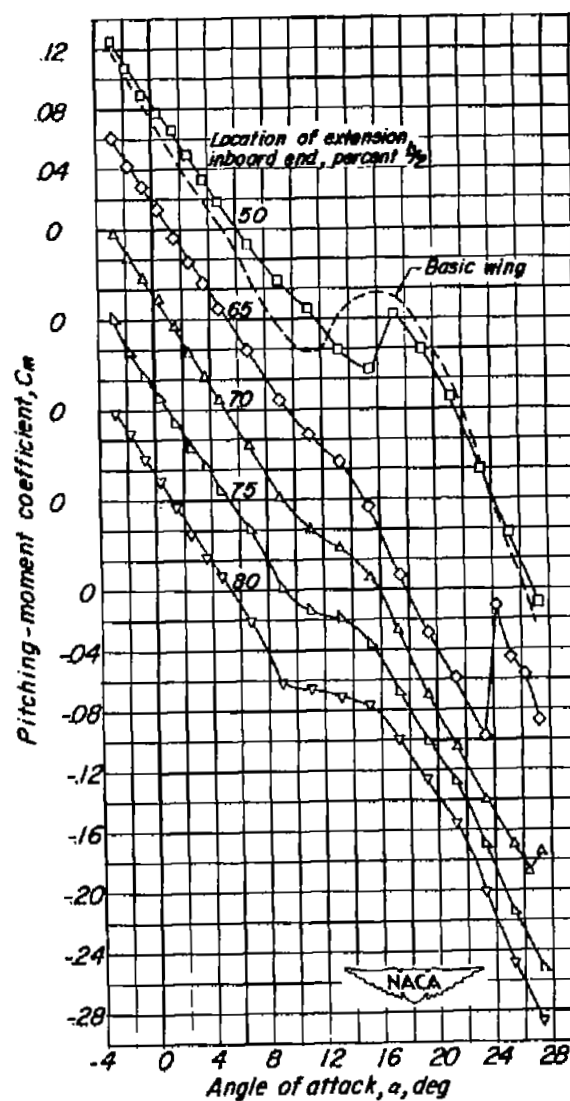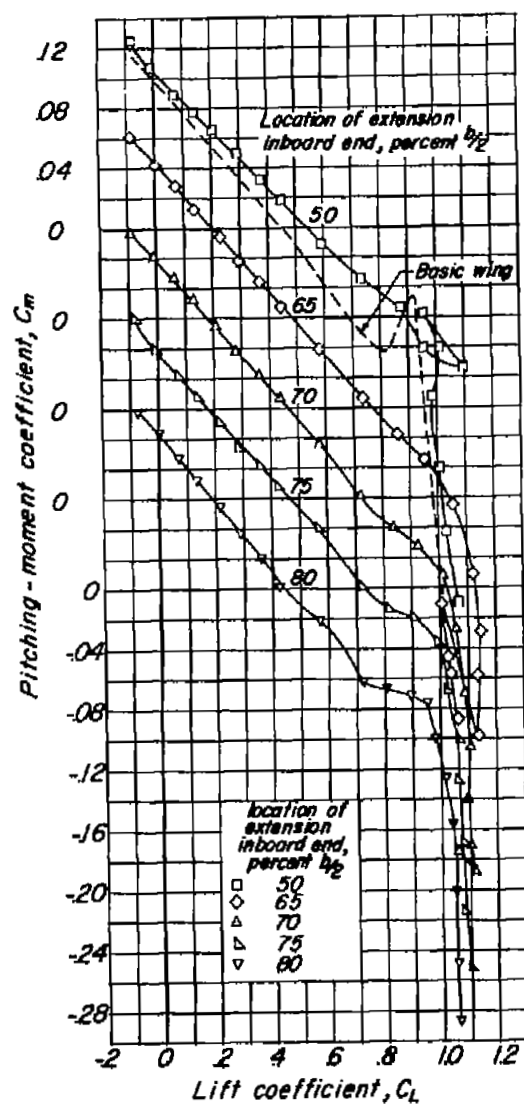
Figure 21.- Concluded.
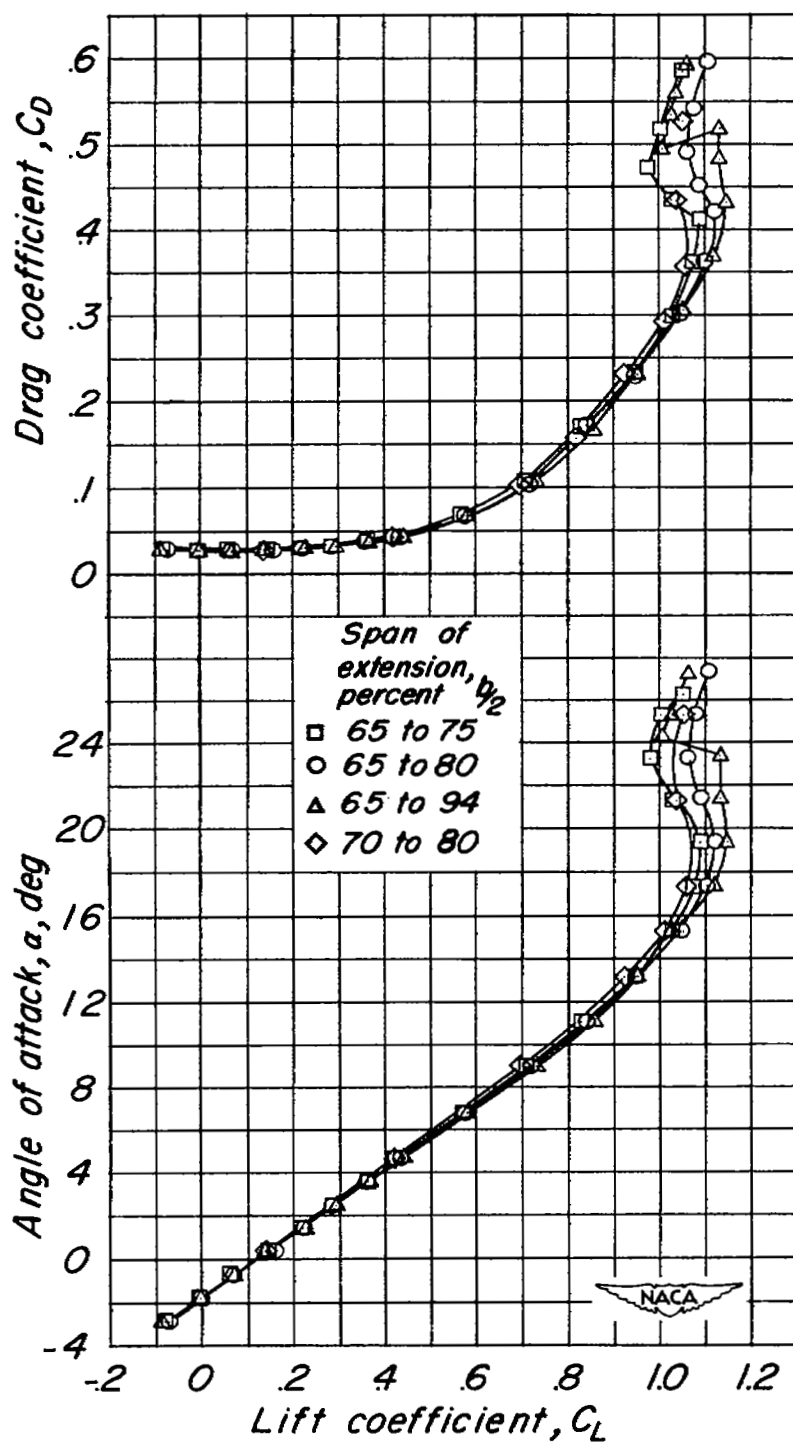
Figure 22.- Effect of spanwise extent of 0.10c leading-edge chord-
extensions. $\delta_f = \delta_s = i_t = 0°$.
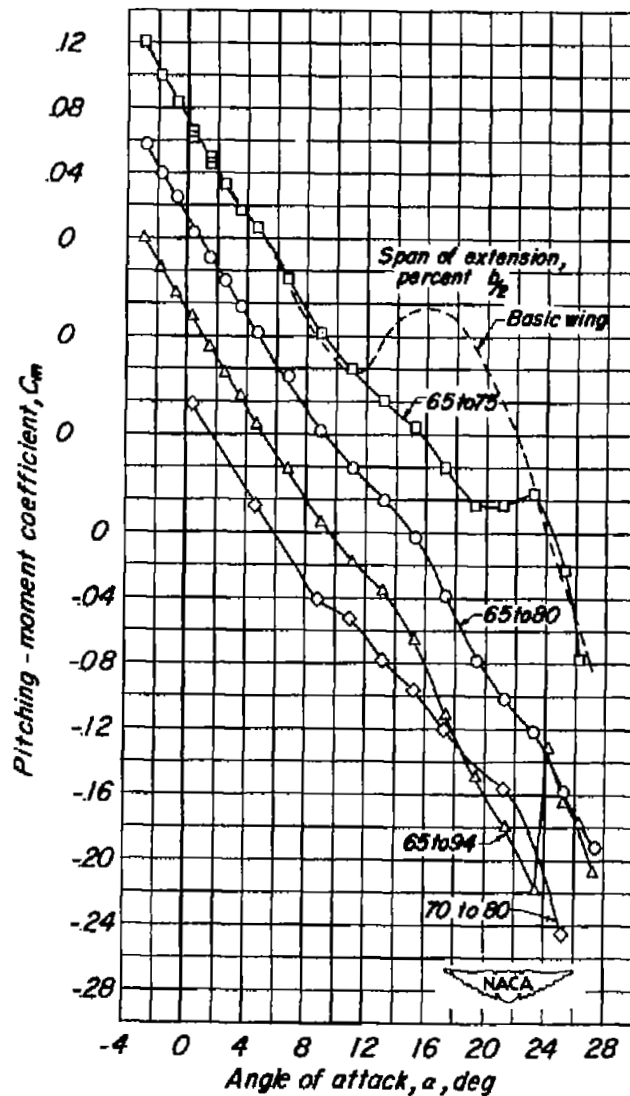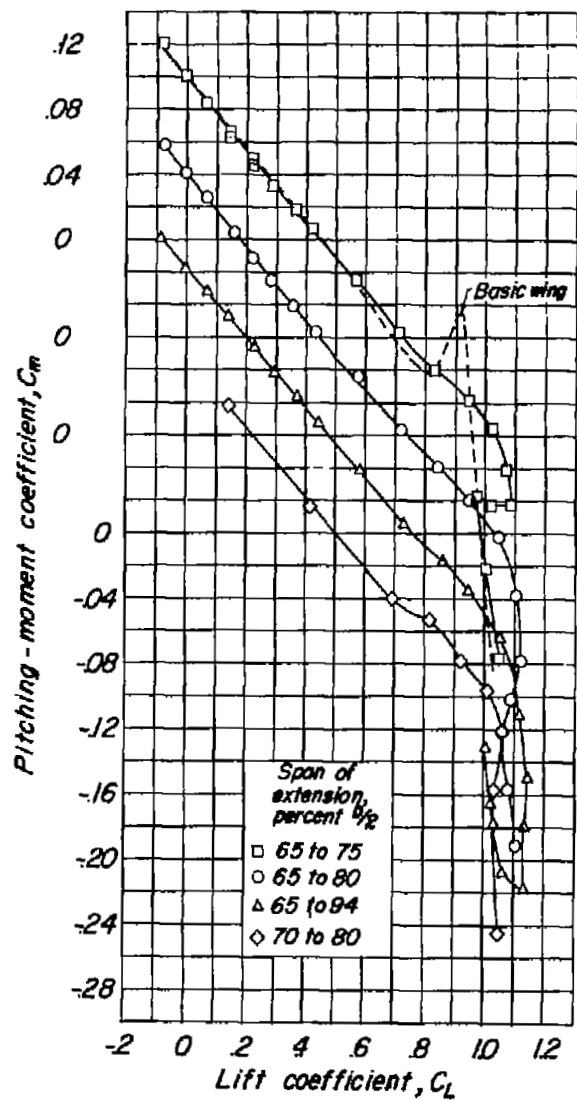
Figure 22.- Concluded.
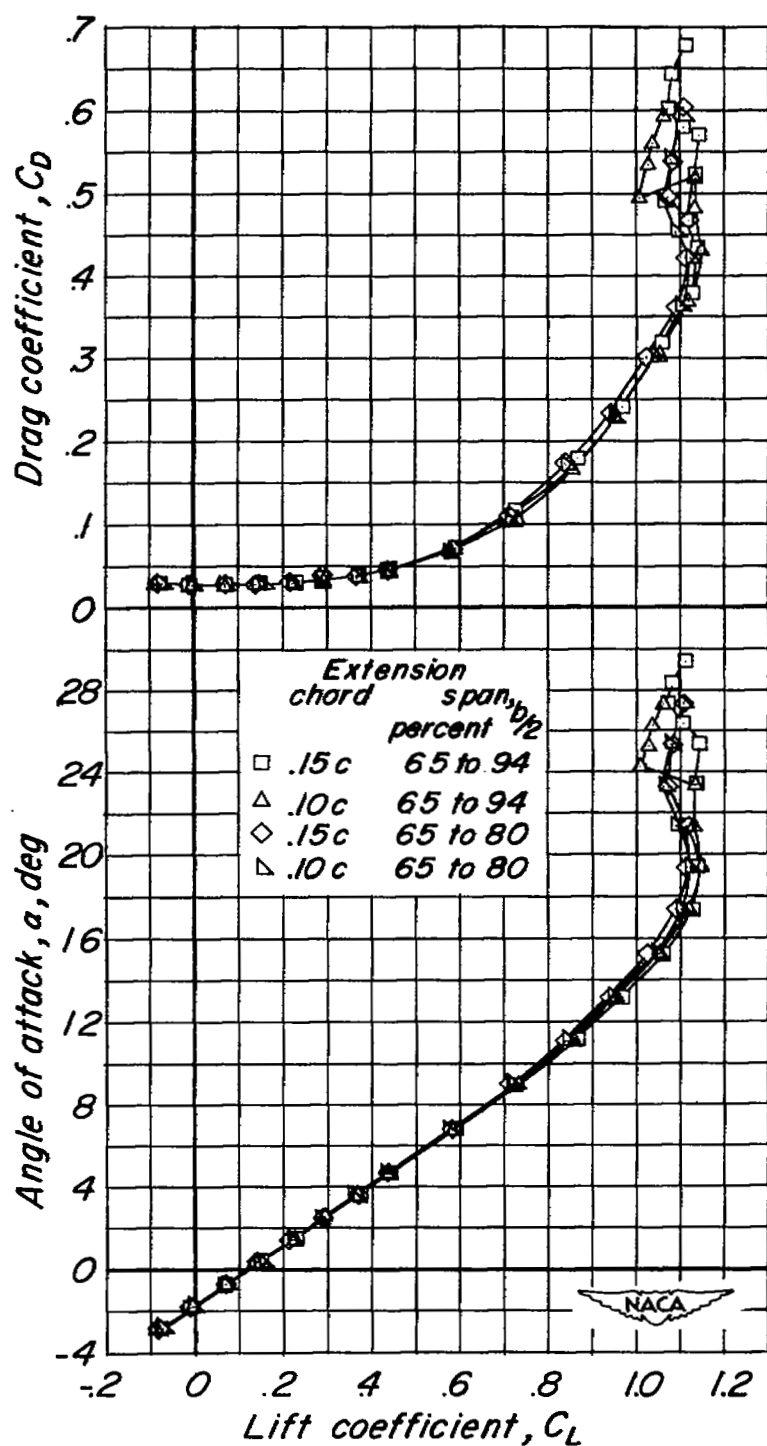
Figure 23.- Effect of chordwise extent of leading-edge chord-extensions. $\delta_f = \delta_s = i_t = 0°$.
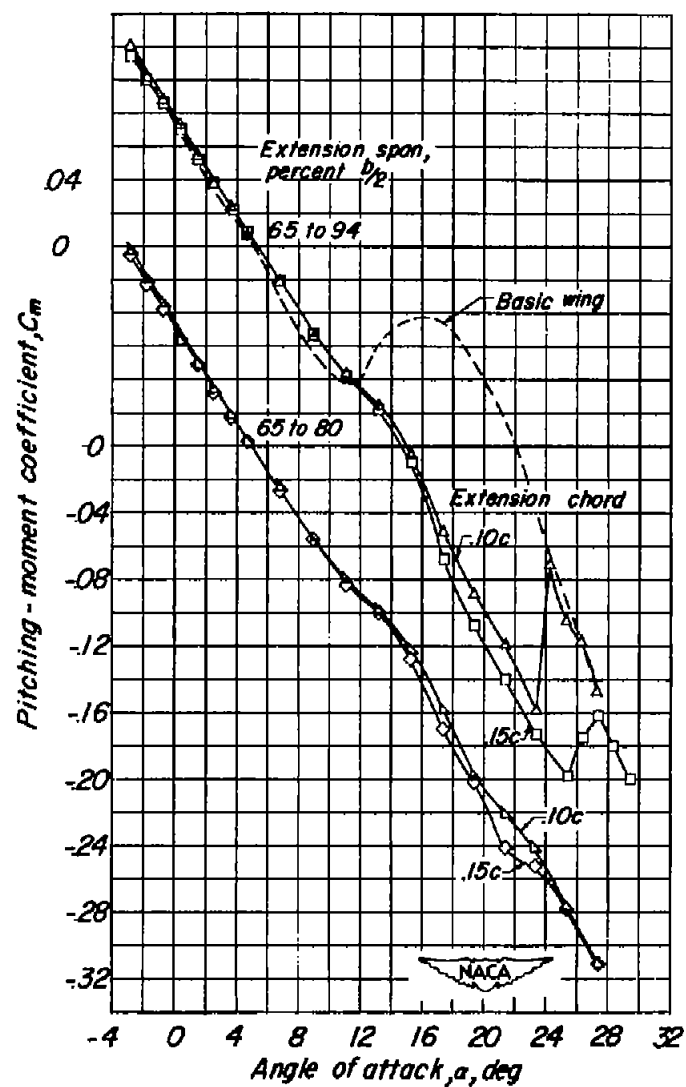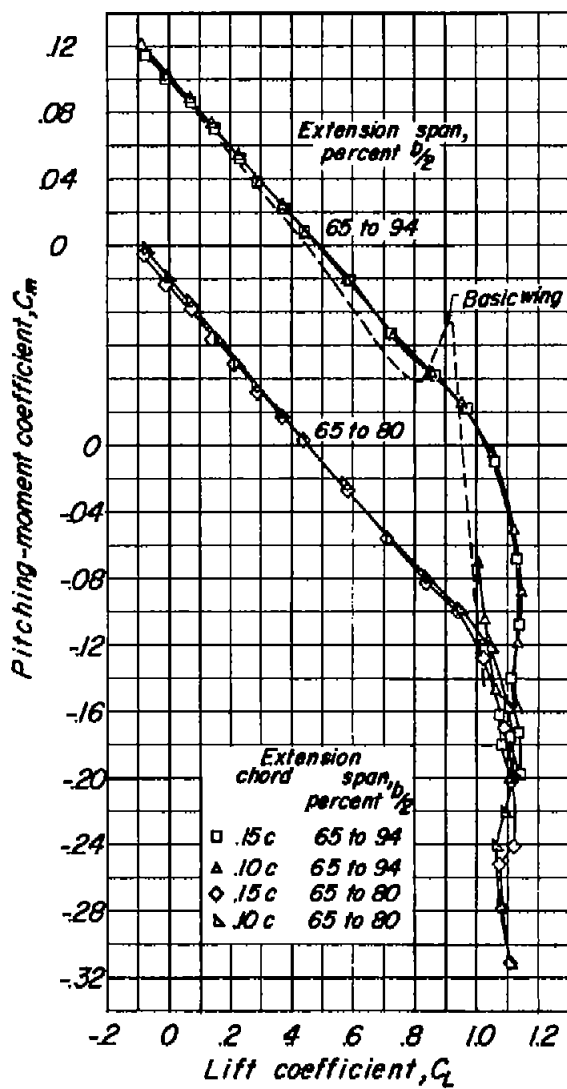
Figure 23.- Concluded.
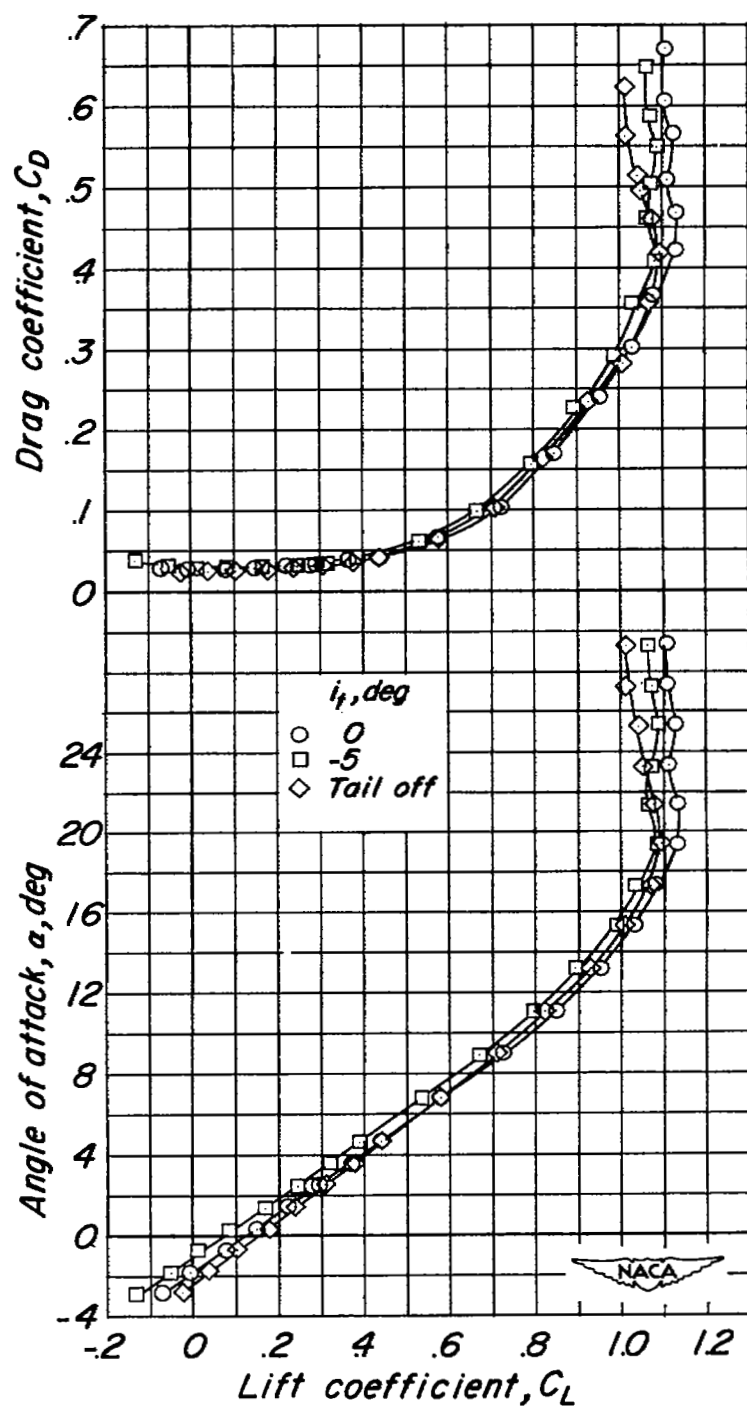
Figure 24.- Effect of stabilizer deflection on the aerodynamic character-
istics of the model with a 0.10c leading-edge chord-extension from
70 to 94 percent semispan.  $\delta_f = \delta_s = 0^\circ$.
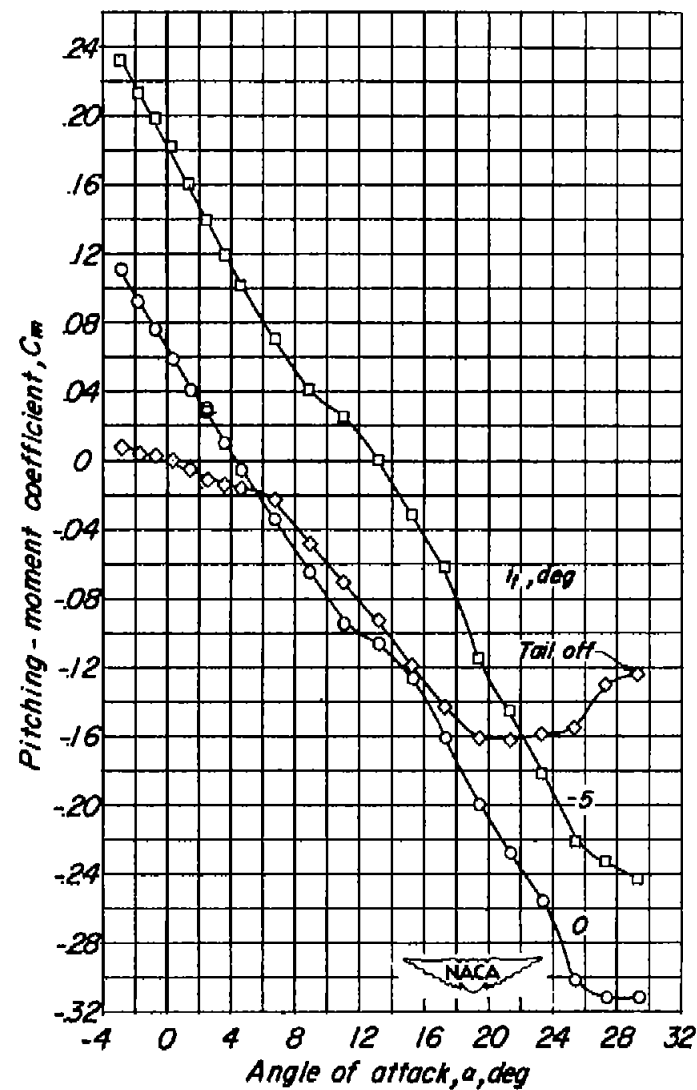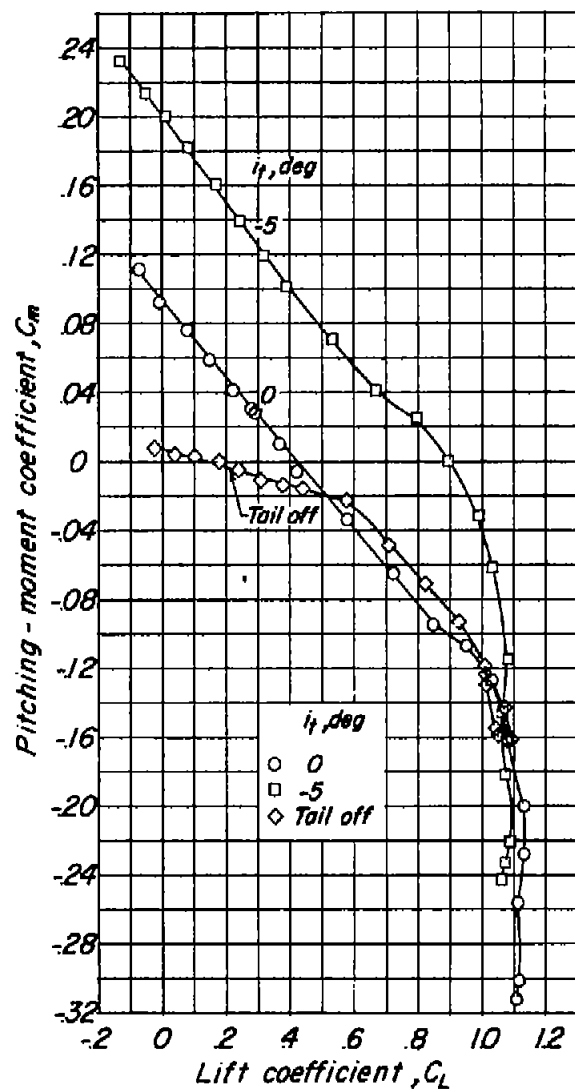
Figure 24.- Concluded.
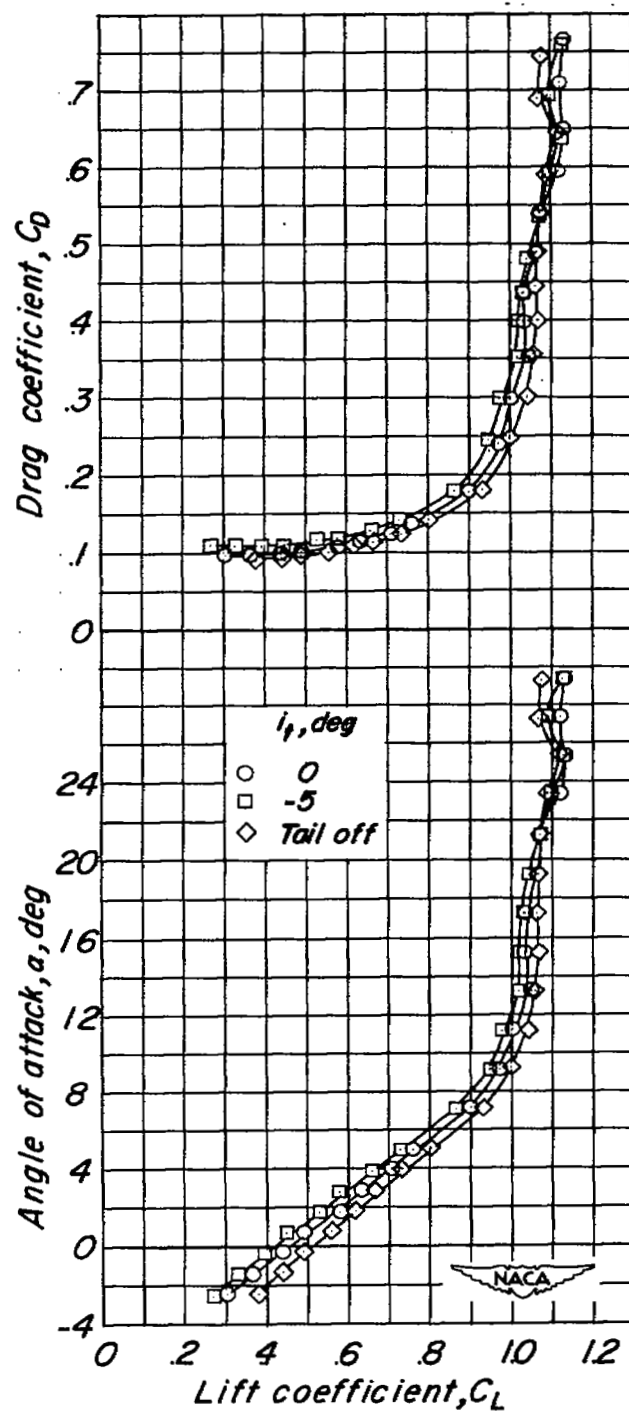
Figure 25.- Effect of stabilizer deflection on the aerodynamic character-
istics of the model with a 0.10c leading-edge chord-extension from
70 to 94 percent semispan.  $\delta_f = 40^\circ$; $\delta_s = 0^\circ$.
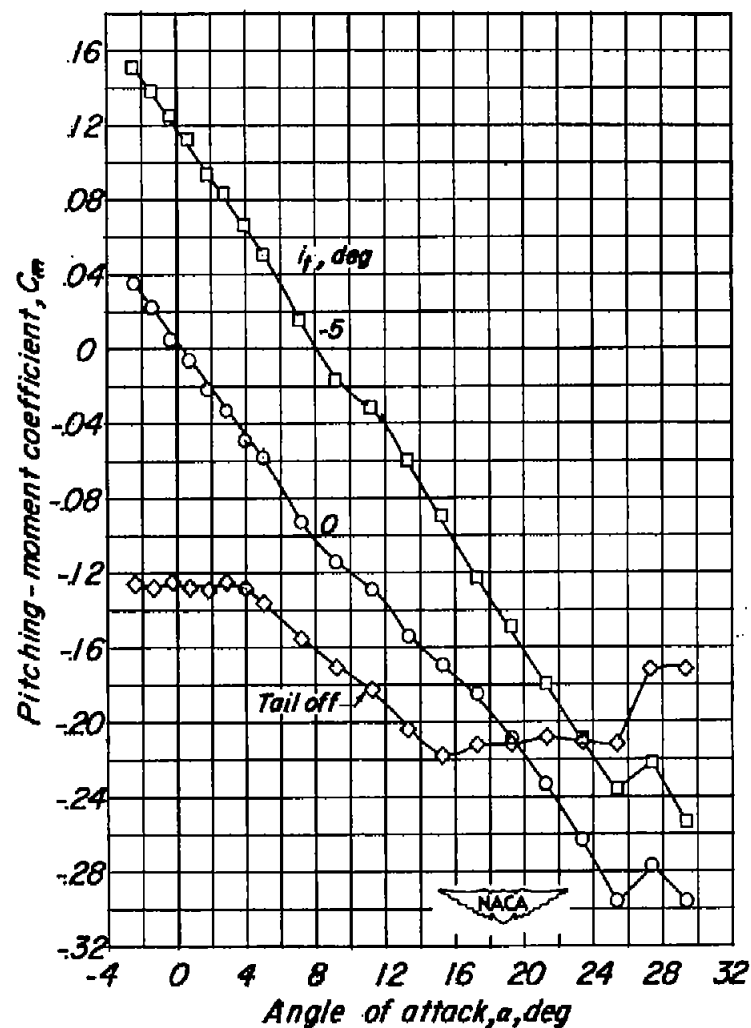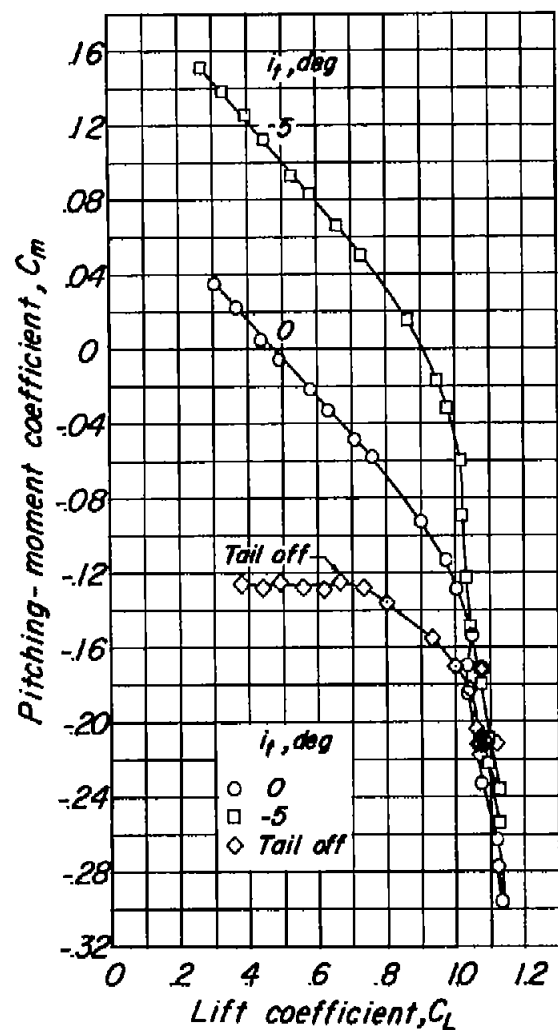
Figure 25.- Concluded.

A - Effect of extension on wing-fuselage contribution
B - Effect of extension on tail contribution
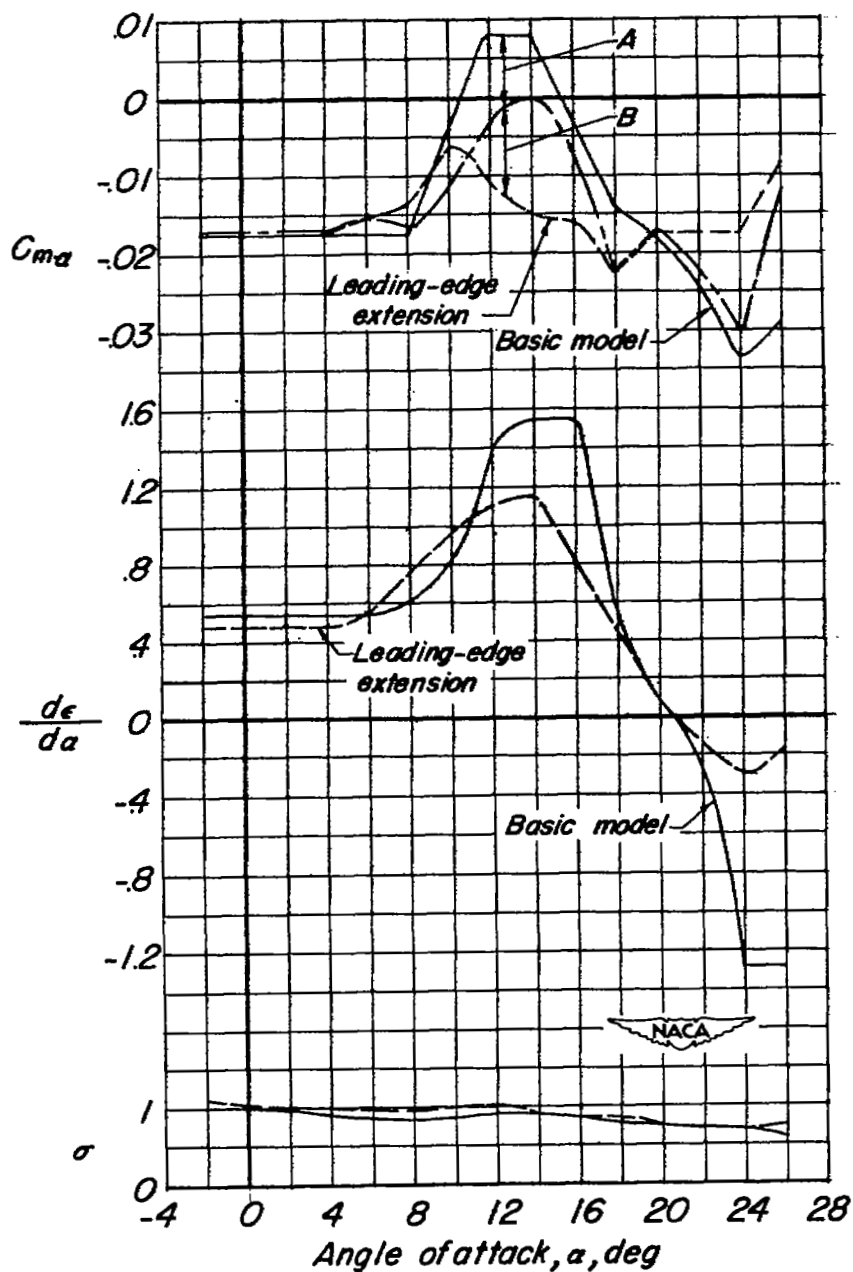


(a)  $\delta_f = \delta_s = 0^\circ$.

Figure 26.- Analysis of effect of leading-edge chord-extension on
longitudinal stability characteristics.

A-Effect of extension on wing-fuselage contribution
B-Effect of extension on tail contribution
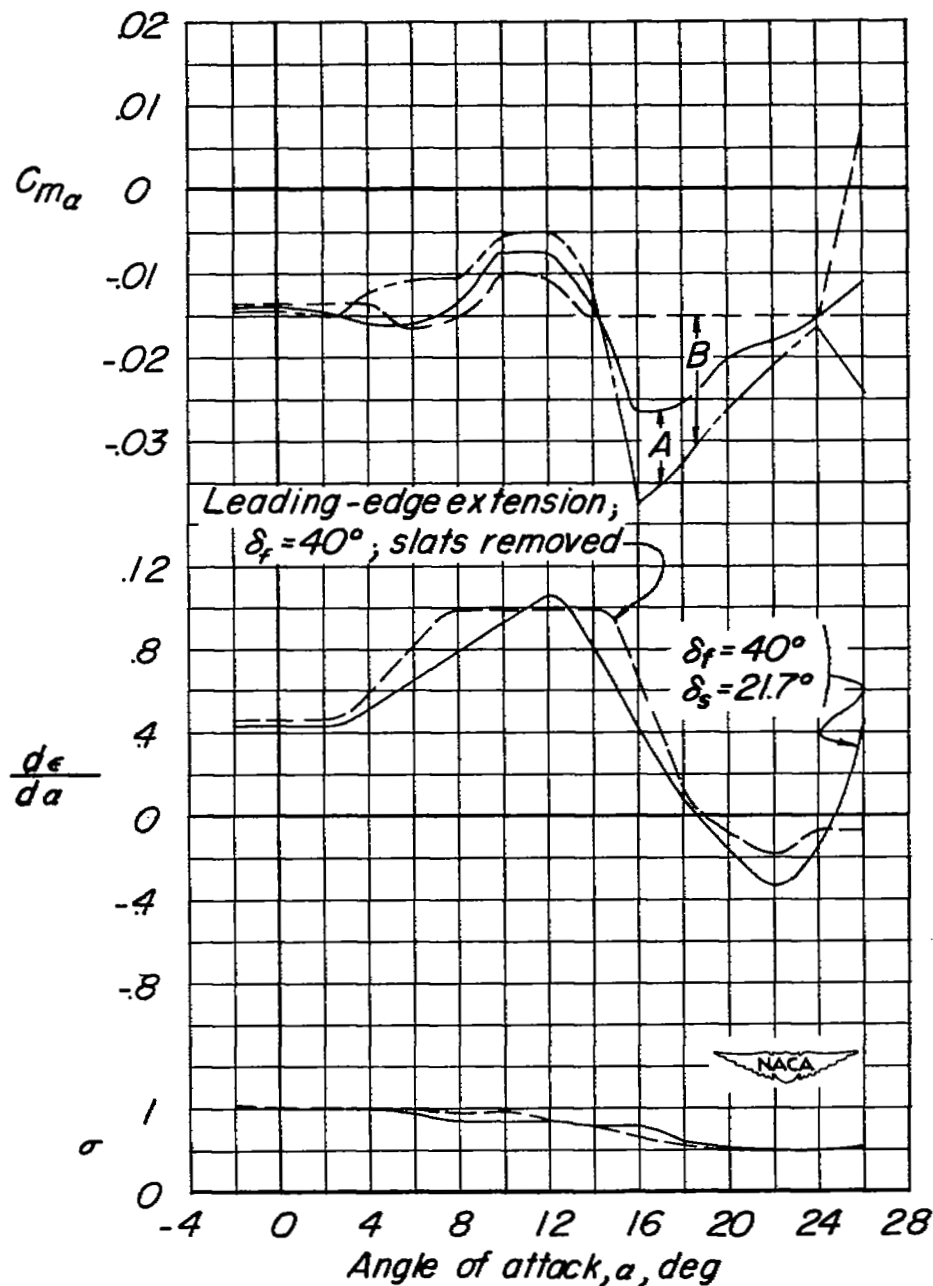


(b)  $\delta_f = 40^\circ$.

Figure 26.- Concluded.
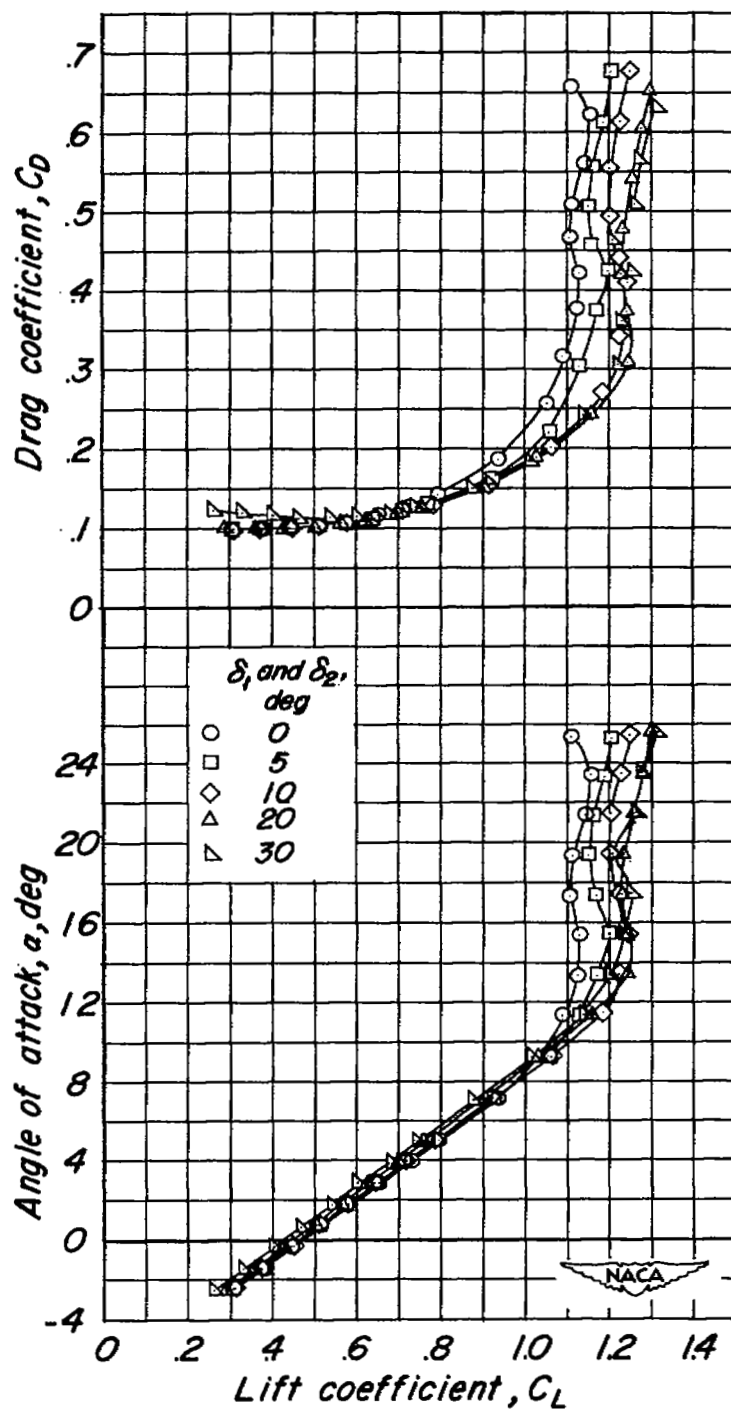
Figure 27.- Effect of leading-edge droop angle with 0.10c leading-edge chord-extension from 65 to 94 percent semispan.  $\delta_f = 40^\circ$; $i_t = 0^\circ$; slats removed.
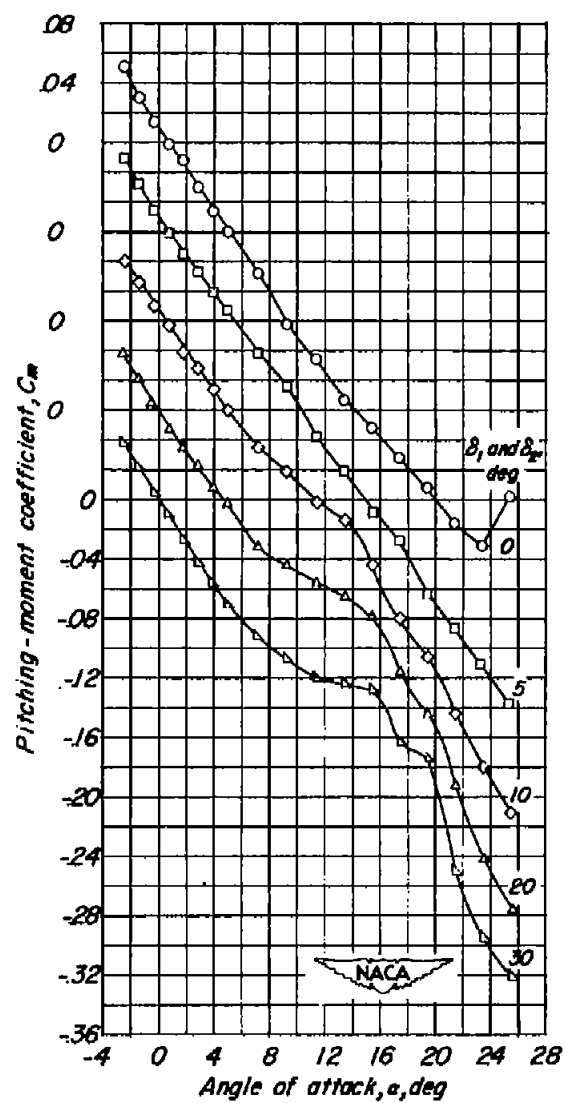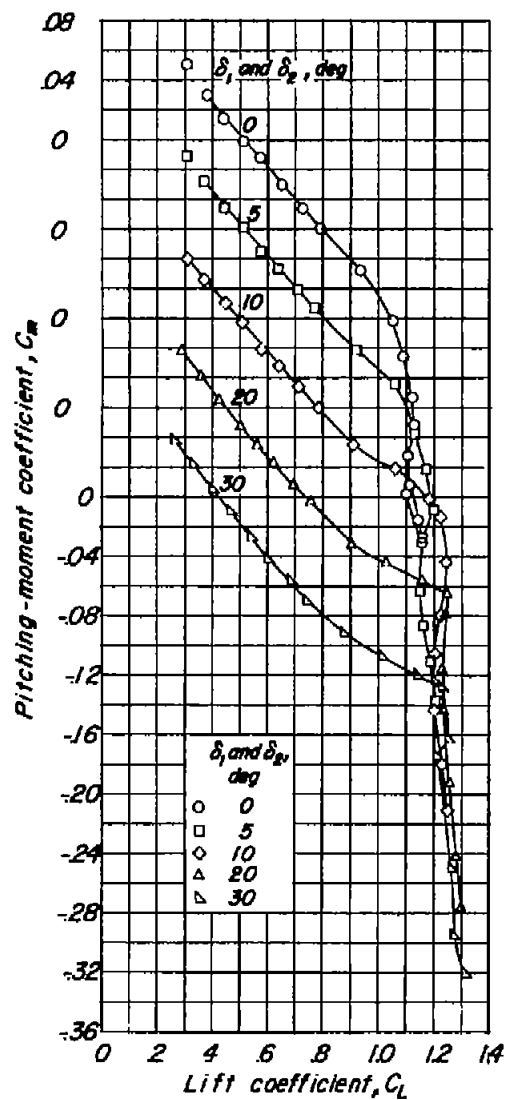
Figure 27.- Concluded.
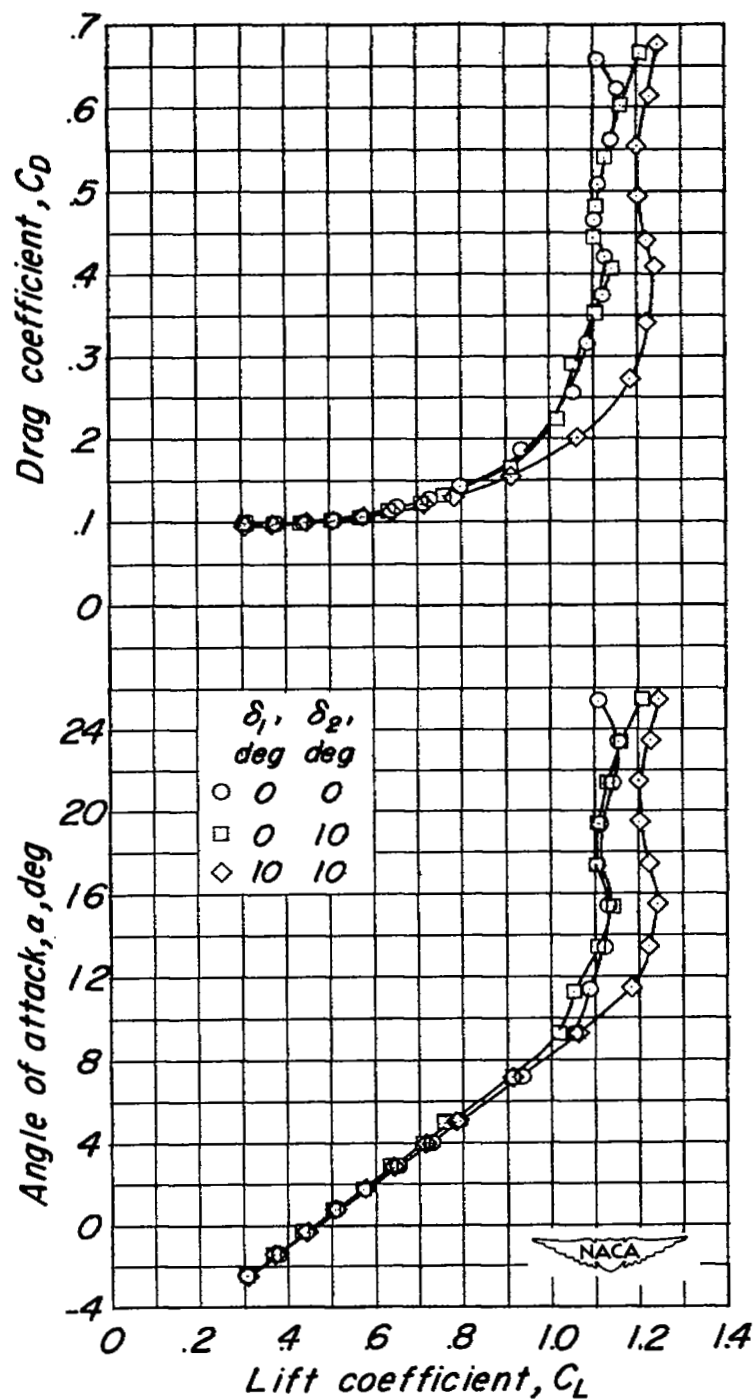
Figure 28.- Effect of spanwise extent of leading-edge droop with 0.10c leading-edge chord-extension from 65 to 94 percent semispan.  $\delta_f = 40^\circ$; $i_t = 0^\circ$; slats removed.
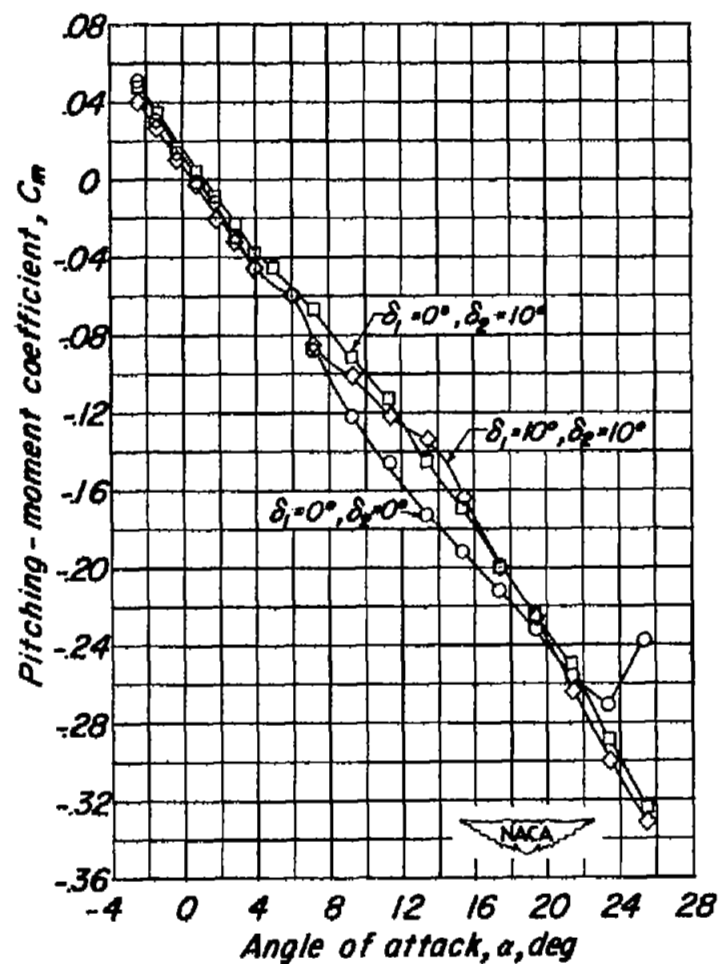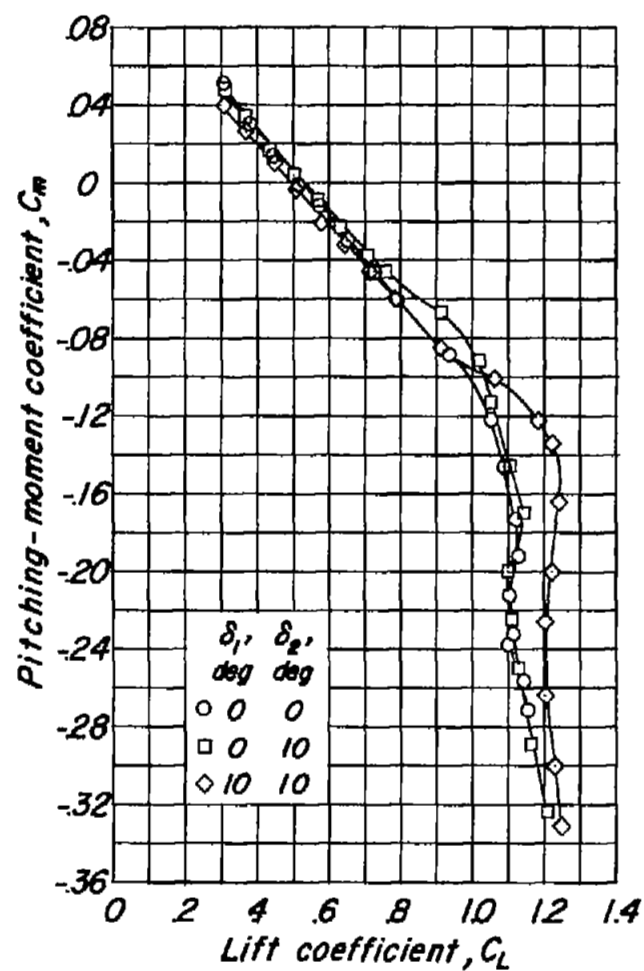
Figure 28.- Concluded.
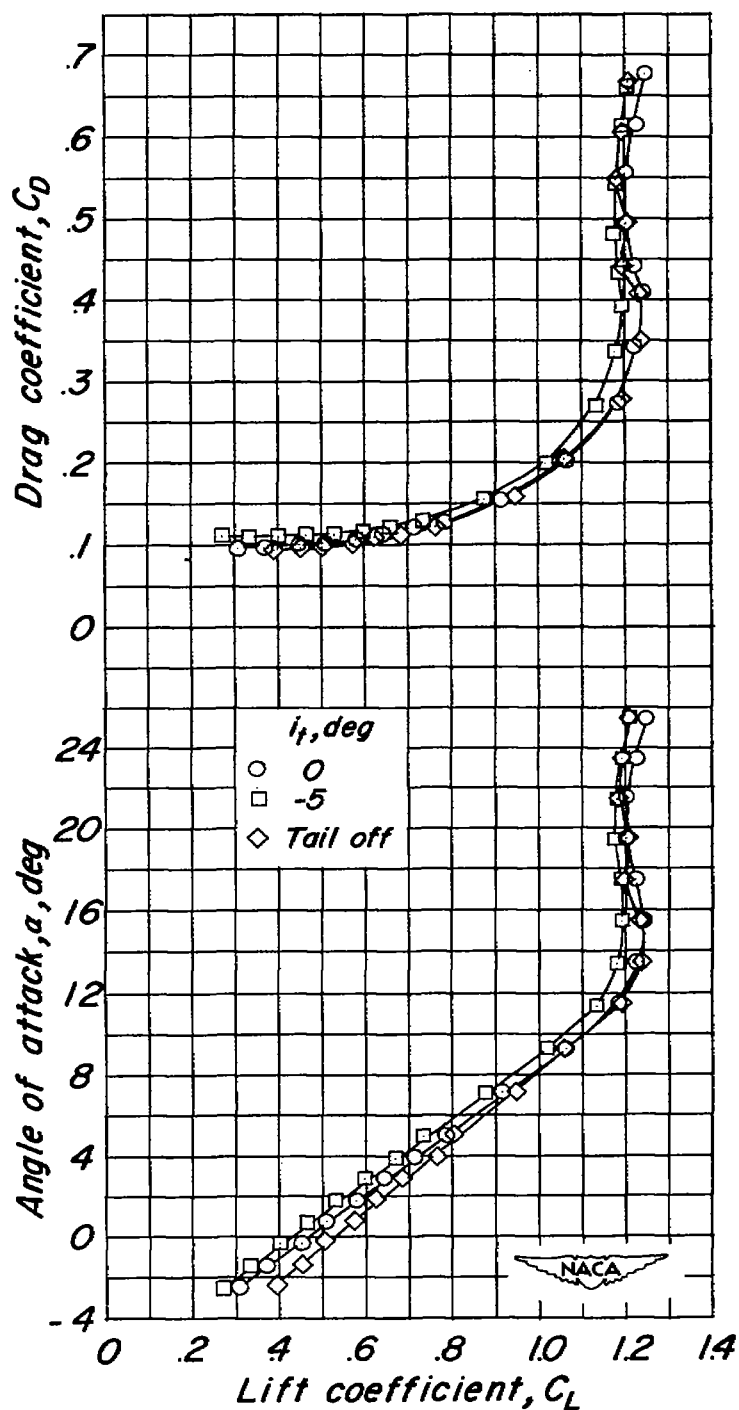
Figure 29.- Effect of stabilizer deflection on the aerodynamic character-
istics of the model with drooped 0.10c leading-edge chord-extension
from 65 to 94 percent semispan. $\delta_1 = 10^\circ$; $\delta_2 = 10^\circ$; $\delta_f = 40^\circ$; slats
removed.
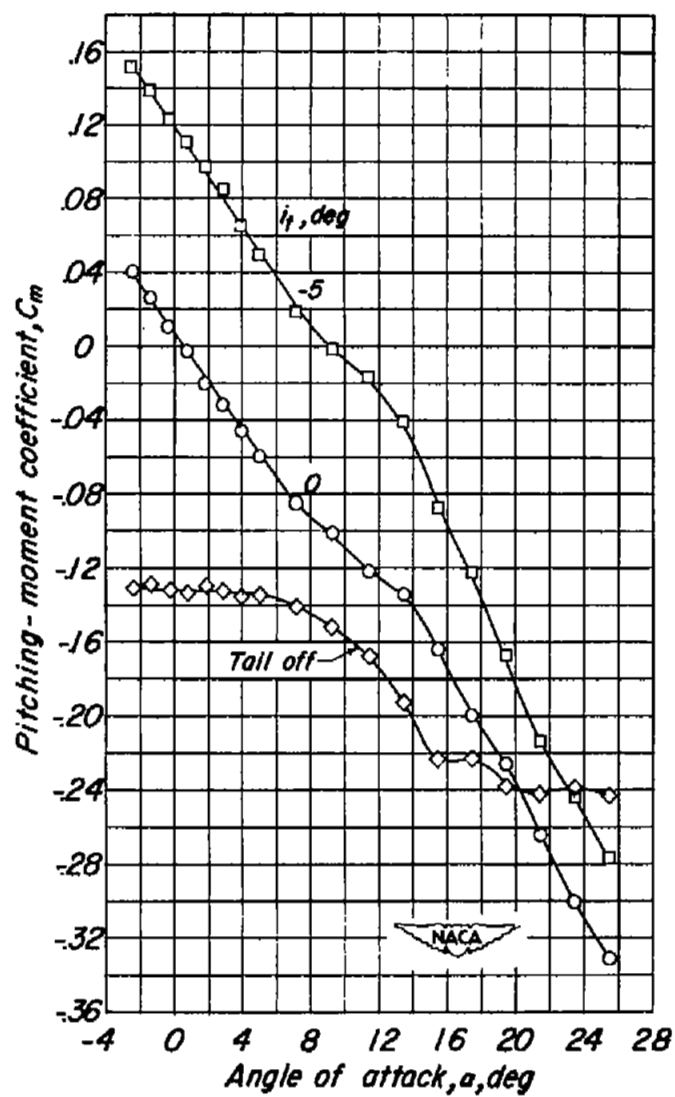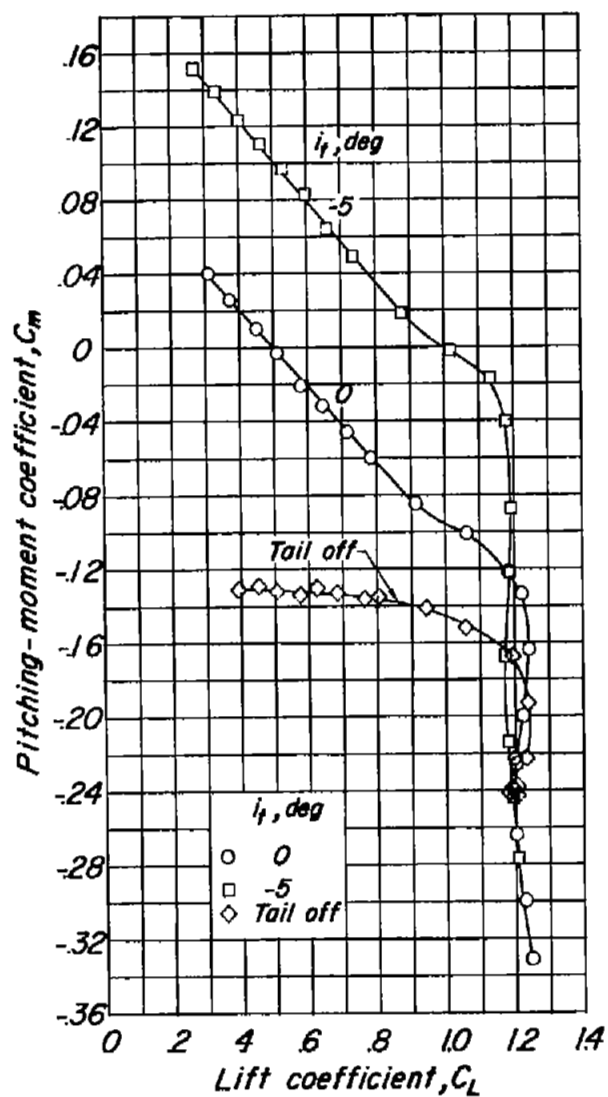
Figure 29.— Concluded.
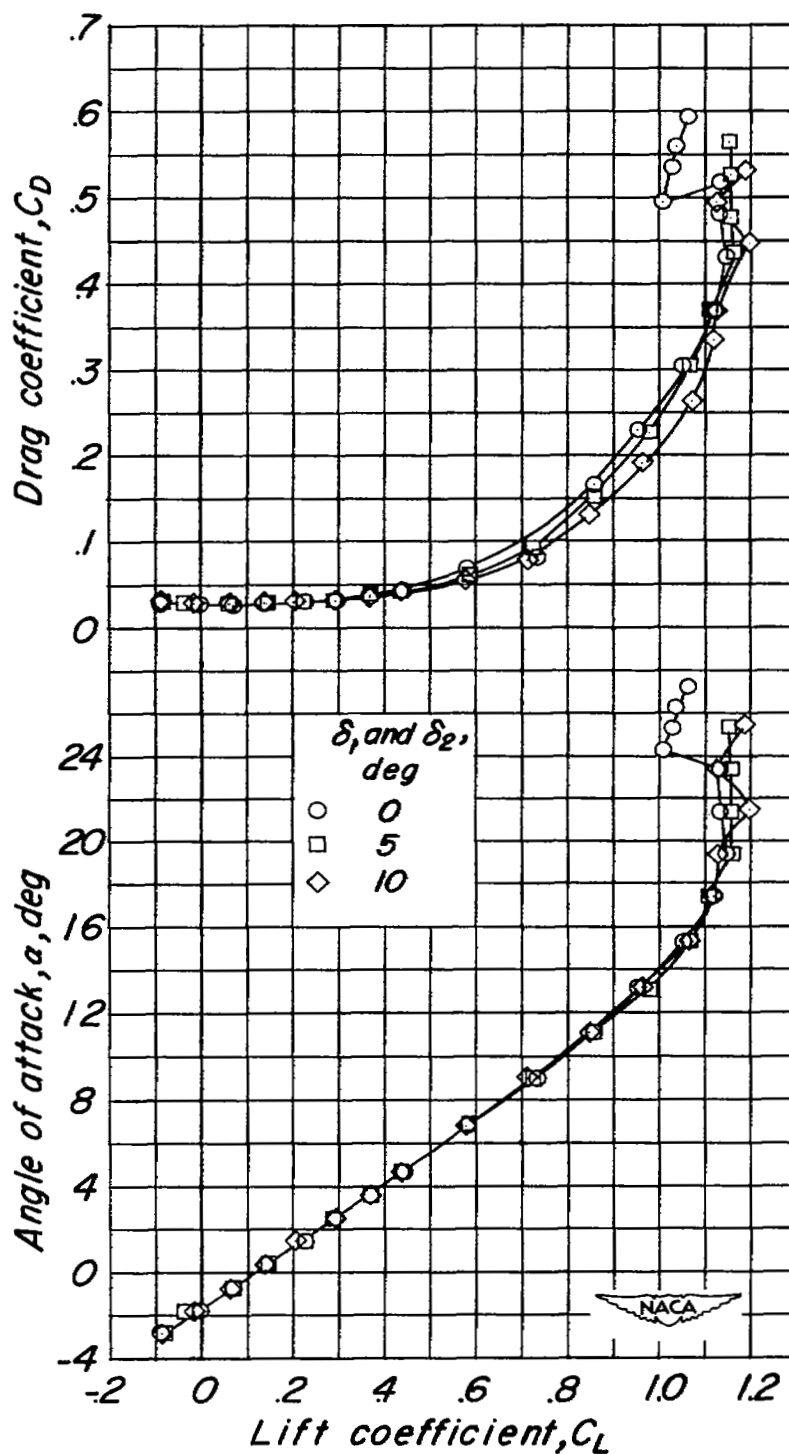
Figure 30.- Effect of leading-edge droop angle with 0.10c leading-edge chord-extension from 65 to 94 percent semispan.  $\delta_f = 0^\circ$.
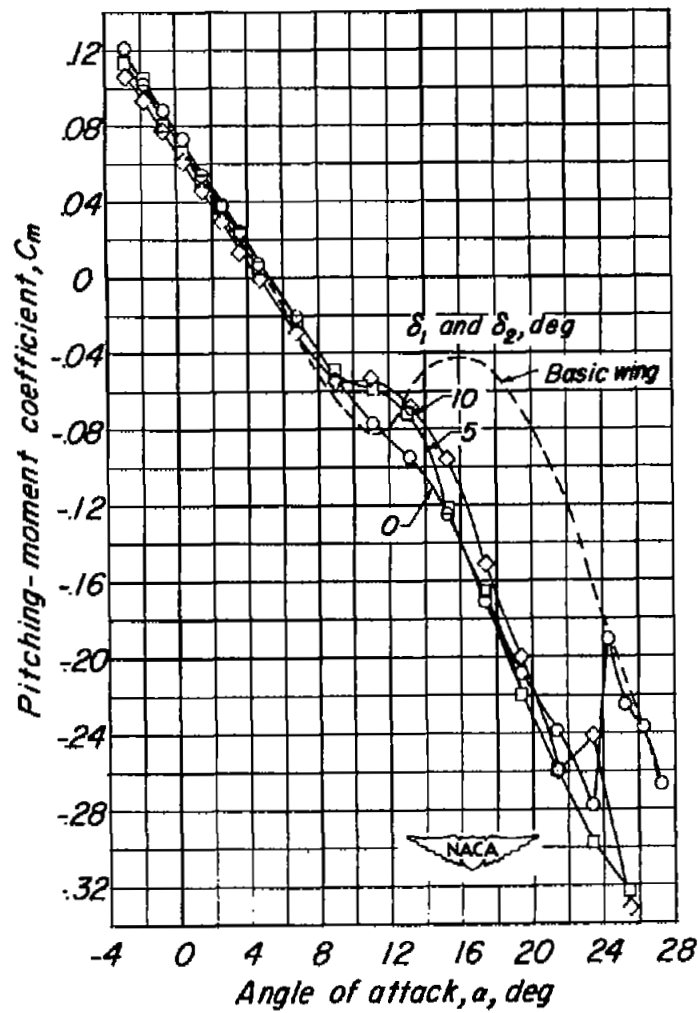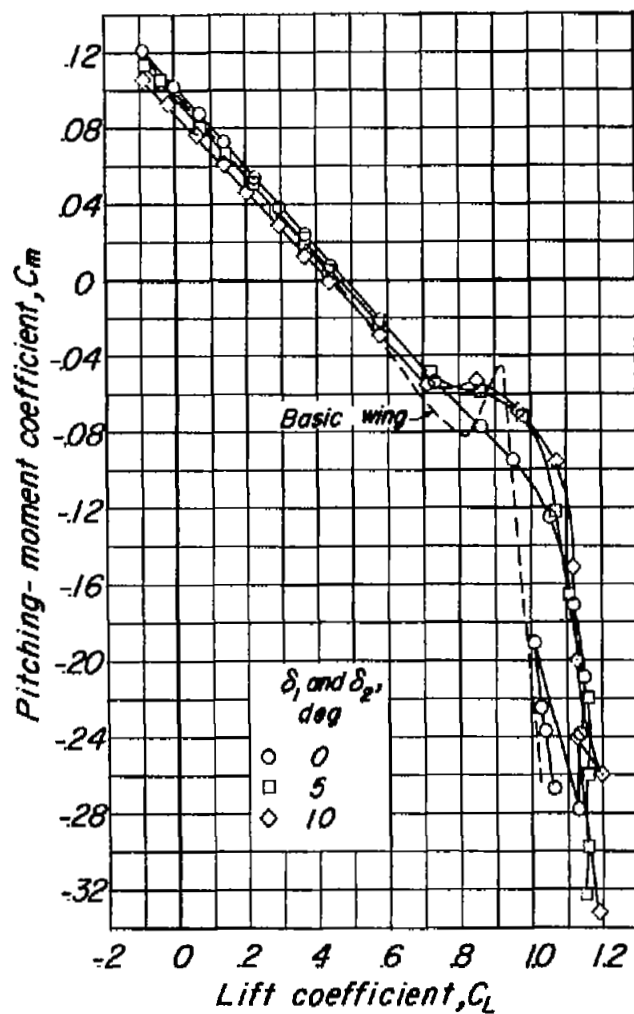
Figure 30.- Concluded.
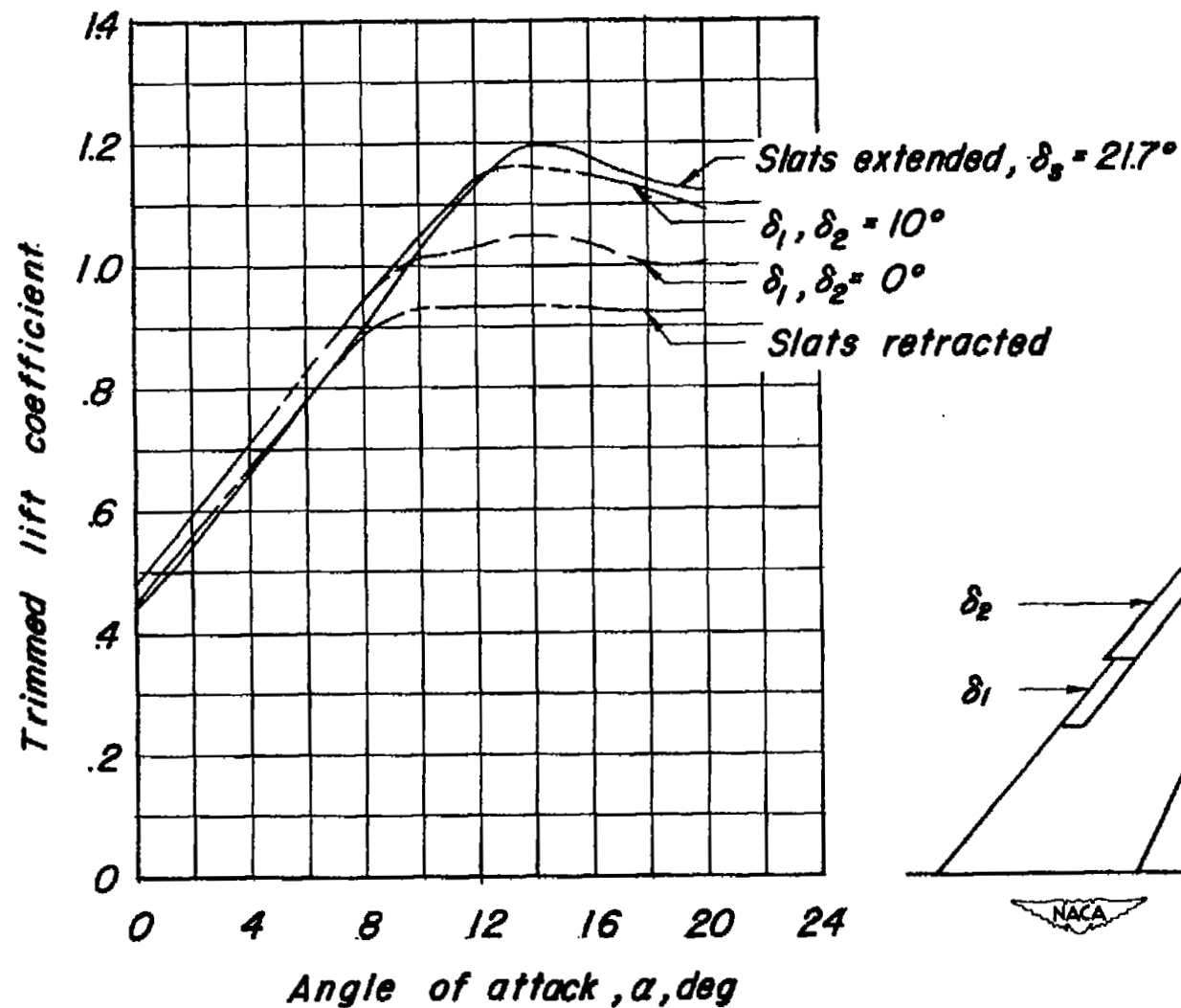
Figure 31.- Summary of effects of leading-edge chord-extensions on trimmed lift characteristics. $\delta_f = 40°$.

Figure 32.- Effect of stabilizer deflection on the aerodynamic character-
istics of the model with the large inlet. $\delta_f = \delta_s = 0^\circ$.
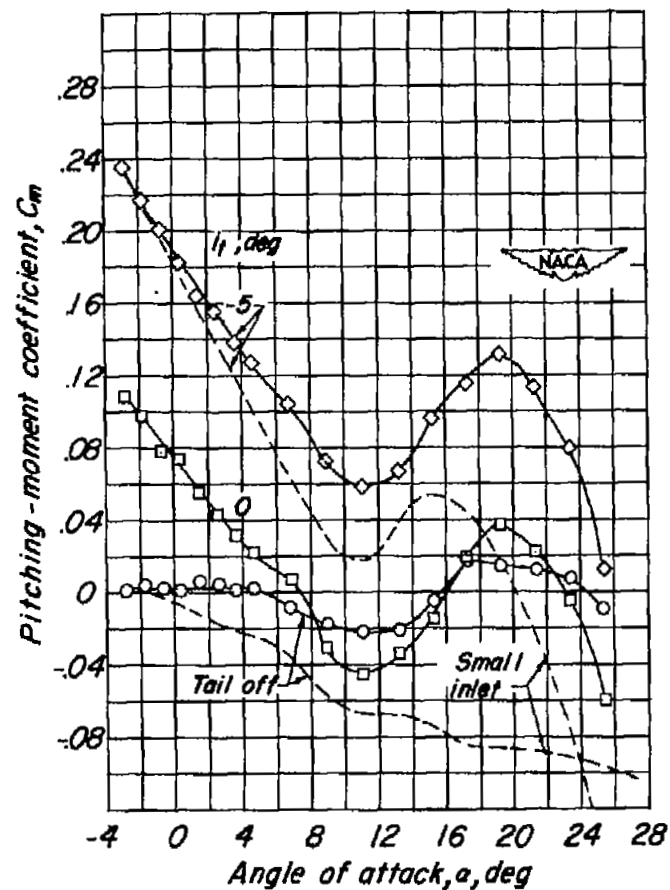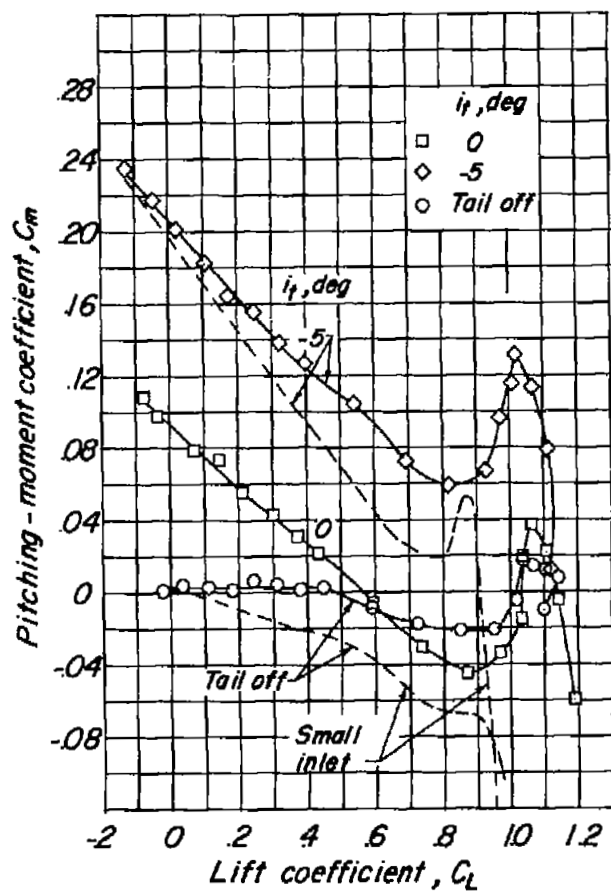
Figure 32.- Concluded.
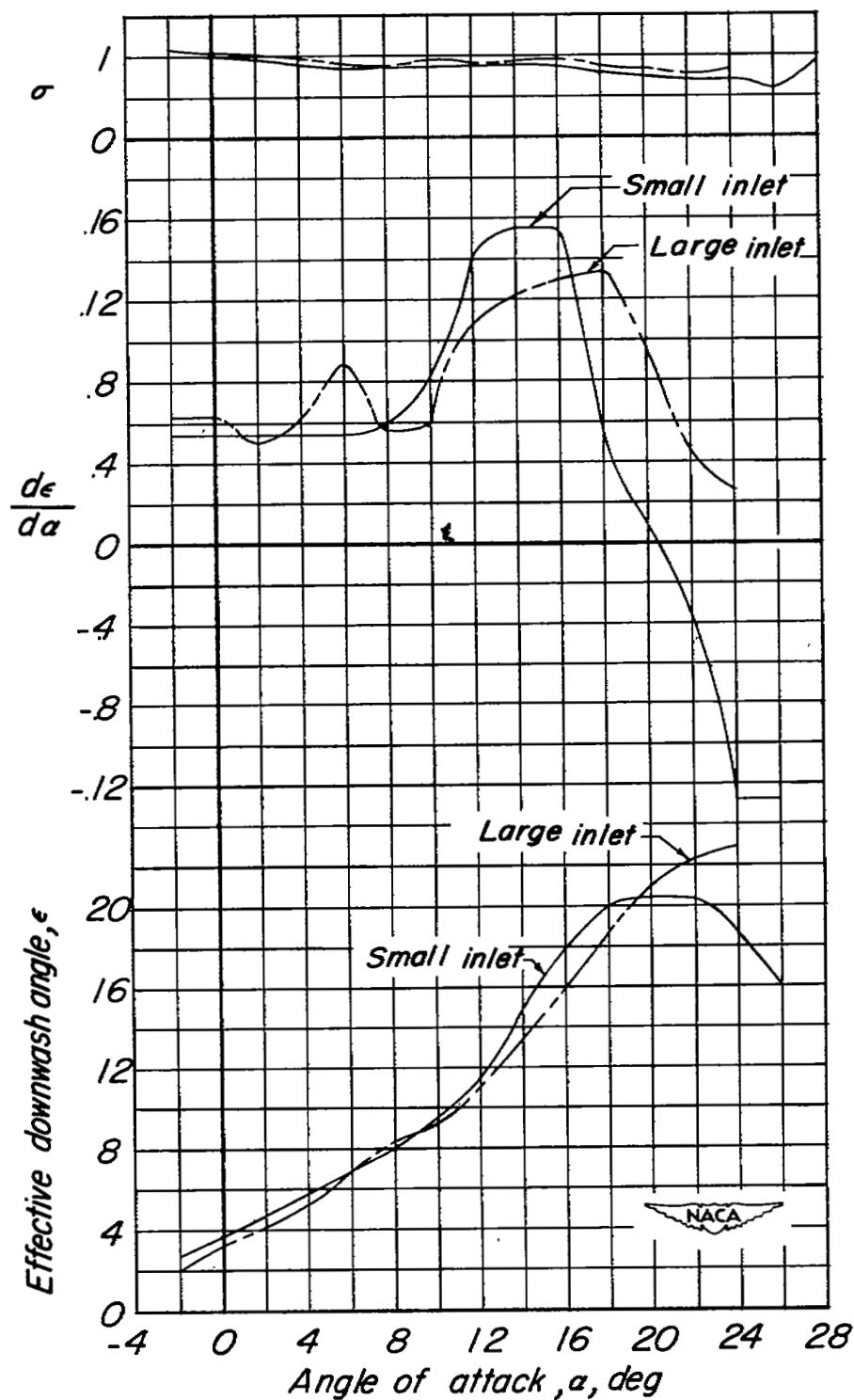
Figure 33.- Effect of inlet size on the effective downwash and tail effectiveness parameter. $\delta_f = \delta_s = 0^\circ$.
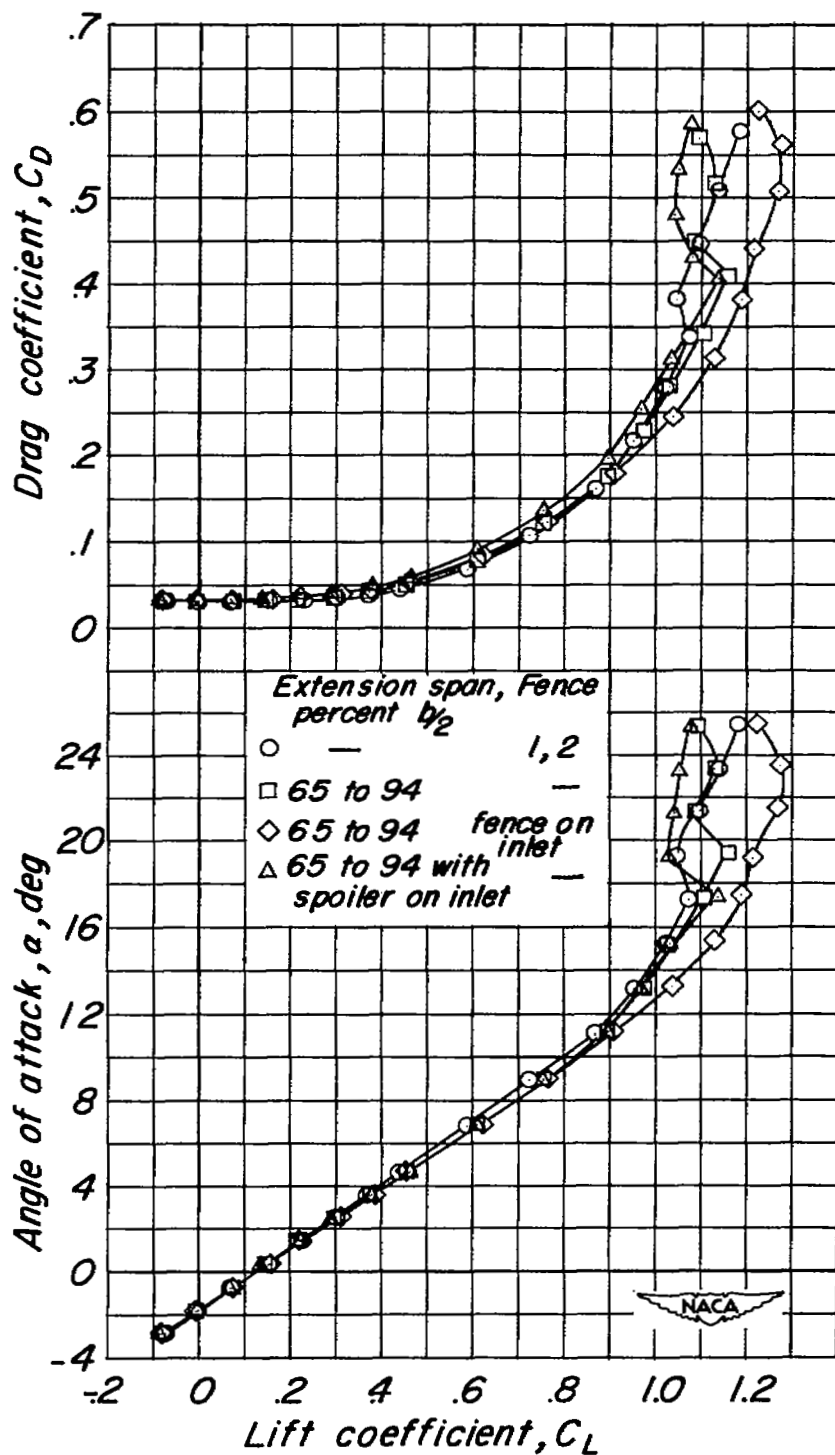
Figure 34.- Effect of fences and chord-extensions on characteristics of the model with the large inlet. $\delta_f = \delta_s = 0°$.
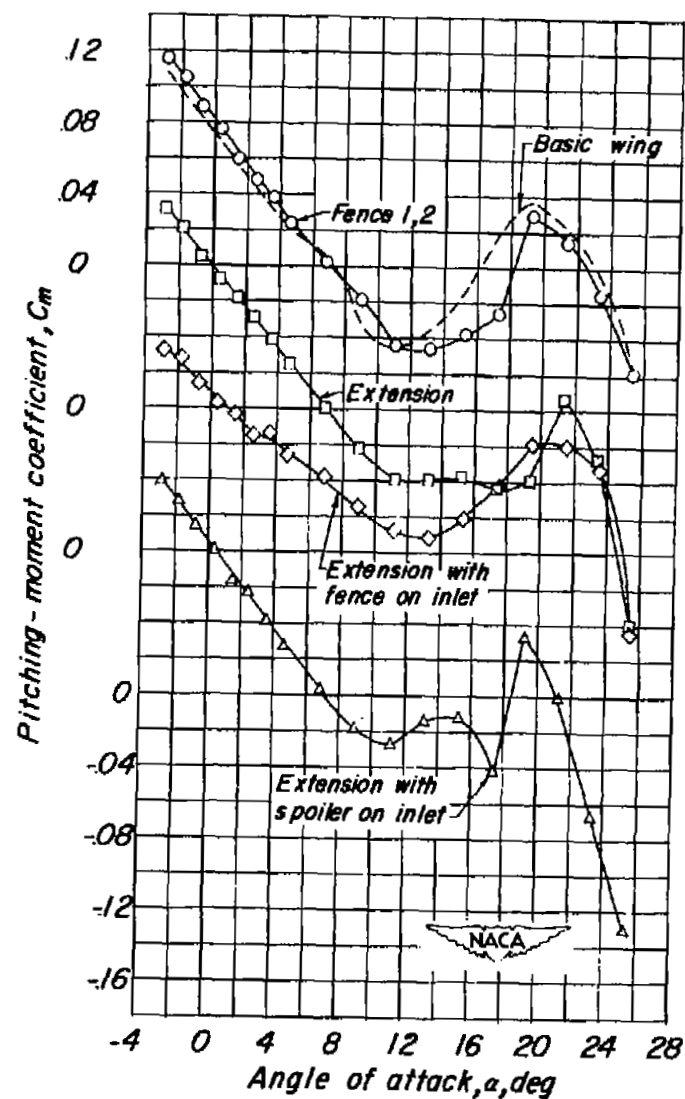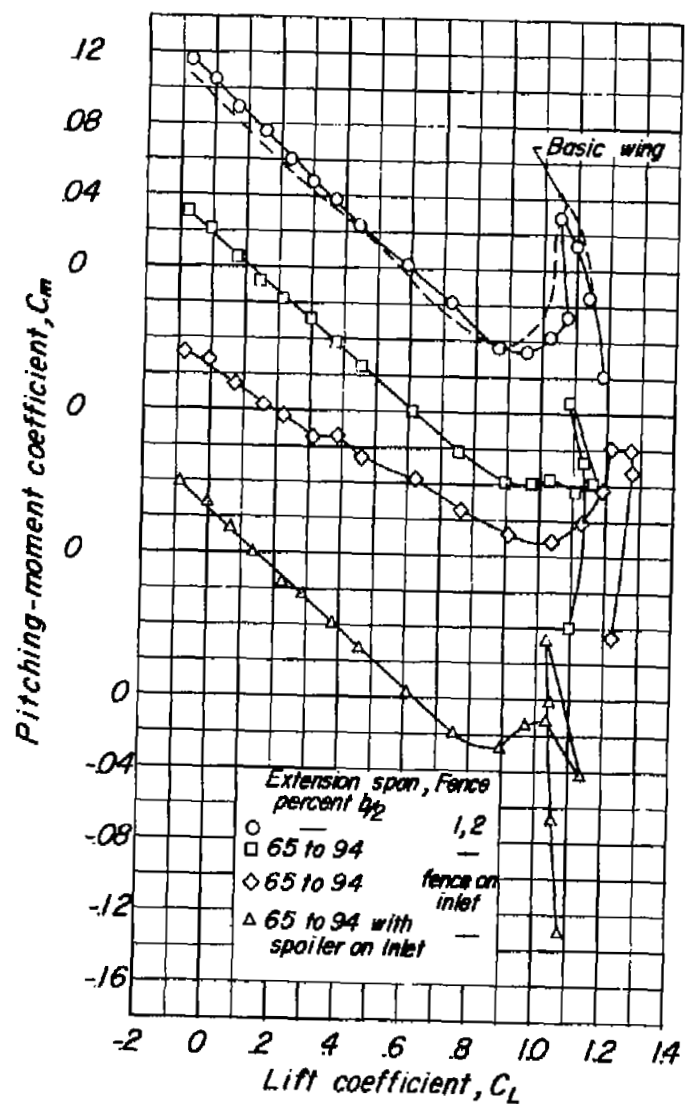
Figure 34.- Concluded.
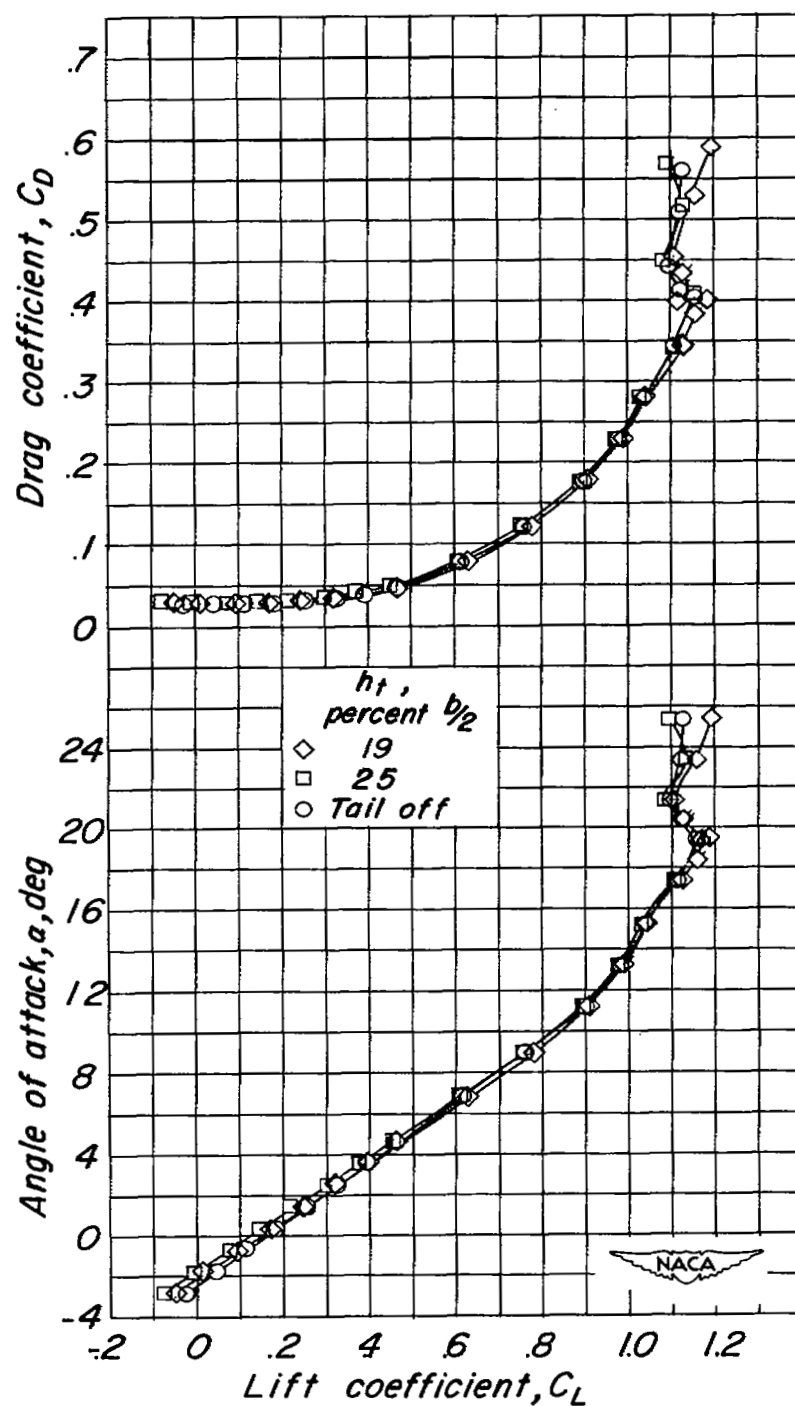
Figure 35.- Effect of lowering the horizontal tail on characteristics of the model with the large inlet. Leading-edge chord-extensions from 65 to 94 percent semispan. $\delta_f = \delta_s = 0^\circ$.
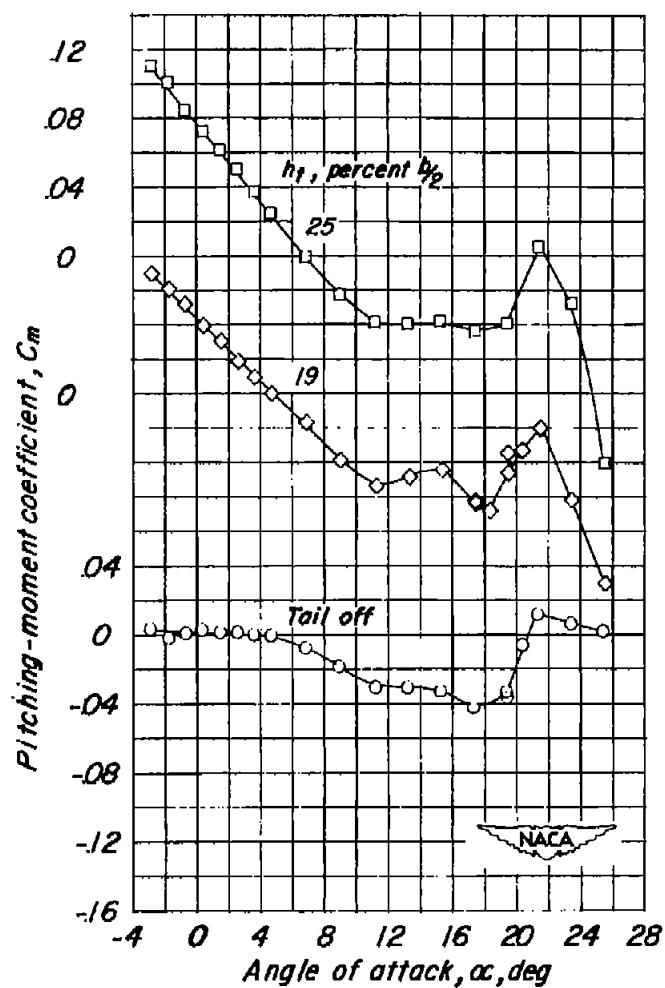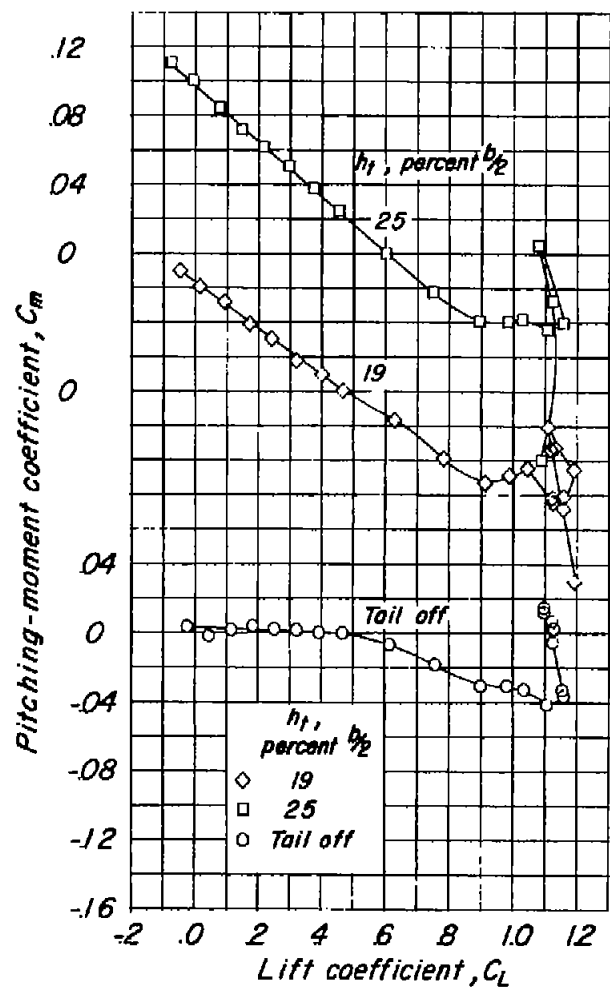
Figure 35.- Concluded.
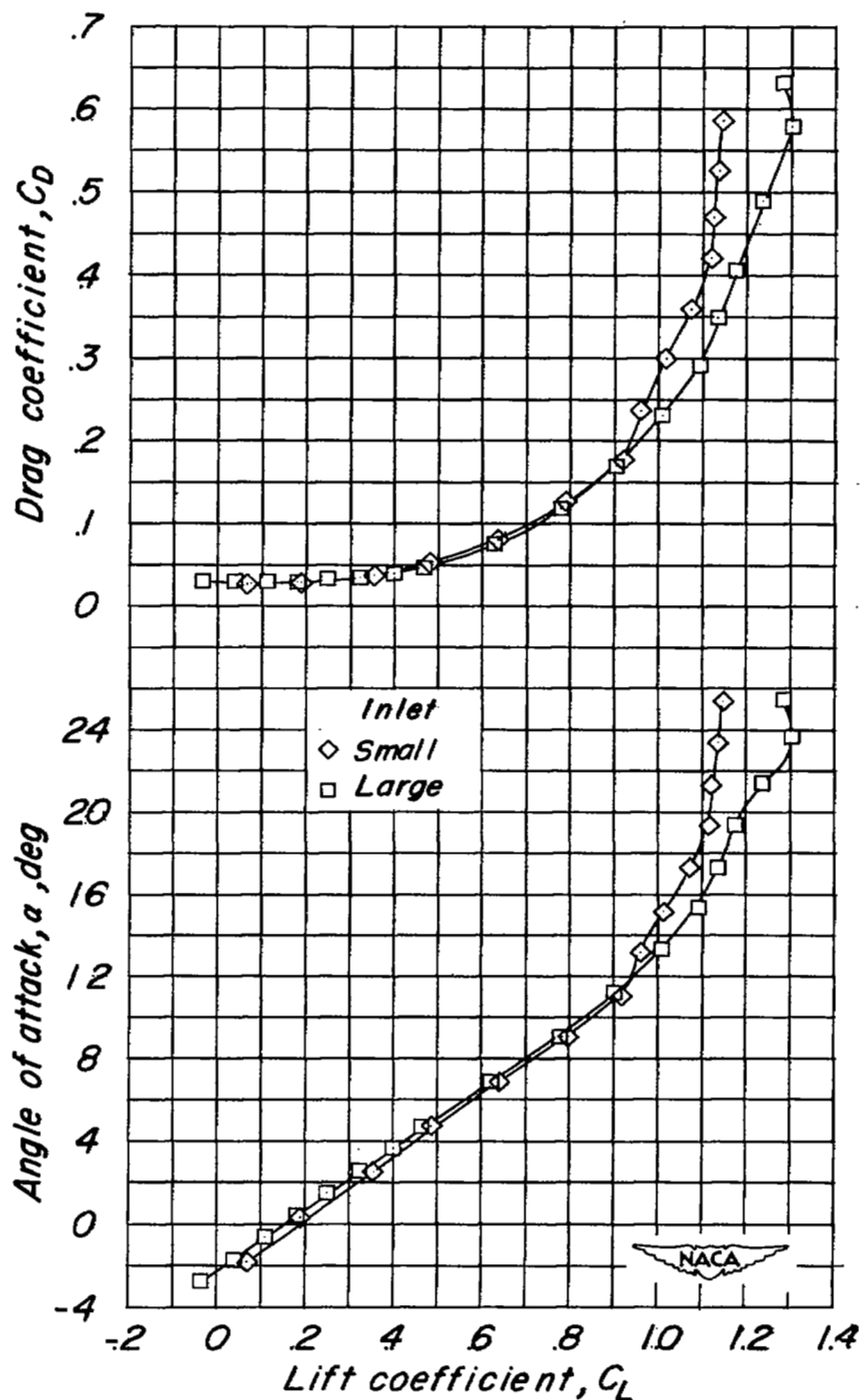
Figure 36.- Effect of inlet size on aerodynamic characteristics of the
model with horizontal tail located 7 percent semispan below fuselage
center line. $\delta_f = \delta_s = i_t = 0^\circ$.
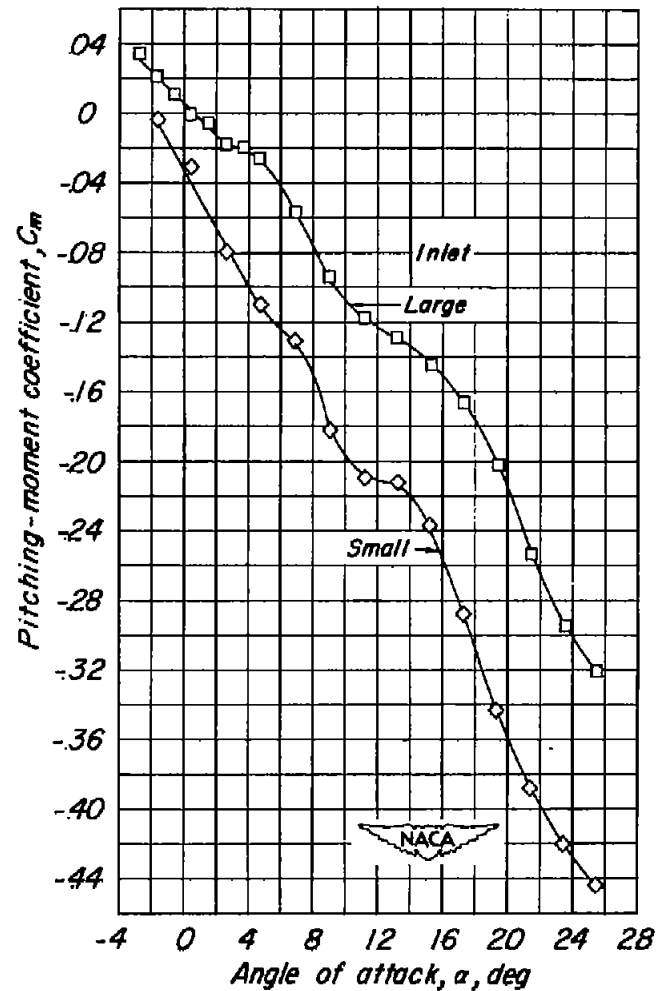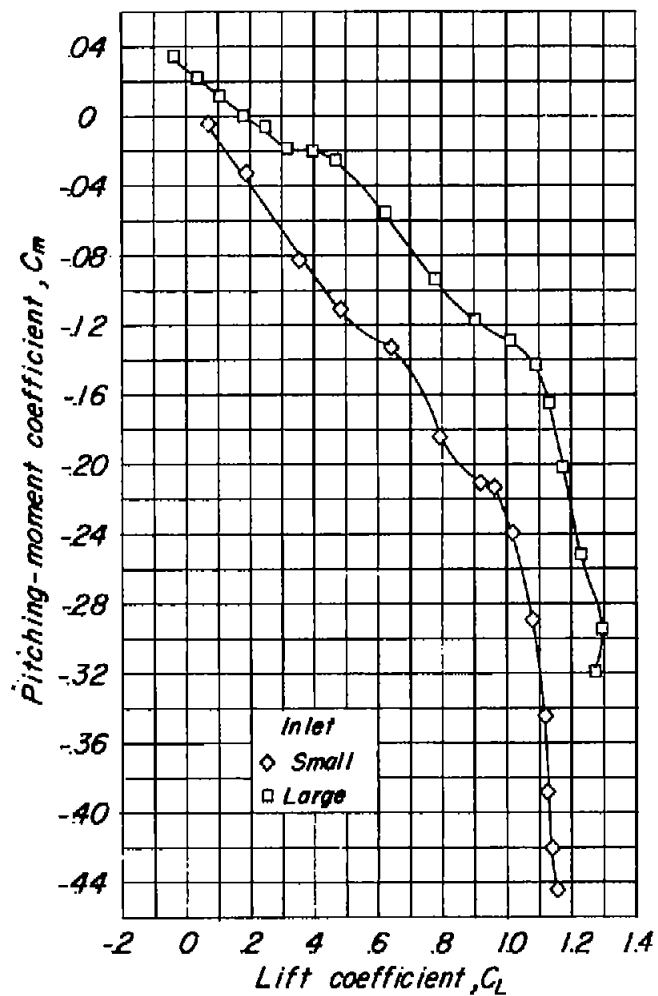
Figure 36.- Concluded.
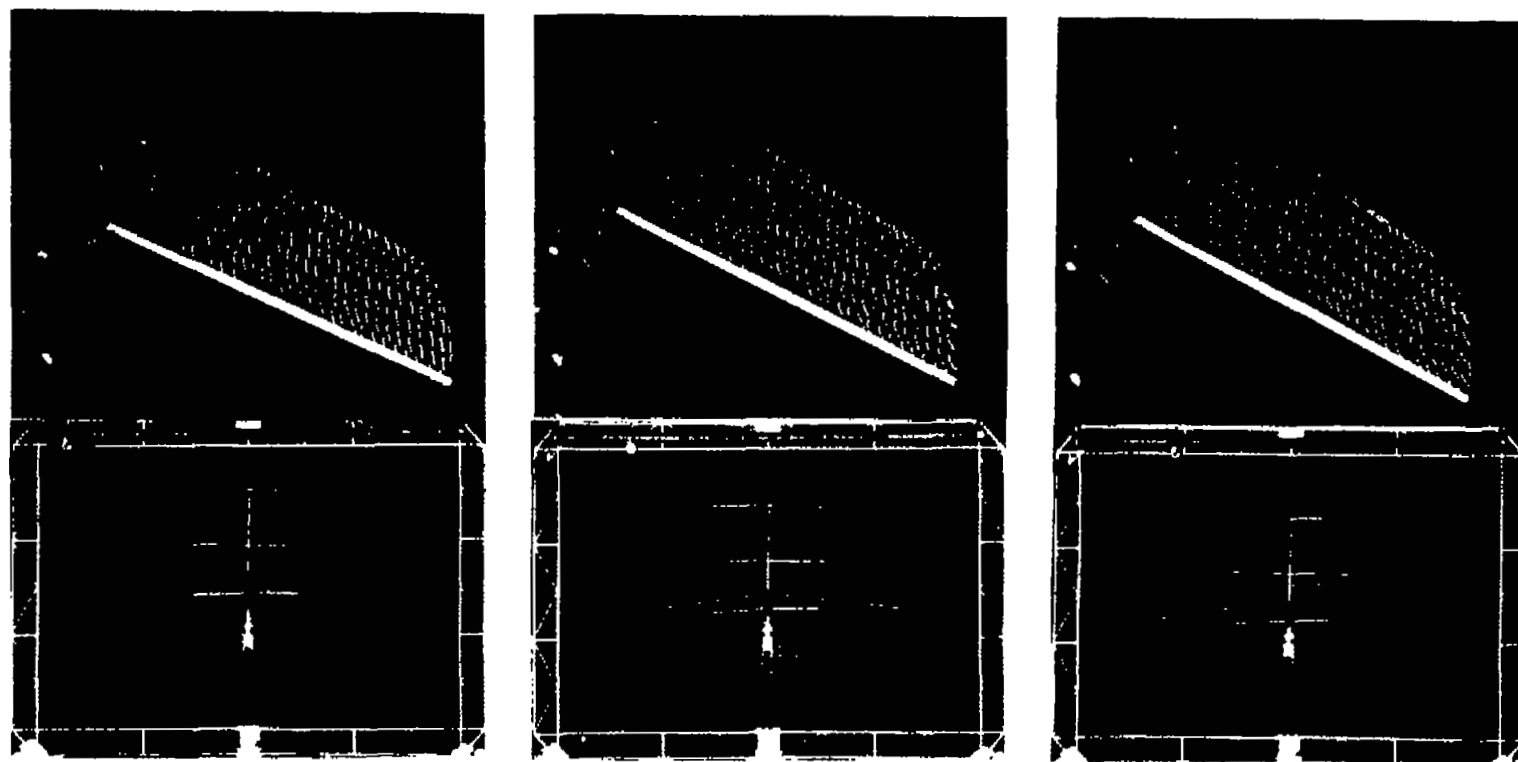
$a=0.3°; C_L=0.19$          $a=4.6°; C_L=0.44$          $a=6.8°; C_L=0.57$

Figure 37.- Tuft-grid and surface-tuft photographs for basic model configuration. $\delta_f = \delta_g = 0°$.

L-77949
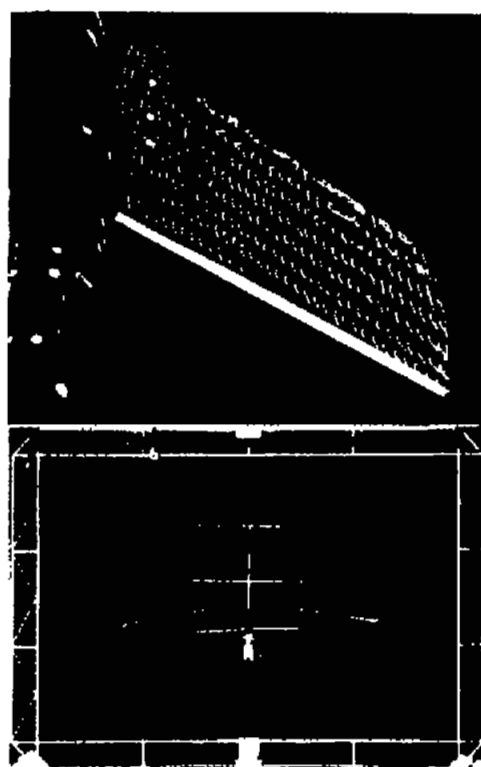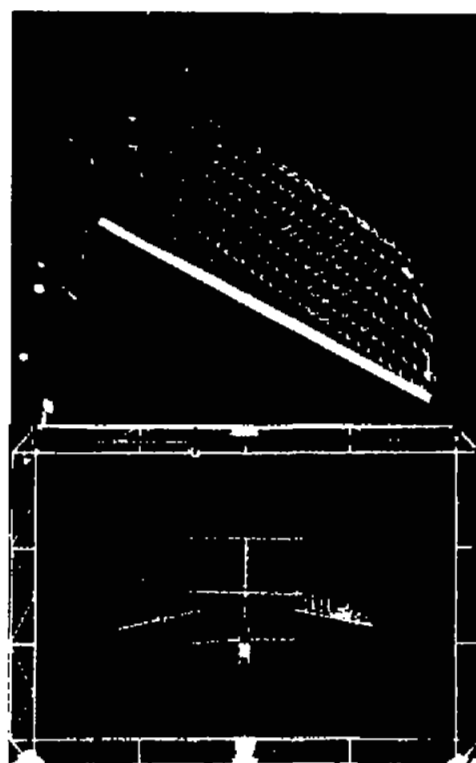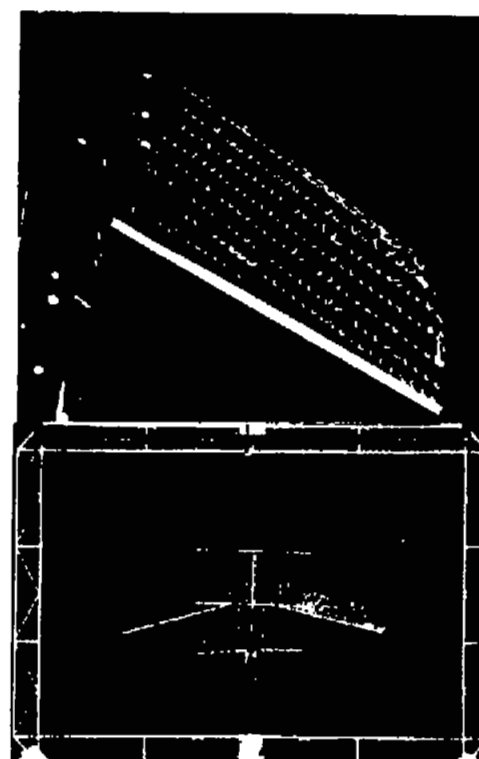
$\alpha=8.9°; C_L=0.72$        $\alpha=13.1°; C_L=0.92$        $\alpha=17.1°; C_L=0.94$

Figure 37.- Concluded.

L-77950
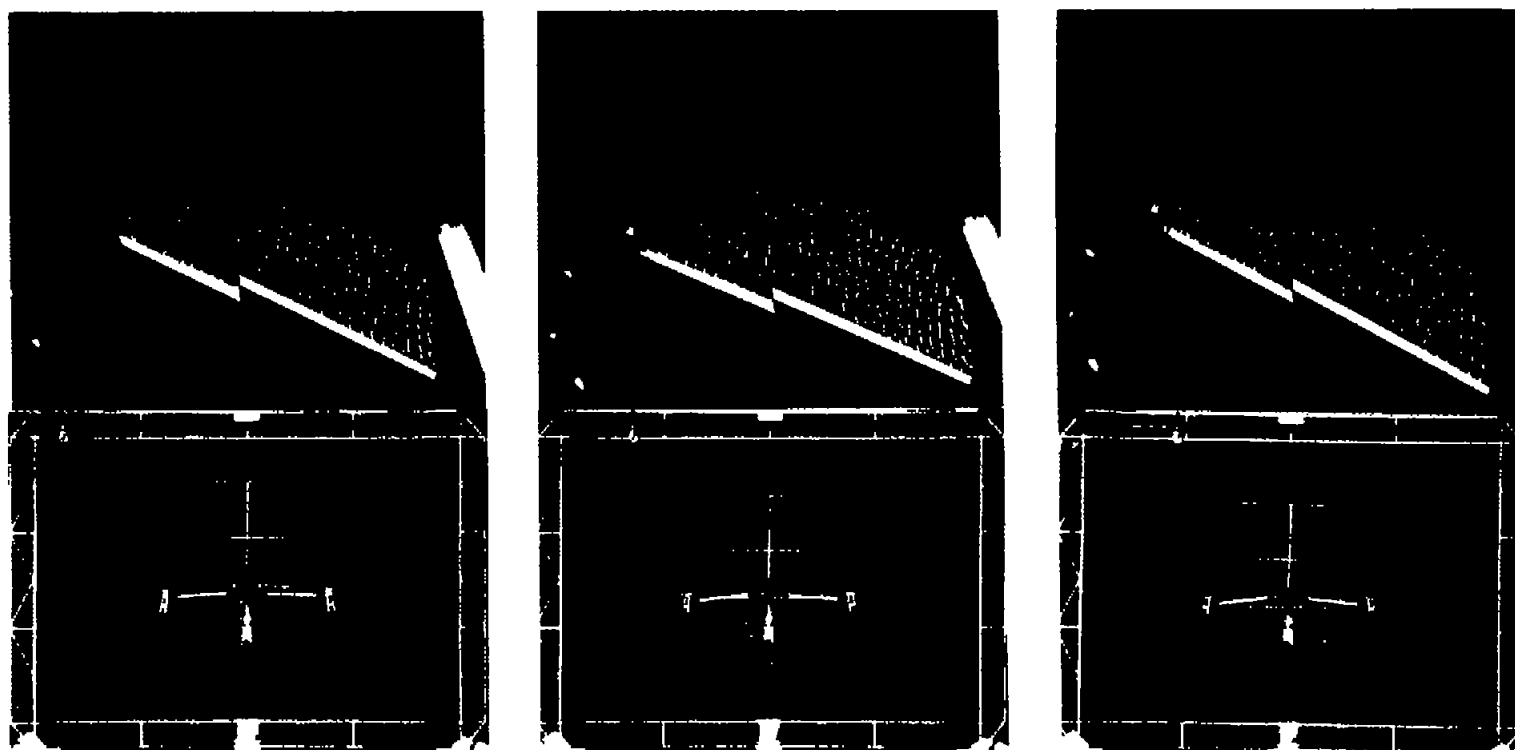
$a = 0.6°; C_L = 0.53$　　　$a = 4.9°, C_L = 0.77$　　　$a = 7.1°; C_L = 0.91$

Figure 38.- Tuft-grid and surface-tuft photographs for basic model configuration. $\delta_f = 40°$; $\delta_s = 21.7°$.

L-77951
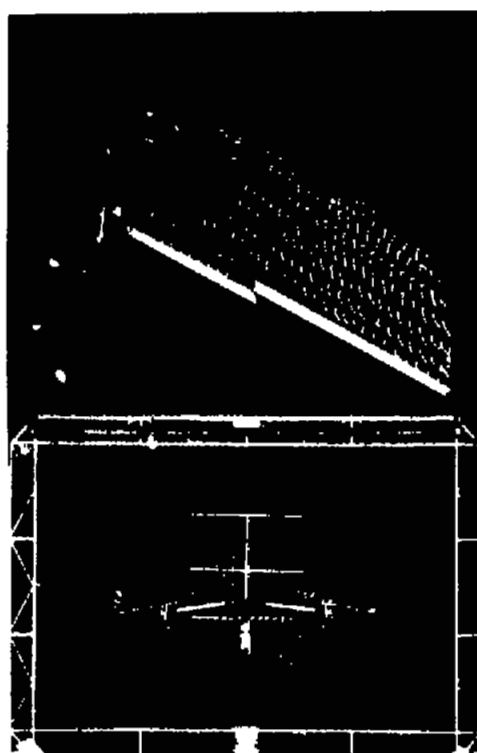
$a=9.2°;\ C_L=1.04$
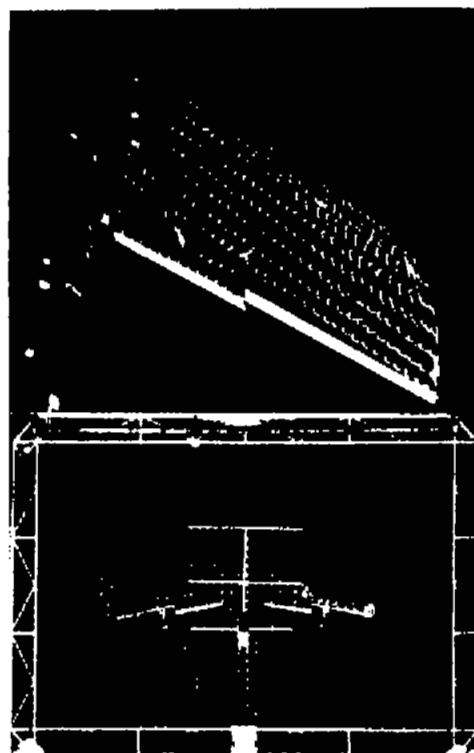
$a=13.4°;\ C_L=1.26$
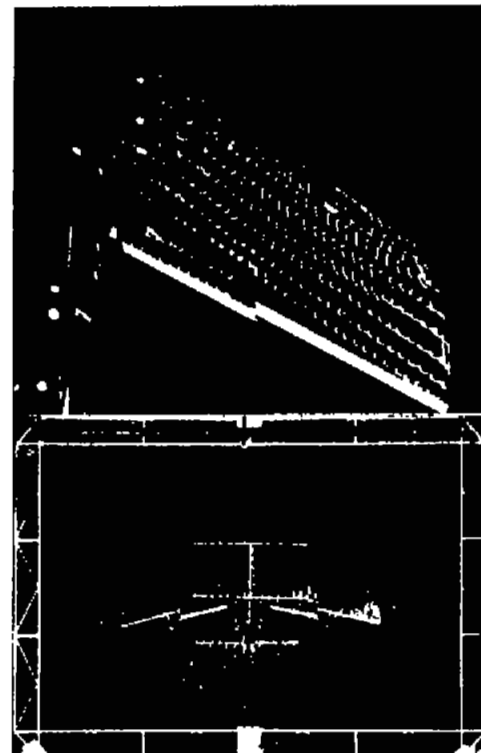
$a=17.4°;\ C_L=1.24$

Figure 38.- Concluded.

L-77952
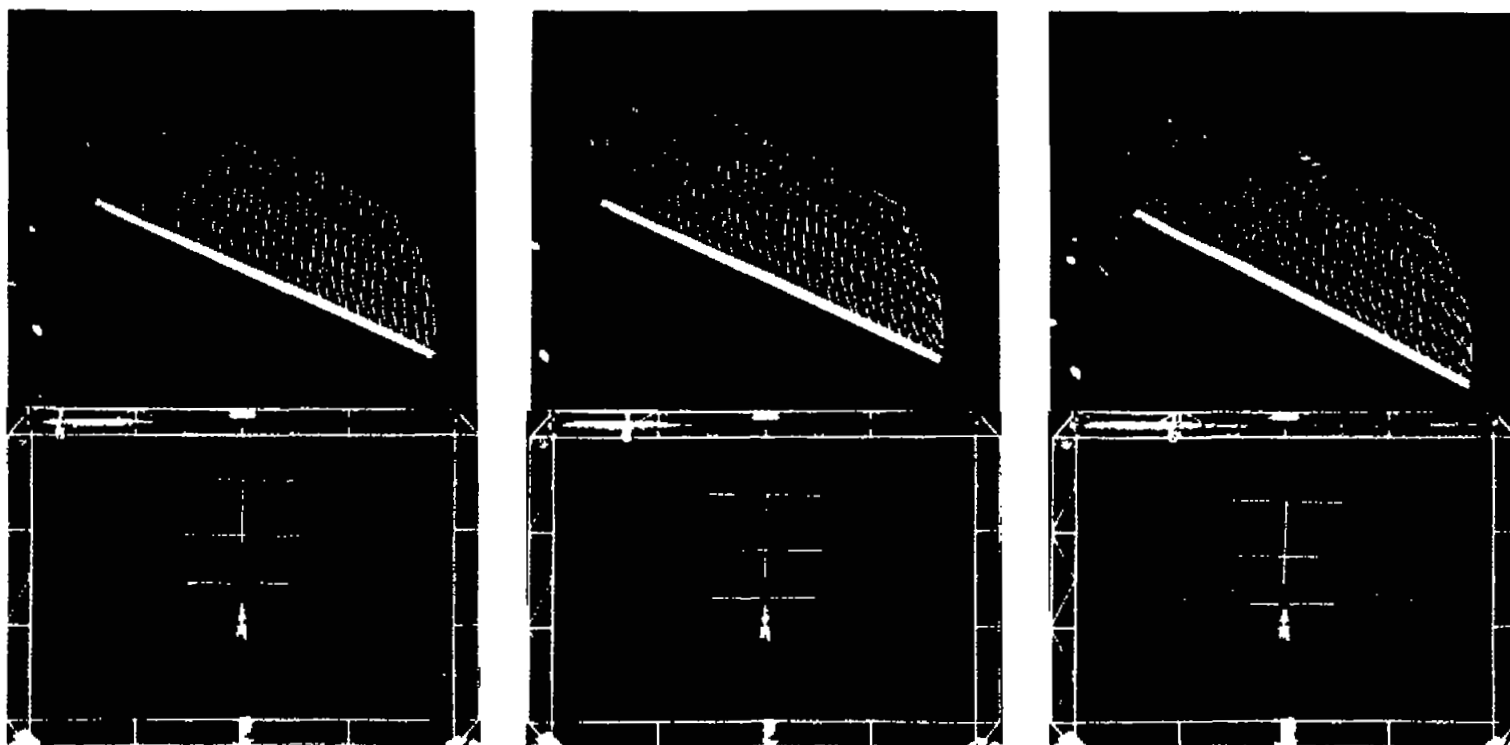
$a=0.3°, \quad C_L=0.18$       $a=4.6°, C_L=0.44$       $a=6.8°, \quad C_L=0.58$

L-77953

Figure 39.- Tuft-grid and surface-tuft photographs of model with leading-
edge chord-extension from 65 to 94 percent semispan. $\delta_f = \delta_s = 0°$.
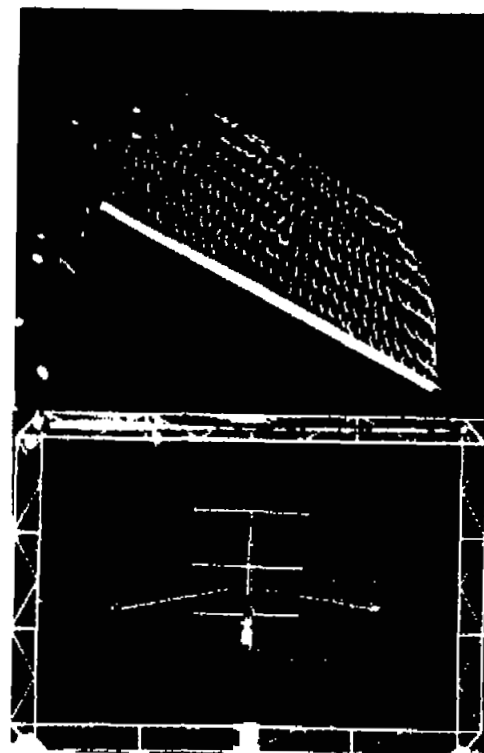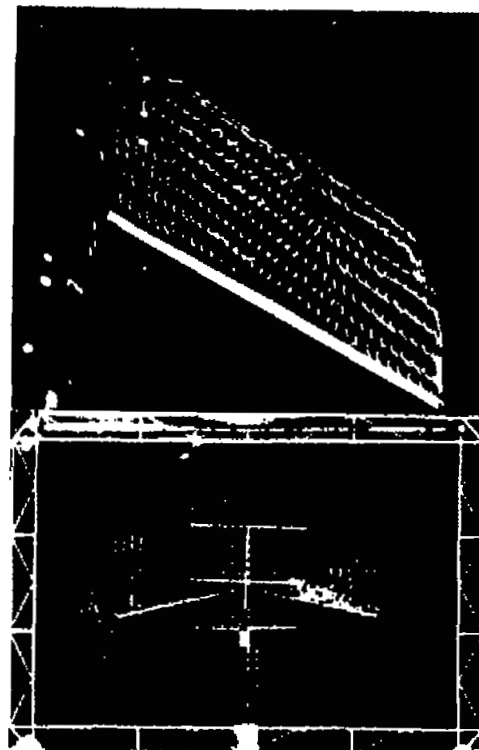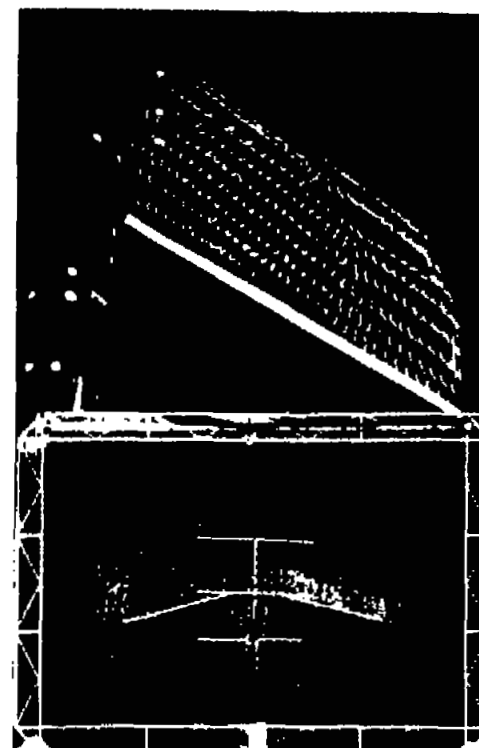
$\alpha = 8.9°$;   $C_L = 0.72$          $\alpha = 13.1°$;   $C_L = 0.93$          $\alpha = 17.2°$;   $C_L = 1.10$

Figure 39.- Concluded.          L-77954
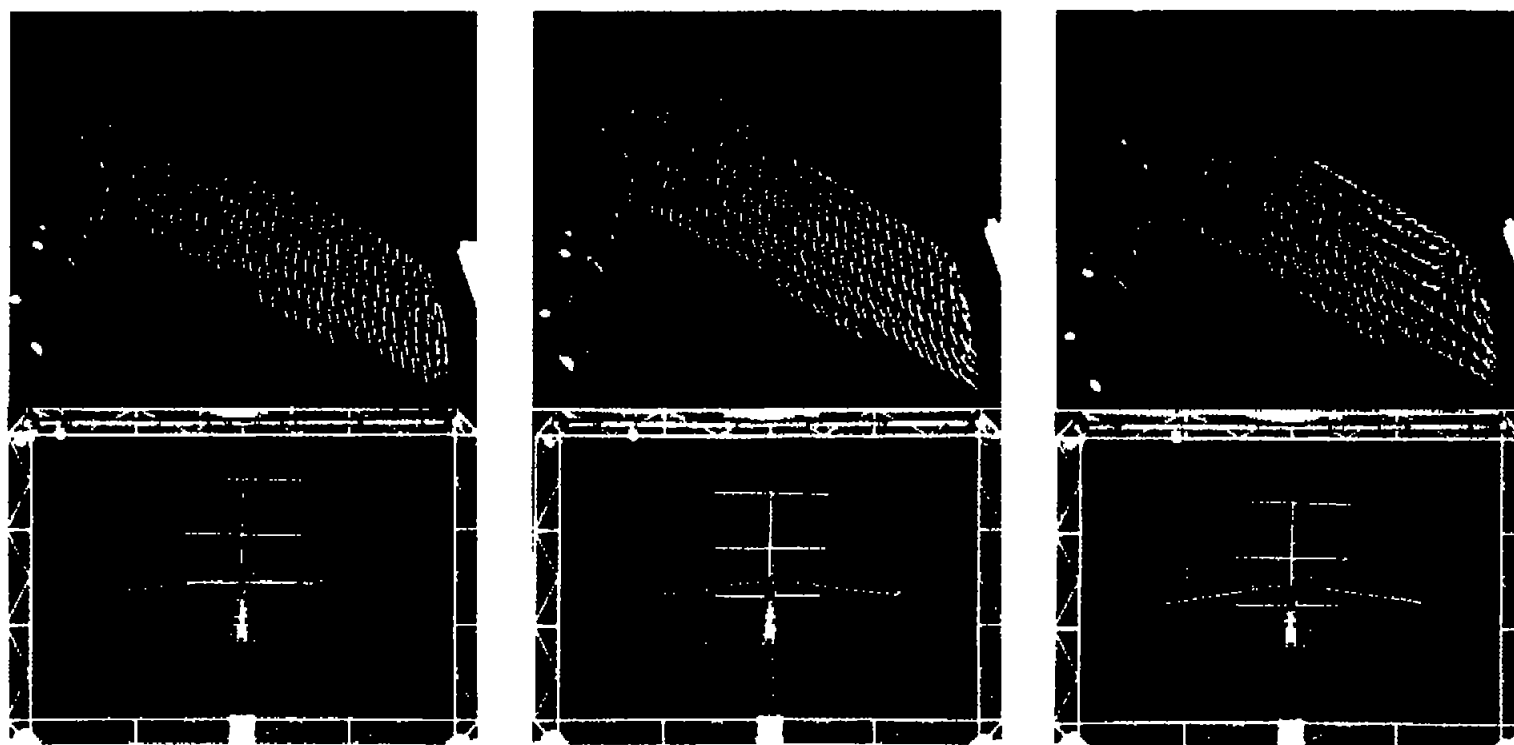
$a=0.4°; C_L=0.18$        $a=4.6°; C_L=0.45$        $a=6.8°; C_L=0.59$

Figure 40.- Tuft-grid and surface-tuft photographs of model with large
inlet. $\delta_f = \delta_s = 0°$.
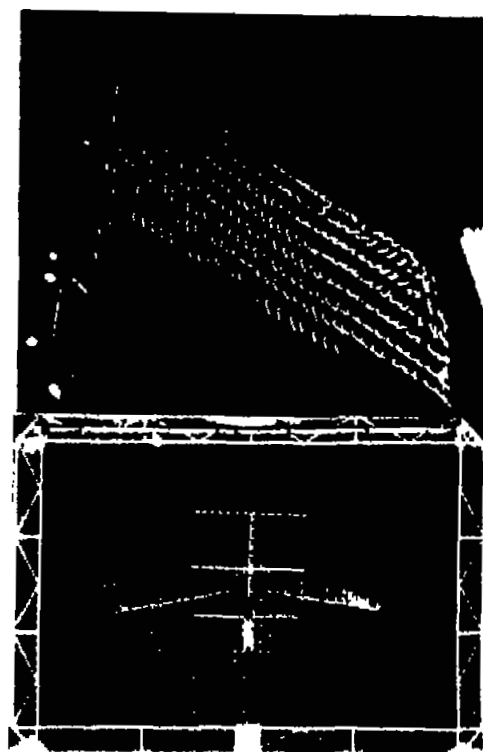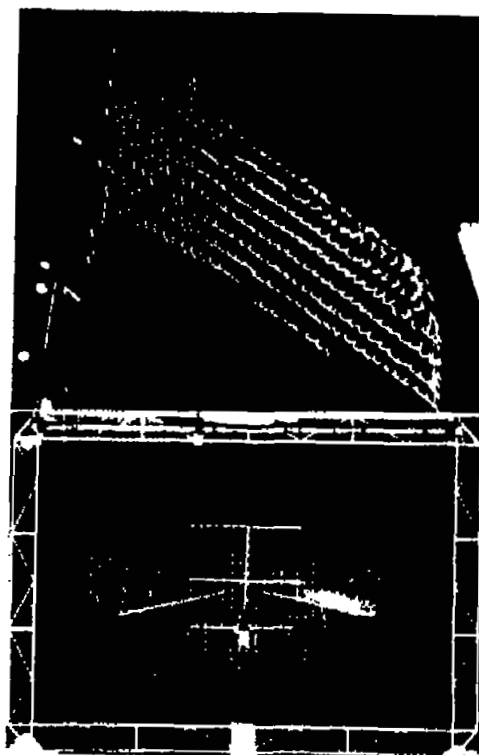
L-77955
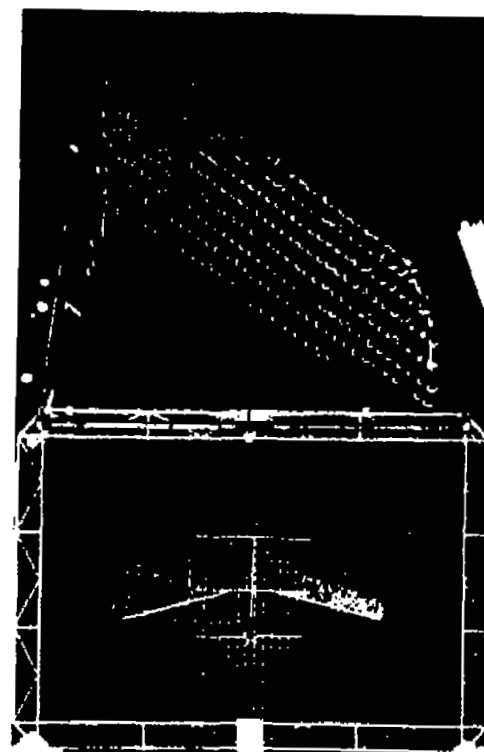
$a = 9.0°, C_L = 0.73$    $a = 13.2°; C_L = 0.95$    $a = 17.2°, C_L = 1.04$

Figure 40.- Concluded.    L-77956
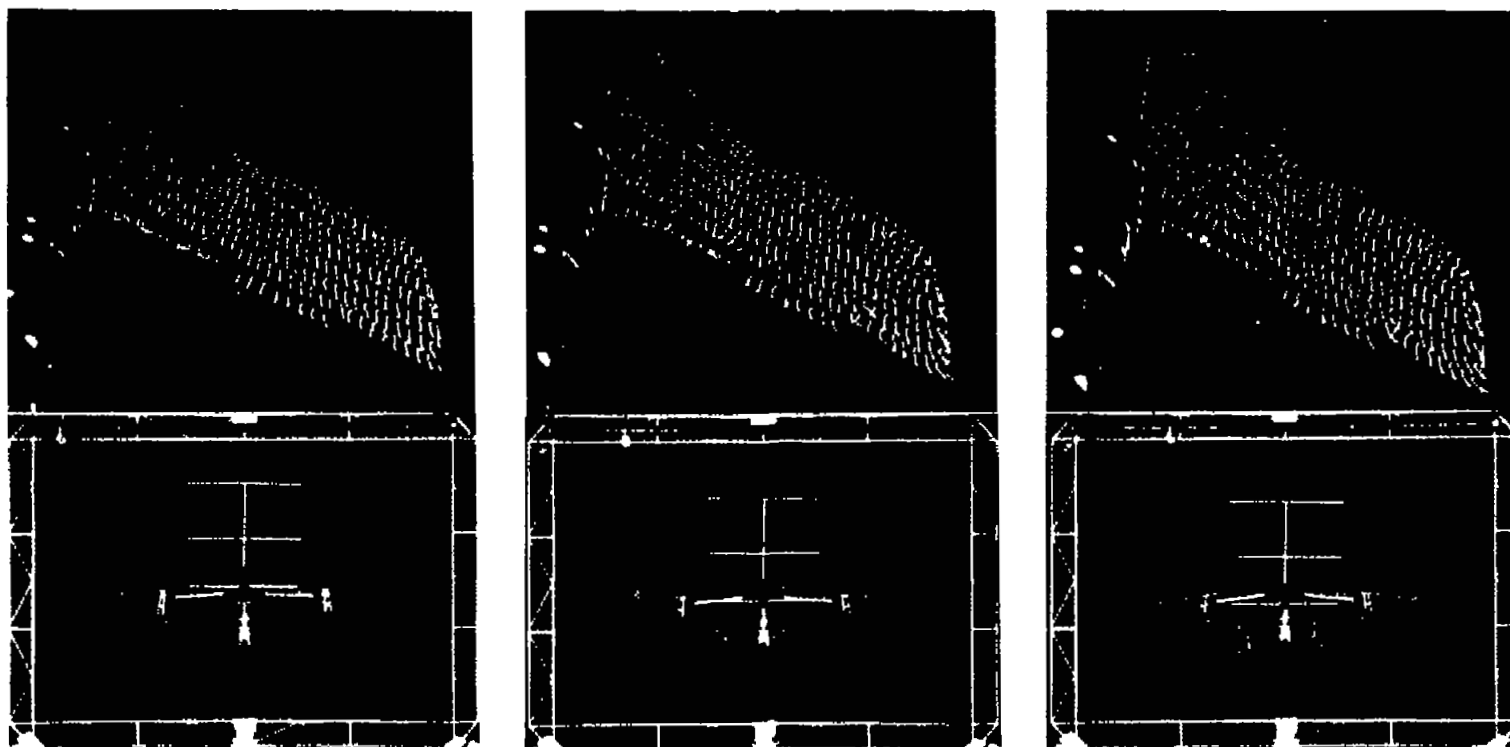
$\alpha = 0.7°$, $C_L = 0.54$      $\alpha = 5.0°$; $C_L = 0.82$      $\alpha = 7.2°$; $C_L = 0.97$

Figure 41.- Tuft-grid and surface-tuft photographs of model with large inlet. $\delta_f = 40°$; $\delta_s = 21.7°$.
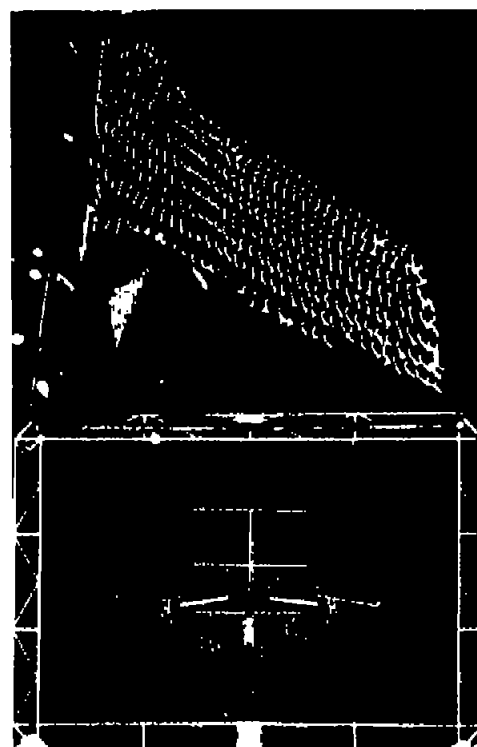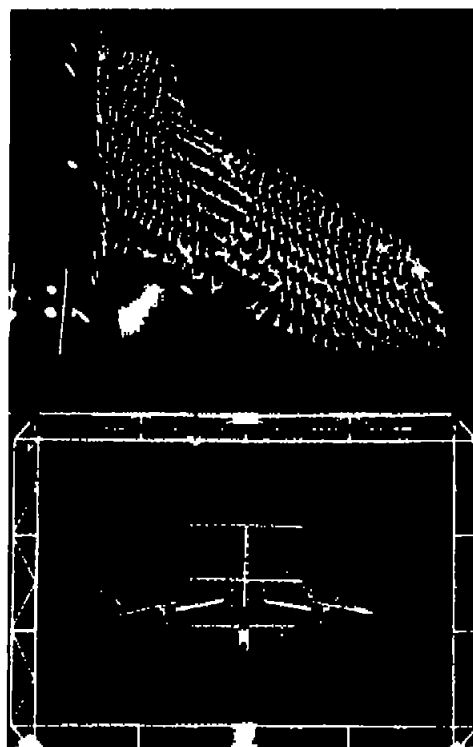
L-77957
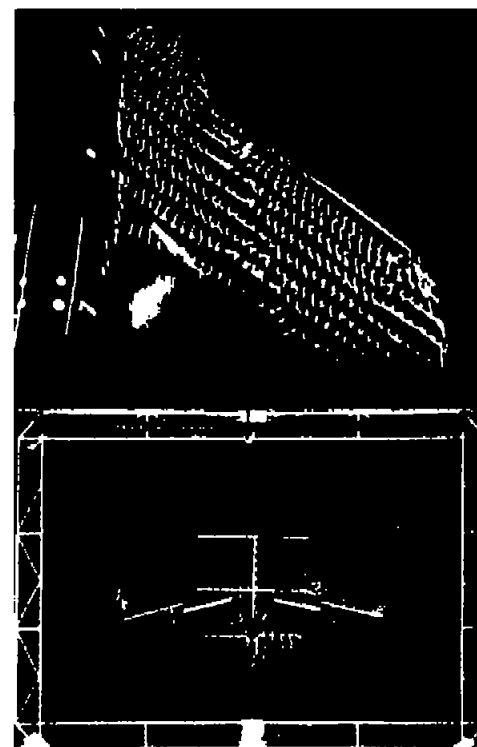
$a=9.2°;\quad C_L=1.08$      $a=13.3°;\quad C_L=1.20$      $a=17.5°;\quad C_L=1.29$

Figure 41.- Concluded.

L-77958
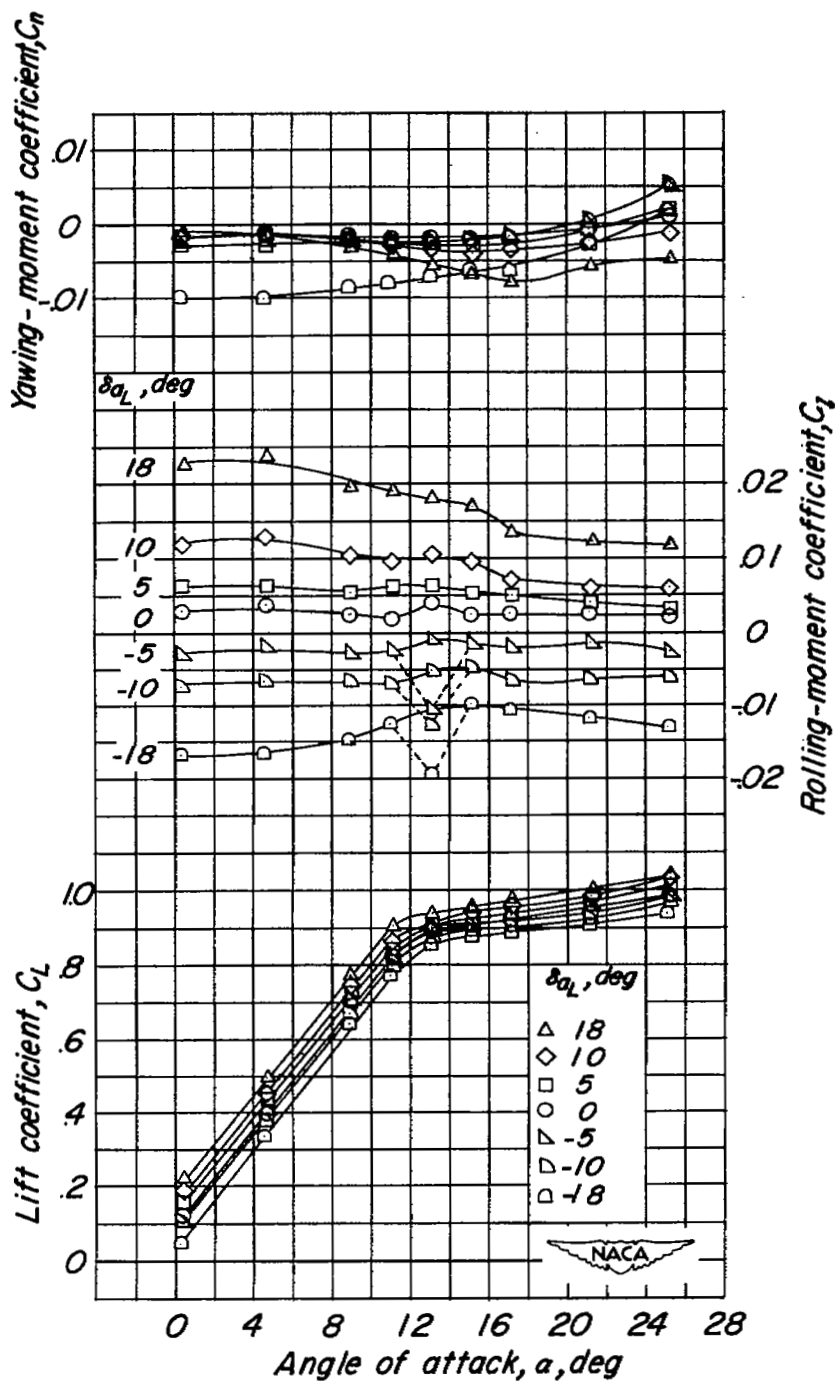
(a)  $\delta_f = \delta_s = 0^\circ$.

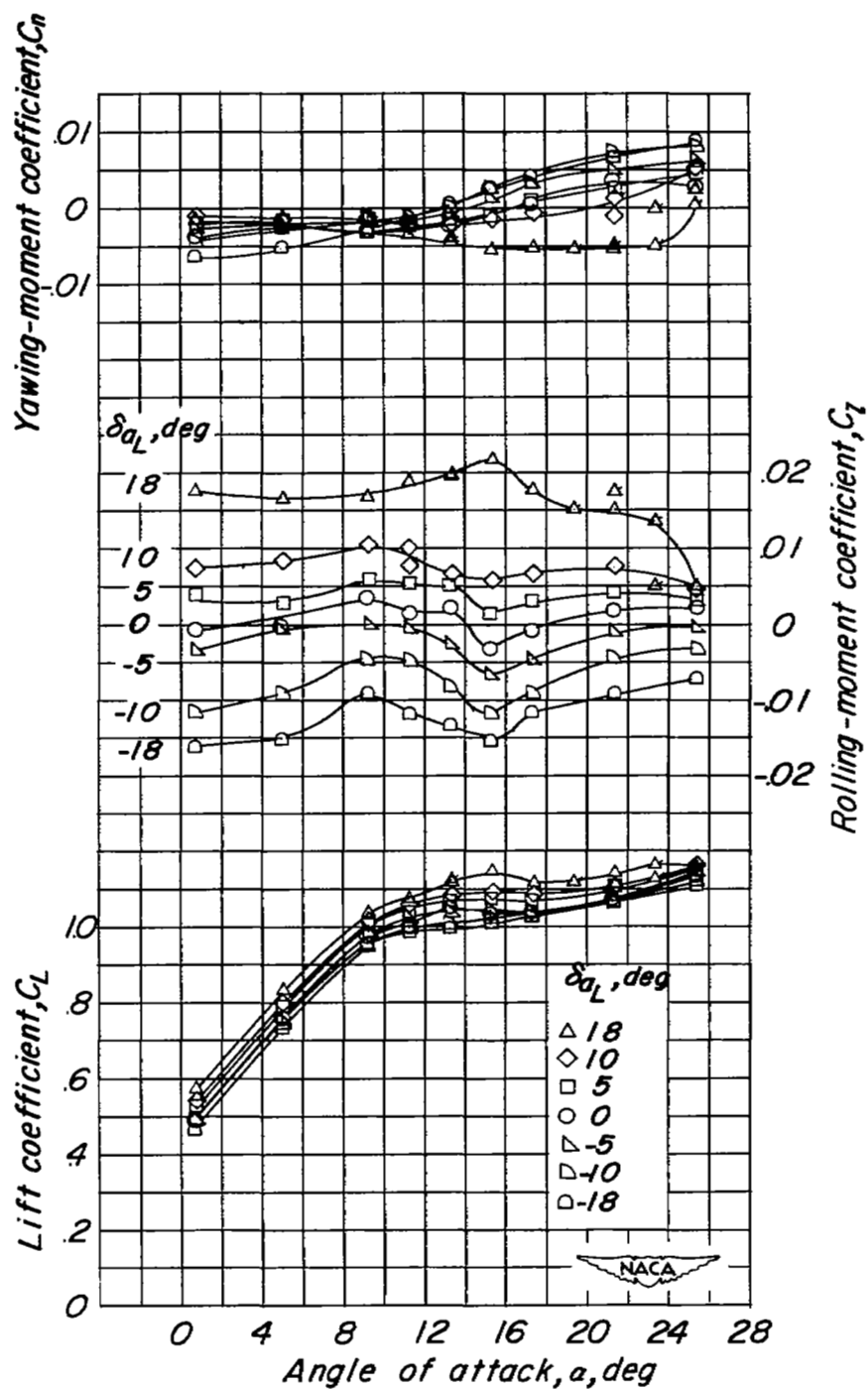Figure 42.- Effect of left-aileron deflection on the aerodynamic charac-
teristics of the basic model.  $i_t = 0^\circ$.
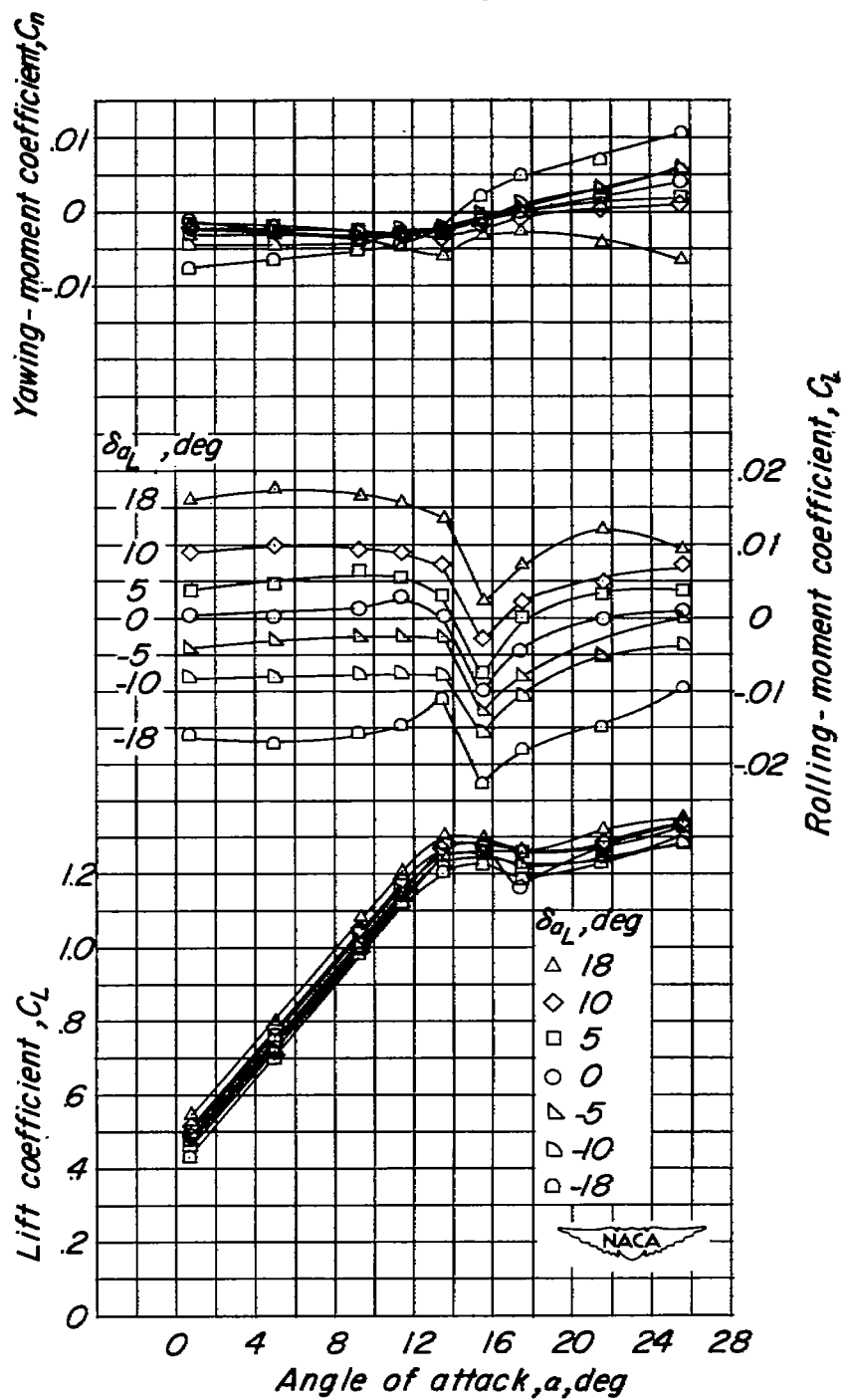
(b)   $\delta_f = 40°$;   $\delta_s = 21.7°$.

Figure 42.- Concluded.
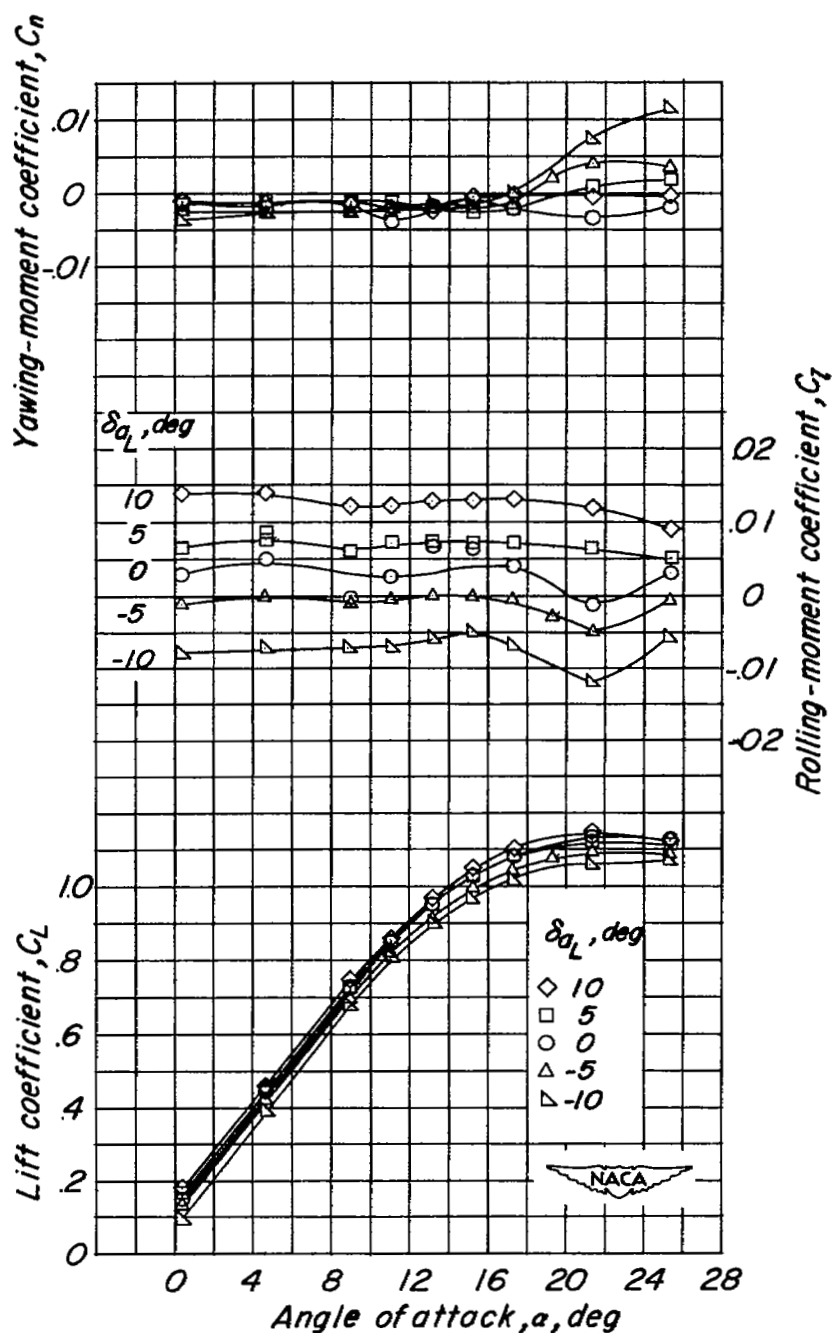
(a)  $\delta_f = \delta_s = 0°$.

Figure 43.- Effect of left-aileron deflection on the aerodynamic characteristics of the model with a 0.10c leading-edge chord-extension from 70 to 94 percent semispan.  $i_t = 0°$.
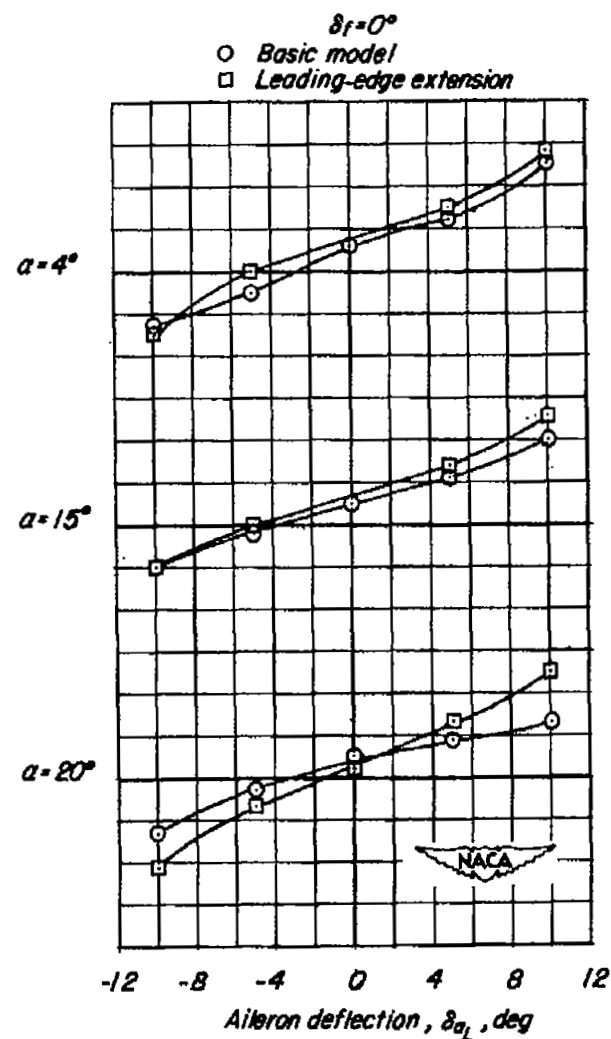
(b)  $\delta_f = 40°$.

Figure 43.- Concluded.

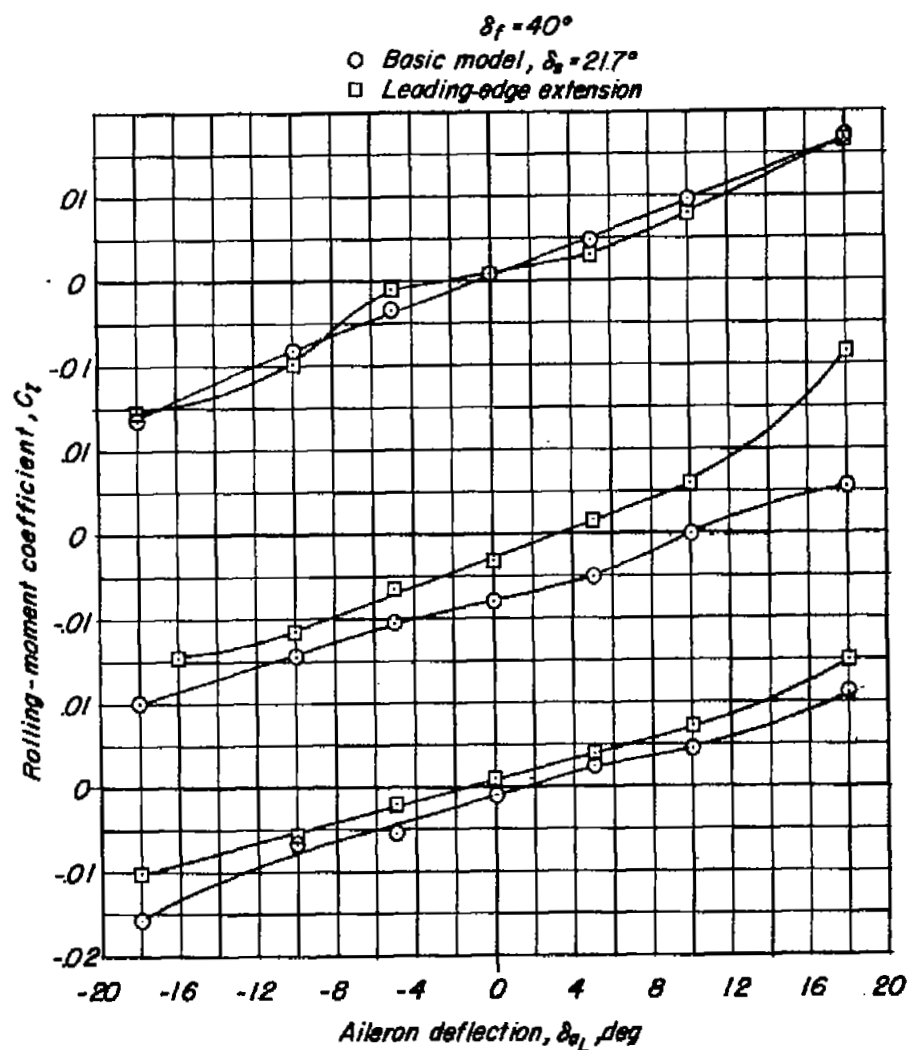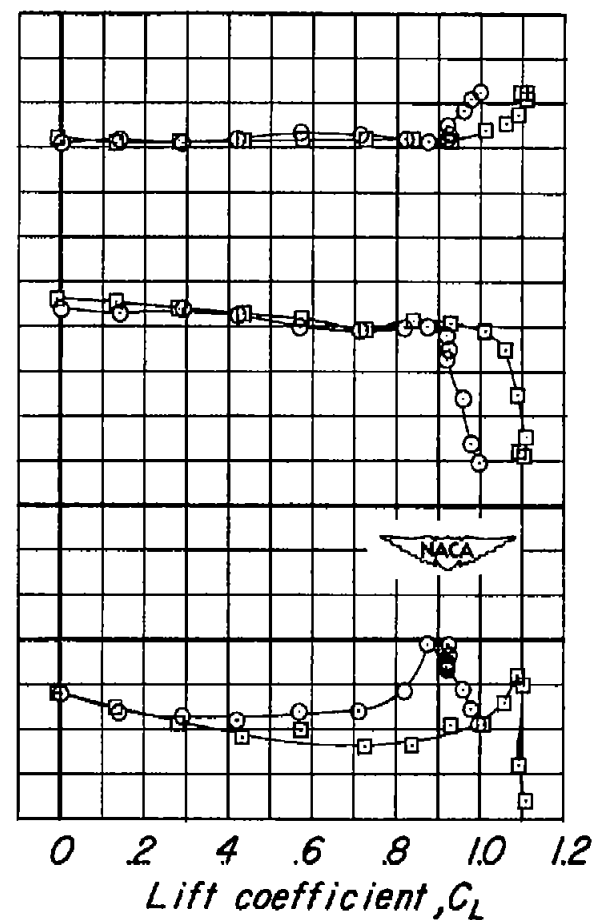$\delta_f = 40°$
O  Basic model, $\delta_a = 21.7°$
□  Leading-edge extension

$\delta_f = 0°$
O  Basic model
□  Leading-edge extension



Rolling-moment coefficient, $C_l$

Aileron deflection, $\delta_{a_L}$, deg
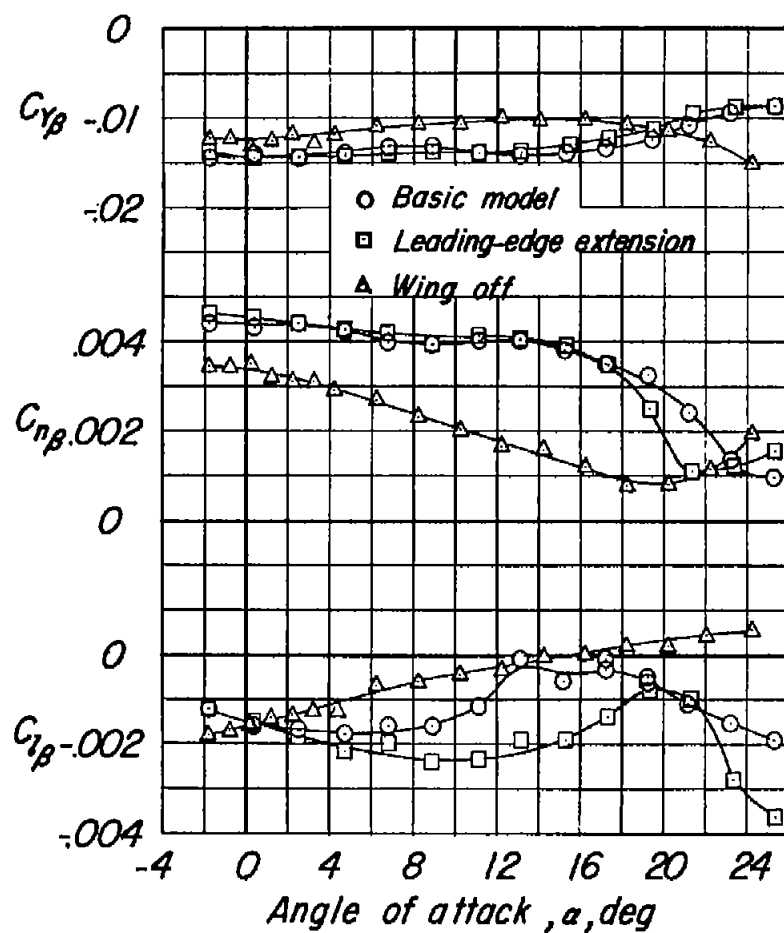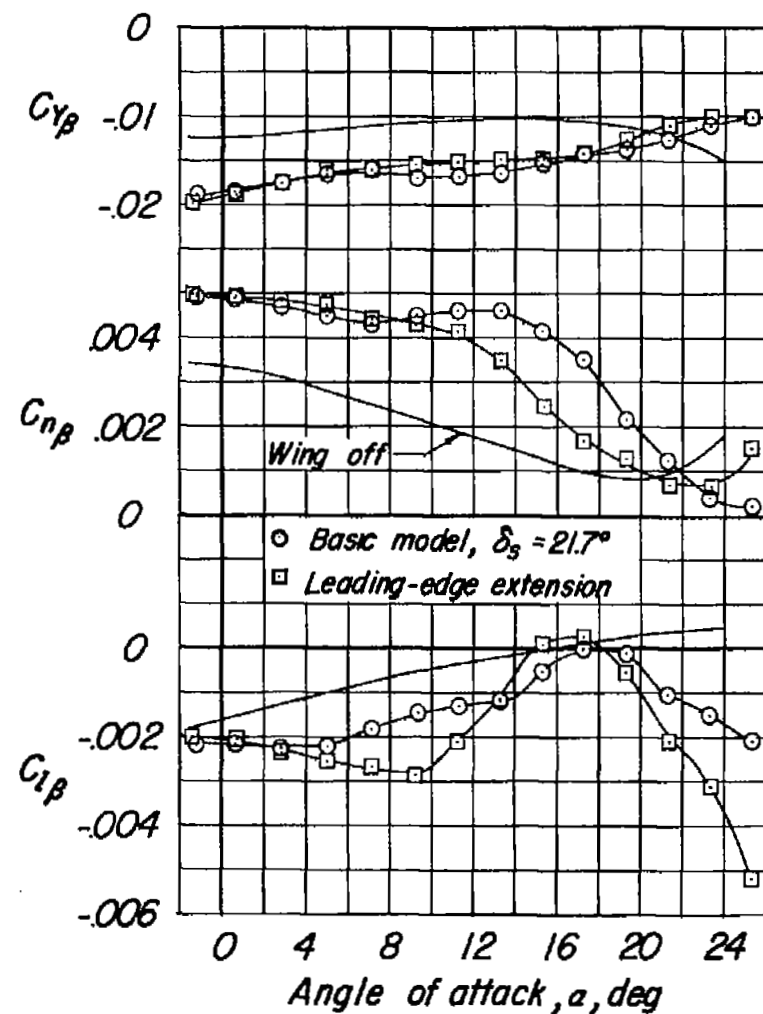
$a = 4°$

$a = 15°$

$a = 20°$

Aileron deflection, $\delta_{a_L}$, deg

Figure 44.- Comparison of aileron effectiveness with and without a
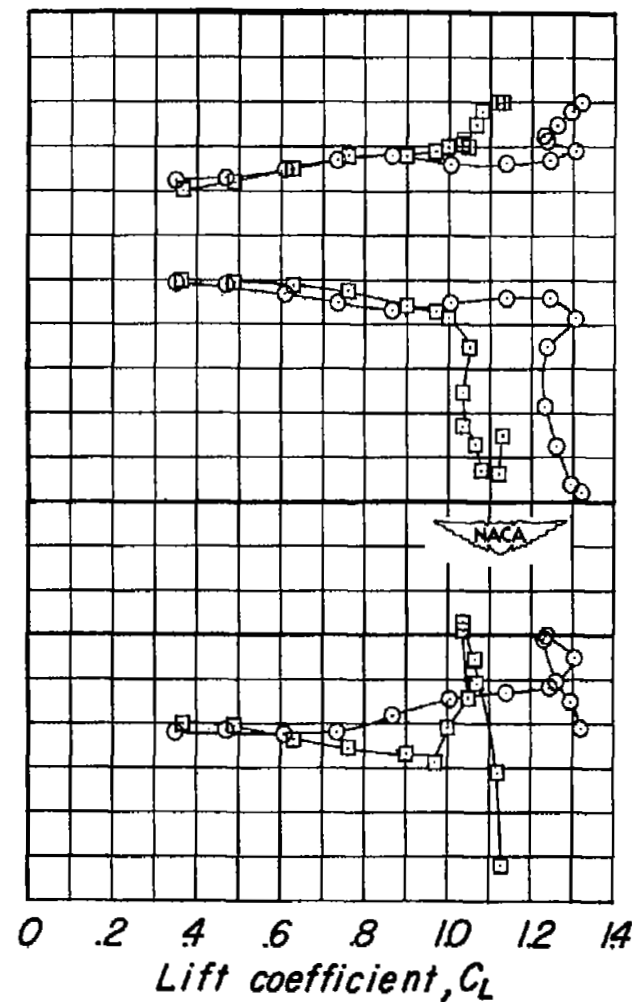0.10c leading-edge chord-extension from 70 to 94 percent semispan.

(a) $\delta_f = \delta_s = \delta_1 = \delta_2 = 0°$.

Figure 45.- Effect of leading-edge chord-extension on the lateral-
stability derivatives.  0.10 chord-extension from 70 to 94 percent
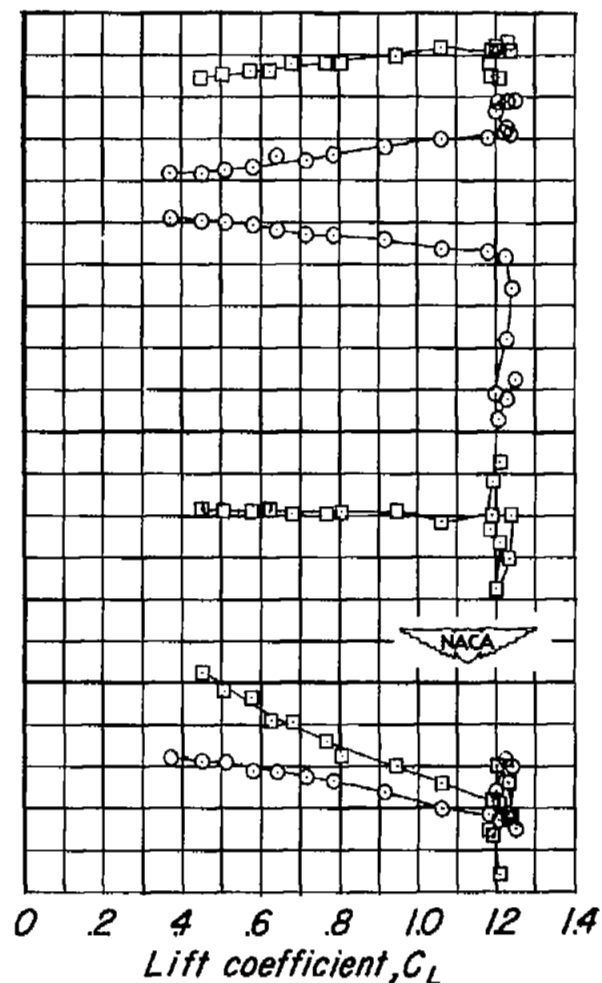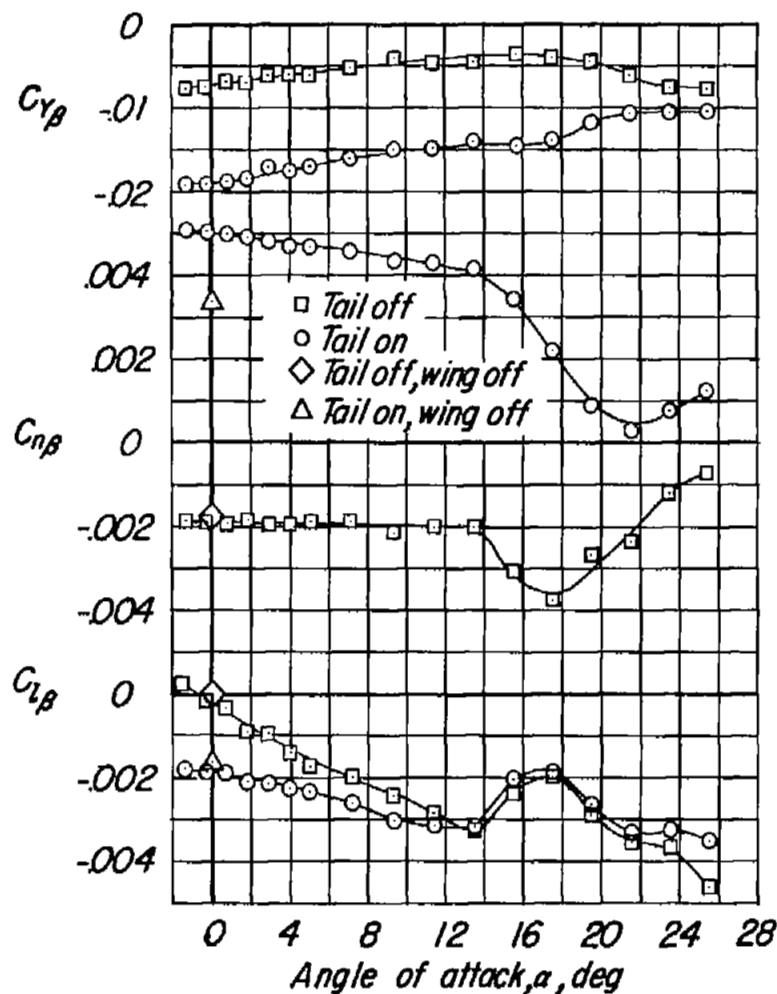semispan.

(b)  $\delta_f = 40^\circ$.

Figure 45.- Concluded.

Figure 46.- Lateral-stability derivatives with drooped chord-extension.
0.10 chord-extension from 65 to 94 percent semispan. $\delta_f = 40^\circ$;
$\delta_1 = \delta_2 = 10^\circ$.